



**THESIS APPROVAL**  
**GRADUATE SCHOOL, KASETSART UNIVERSITY**

Doctor of Philosophy (Plant Pathology)

DEGREE

Plant Pathology

FIELD

Plant Pathology

DEPARTMENT

**TITLE:** The Role of *luxR* Homolog of *Xanthomonas axonopodis* pv. *glycines* is Important for Virulent in Soybean

**NAME:** Miss Tiyakhon Chatnaparat

**THIS THESIS HAS BEEN ACCEPTED BY**

THESES ADVISOR

( Associate Professor Sutruedee Prathuangwong, Ph.D. )

THESES CO-ADVISOR

( Professor Steven E. Lindow, Ph.D. )

DEPARTMENT HEAD

( Associate Professor Somsiri Sangchote, Ph.D. )

APPROVED BY THE GRADUATE SCHOOL ON \_\_\_\_\_

DEAN

( Associate Professor Gunjana Theeragool, D.Agr. )

THESIS

THE ROLE OF *luxR* HOMOLOG OF *Xanthomonas axonopodis* pv.  
*glycines* IS IMPORTANT FOR VIRULENT IN SOYBEAN



TIYAKHON CHATNAPARAT

A Thesis Submitted in Partial Fulfillment of  
the Requirements for the Degree of  
Doctor of Philosophy (Plant Pathology)  
Graduate School, Kasetsart University  
2012

Tiyakhon Chatnaparat 2012: The Role of *luxR* Homolog of *Xanthomonas axonopodis* pv. *glycines* is Important for Virulent in Soybean. Doctor of Philosophy (Plant Pathology), Major Field: Plant Pathology, Department of Plant Pathology.  
Thesis Advisor: Associate Professor Sutruedee Prathuangwong, Ph.D. 176 pages.

This study reports the role of a novel *luxR* homolog, *XagR*, in *Xanthomonas axonopodis* pv. *glycines* strain 12-2 (*Xag*), the cause of soybean pustule disease. *XagR* controlled expression of *pip*, proline iminopeptidase; *yapH*, a homolog of *Yersinia* auto-transporter-like protein H; and at least 77 other genes. *XagR* and *Pip* were required for full virulence of *Xag* to soybean while constitutive over-production of *XagR* suppressed infection. The *xagR*-dependent induction of *pip* occurred *in planta* only 2 days or more after inoculation. While the transcription of *xagR* appeared constitutive, *XagR* accumulated only in cells that had colonized soybean plants for more than 2 days. This event suggested that some component(s) produced during the infection process mediated post-transcriptional control, likely by protecting *XagR* from proteolytic degradation. *XagR* modulated the adhesiveness of the pathogen during the infection process by suppressing the adhesin *YapH*. The *yapH* mutant incited more infections of soybean leaves than the wild type strain when topically applied under dry conditions, while it caused fewer infections when leaves were subject to simulated rain events after inoculation. Likewise, *yapH* mutant and strain in which *XagR* was over-expressed exhibited much more egress from infected leaves than the wild type strain. Thus *XagR* differentially modulates expression of a variety of genes during the infection process in response to feedback from plant molecules elaborated during infection to coordinate processes such as invasion, infection, and cell egress needed to complete the disease cycle.

To identify the genes in *Xag*12-2 that are altered in expression during infection of soybean plants compared to growth in a minimal medium *in vitro*, *Xag* draft genome was developed and transcriptome analysis using deep RNA sequencing of mRNA was performed. Of 5062 predicted genes in the *Xag* draft genome, 534 genes were identified as being up-regulated in the plant while 289 were down-regulated. Plant up-regulated genes included the *hrp* cluster, and genes encoding avirulence and type III effector proteins, extracellular enzymes, chemotaxis components, and several other known or new putative virulence factors. Plant down-regulated genes included those involved in attachment and the movement process. This study is the first to report on *Xag* gene expression during infection of soybean and the insights into the behavior of the pathogen should prove useful for developing strategies for controlling disease in this important agricultural crop.

---

Student's signature

---

Thesis Advisor's signature

## ACKNOWLEDGEMENTS

I offer my sincerest gratitude to my thesis advisor, Assoc. Prof. Dr. Sutruedee Prathuangwong, who has supported me throughout my thesis with her advice and suggestion and giving me the wonderful opportunity and partially financial support for this work.

Special thanks to Professor Steven E. Lindow, my co-advisor for his patience and knowledge whilst allowing me to use the excellent working facilities and giving me partially financial support for this work at his laboratory in University of California, Berkeley USA.

Also, I would also like to thank to Assoc. Prof. Sutruedee's laboratory, as well as the graduate students and research assistant of Prof. Steven E. Lindow for their kind cooperation with a friendly and cheerful.

This research was financially supported by a grant from the Thailand Research Fund (TRF) for providing the Royal Golden Jubilee (RGJ-Ph.D program) Scholarship.

Finally, this thesis is dedicated to the memory of my beloved parents and family, who stand beside me, give me warmly love, encouragement and inspiration for this study.

Tiyakhon Chatnaparat

February 2012

**TABLE OF CONTENTS**

	<b>Page</b>
TABLE OF CONTENTS	i
LIST OF TABLES	ii
LIST OF FIGURES	iii
INTRODUCTION	1
OBJECTIVES	5
LITERATURE REVIEW	6
MATERIALS AND METHODS	24
RESULTS AND DISCUSSION	41
Results	41
Discussion	111
CONCLUSIONS	128
LITERATURE CITED	130
APPENDIX	156
CURRICULUM VITAE	176

## LIST OF TABLES

<b>Table</b>		<b>Page</b>
1	<i>Xanthomonas</i> published genome sequences	9
2	Bacterial strains and plasmids	24
3	Polymerase chain reaction primers	29
4	The <i>luxR</i> homolog/ <i>pip</i> -like loci found in other bacterial species	46
5	Virulence of <i>Xanthomonas axonopodis</i> pv. <i>glycines</i> mutants on soybean	48
6	Transcriptional analysis of <i>Xanthomonas axonopodis</i> pv. <i>glycines</i> 12-2 genes controlled by <i>xagR</i>	67
7	The differentially plant upregulated genes in <i>Xanthomonas axonopodis</i> pv. <i>glycines</i> 12-2	88
8	The differentially plant downregulated genes in <i>Xanthomonas axonopodis</i> pv. <i>glycines</i> 12-2	103
 <b>Appendix Table</b>		
A1	The unique genes of <i>Xanthomonas axonopodis</i> pv. <i>glycines</i> 12-2	159

## LIST OF FIGURES

<b>Figure</b>		<b>Page</b>
1	<p>The system of <i>Xanthomonas</i> spp. with published genome sequences, and the corresponding host plants on which they cause disease. <i>Xanthomonas campestris</i> pv. <i>campestris</i> (<i>Xcc</i>), <i>Xanthomonas oryzae</i> pv. <i>oryzae</i> (<i>Xoo</i>) and <i>Xanthomonas albilineans</i> (<i>Xalb</i>) spread in vascular system of the host plant, whereas <i>Xanthomonas axonopodis</i> pv. <i>glycines</i> (<i>Xag</i>), <i>Xanthomonas axonopodis</i> pv. <i>citri</i> (<i>Xac</i>), <i>Xanthomonas oryzae</i> pv. <i>oryzicola</i> (<i>Xoc</i>) and <i>Xanthomonas campestris</i> pv. <i>vesicatoria</i> (<i>Xcv</i>) either locally in the apoplast at the infection site.</p>	8
2	<p>Model of known virulence factors from Xanthomonads.</p>	14
3	<p>Sequencing gel. The left lane shows a marker ladder. The smear on the middle lane shows a long insert library and the smear on the right shows a short insert library.</p>	27
4	<p>Overlap extension PCR was used to create constructs in the suicide-delivery vector pTOK2 to create site-directed mutants in <i>Xanthomonas axonopodis</i> pv. <i>glycines</i> 12-2 by recombination (A). An XagR-complementary strain, the 1.4-kb sequence of <i>xagR</i> containing the native promoter was amplified and ligated into the multiple cloning site of vector pBBR1MCS-5(B). XagR-overexpressing strain was constructed by placing the coding region of <i>xagR</i> amplified as a 765 bp fragment from <i>Xag12-2</i> genomic DNA with <i>Sma</i>I sites downstream of the <i>E. coli trp</i> operon promoter pBBR1MCS-5 to yield pTrp::<i>xagR</i> (C).</p>	33

## LIST OF FIGURES (Continued)

Figure		Page
5	Dot blot comparison between draft genome of <i>Xanthomonas axonopodis</i> pv. <i>glycines</i> 12-2 and complete genomes of <i>Xanthomonas axonopodis</i> pv. <i>citri</i> 306 (A), <i>Xanthomonas campestris</i> pv. <i>vesicatoria</i> 85-10 (B), <i>Xanthomonas campestris</i> pv. <i>campestris</i> ATCC 33913 (C) and <i>Xanthomonas oryzae</i> pv. <i>oryzae</i> KACC10331 (D) using RAST subsystem technology.	42
6	Structure of XagR from <i>Xanthomonas axonopodis</i> pv. <i>glycines</i> with schematic representation of the positions of the AHL-binding and the helix-turn-helix-DNA binding domains typical of quorum sensing LuxR family regulators (A). Analysis of the <i>pip</i> promoter locus within the 384-bp intergenic region upstream from the <i>pip</i> gene and location of a putative palindromic <i>lux</i> box sequence (B). Alignment of the putative <i>lux</i> boxes associated with <i>pip</i> genes in <i>X. axonopodis</i> pv. <i>glycines</i> , <i>Xanthomonas campestris</i> pv. <i>campestris</i> and <i>Xanthomonas oryzae</i> pv. <i>oryzae</i> (C).	45
7	Disease severity on susceptible soybean cv. Spencer caused by <i>Xanthomonas axonopodis</i> pv. <i>glycines</i> 12-2 (A), <i>xagR</i> mutant (B), <i>pip</i> mutant (C), <i>xagR/pip</i> double mutant (D), XagR overexpressing strain (E) and <i>xagR</i> complementary strain (F).	49
8	Population size of the wildtype strain of <i>Xanthomonas axonopodis</i> pv. <i>glycines</i> (diamonds), a <i>xagR</i> mutant (squares) and a <i>xagR/pip</i> double mutant (triangles) in soybean at various times after infiltration. The vertical bars represent the standard error of mean log-transformed population sizes.	50

## LIST OF FIGURES (Continued)

<b>Figure</b>		<b>Page</b>
9	<p>pKI- <i>pip</i> promoter-probe vectors contain a common cassette that has four tandem copies of the T1 terminator (T1<sub>(4)</sub>; shaded boxes), a multicloning site (solid box) containing <i>pip</i> promoter was cutted with <i>SacI</i>, <i>inaZ</i> reporter genes (including optimally placed ribosome binding sites and a single <i>rrnB</i> T1 terminator (T1; shaded box) (Miller and Lindow, 1997).</p>	53
10	<p>Ice nucleation activity indicative of <i>pip</i> promoter activity in a wildtype strain of <i>Xanthomonas axonopodis</i> pv. <i>glycines</i> (orange bars) and a <i>xagR</i> mutant (purple bars) harboring a <i>pip:inaZ</i> fusion when grown in various culture media including LB, M9 minimal medium, M9 minimal medium added with fresh macerated soybean, M9 minimal medium added with autoclaved soybean and when inoculated into soybean plants. Vertical bars represent the standard error of mean log-transformed ice nucleation activity.</p>	54
11	<p>Relative abundance of <i>pip</i> transcripts in a wildtype and <i>xagR</i> mutant of <i>Xanthomonas axonopodis</i> pv. <i>glycines</i> grown in M9 minimal media, M9 minimal media containing fresh soybean leaf macerates, or in cells <i>in planta</i> as determined by RT-PCR. The vertical bars represent the standard error of mean relative gene expression.</p>	55

## LIST OF FIGURES (Continued)

Figure		Page
12	Ice nucleation activity indicative of <i>pip</i> promoter activity in a wildtype strain of <i>Xanthomonas axonopodis</i> pv. <i>glycines</i> (open bars) and a <i>xagR</i> mutant (solid bars) harboring a <i>pip:inaZ</i> fusion when recovered from rice, cabbage, soybean cv. Spencer (susceptible), soybean cv. Williams 82 (resistant) and tobacco two days after inoculation. The vertical bars represent the standard error of mean log-transformed ice nucleation activity.	56
13	Ice nucleation activity indicative of <i>pip</i> promoter activity in a wildtype strain of <i>Xanthomonas axonopodis</i> pv. <i>glycines</i> (circles) and a <i>xagR</i> mutant (triangles) harboring a <i>pip:inaZ</i> fusion at various times after infiltration into soybean leaves (A). Population size of the wildtype strain of <i>X. axonopodis</i> pv. <i>glycines</i> (circles) and a <i>xagR</i> mutant (triangles) at various times after infiltration (B). The vertical bars represent the standard error of mean log-transformed ice nucleation activity or population sizes.	58
14	pXagR-KI contain a common cassette that has four tandem copies of the T1 terminator (T1 <sub>(4)</sub> ; shaded boxes), a multicloning site (solid box) containing <i>XagR</i> promoter was cutted with <i>SacI</i> <i>inaZ</i> reporter genes (including optimally placed ribosome binding sites and a single <i>rrnB</i> T1 terminator (T1; shaded box) (Miller and Lindow, 1997).	60

## LIST OF FIGURES (Continued)

Figure		Page
15	Ice nucleation activity indicative of <i>xagR</i> promoter activity in a wildtype strain of <i>Xanthomonas axonopodis</i> pv. <i>glycines</i> (red bars) and a <i>xagR</i> mutant (blue bars) harboring a <i>xagR:inaZ</i> fusion when grown in various culture media including LB, M9 minimal medium, M9 minimal medium added with fresh macerated soybean, M9 minimal medium added with autoclaved soybean and when inoculated into soybean plants. The vertical bars represent the standard error of mean log-transformed ice nucleation activity or population sizes.	61
16	Relative abundance of <i>xagR</i> transcripts in a wildtype strain of <i>Xanthomonas axonopodis</i> pv. <i>glycines</i> grown in M9 minimal media, M9 minimal media containing fresh soybean leaf macerates, or in cells <i>in planta</i> as determined by RT-PCR. The vertical bars represent the standard error of mean relative gene expression.	62
17	Western blot analysis of XagR in different strains of <i>Xanthomonas axonopodis</i> pv. <i>glycines</i> including wildtype strain, <i>xagR</i> mutant and XagR overexpressing strain grown in minimal medium (left three lanes) or in media containing fresh soybean leaf macerates (left panel) or in uninoculated soybean leaves or leaves inoculated with the <i>X. axonopodis</i> pv. <i>glycines</i> wildtype strain 72 hours after inoculation (right panel).	63
18	The relationship between concentration and fold-change across the genes compared between XagR overexpressing strain and <i>X. axonopodis</i> pv. <i>glycines</i> wildtype. The differentially expressed genes are colored red and the non-differentially expressed are colored black. The blue line is added at a log fold change of 2 to represent a level for biological significance.	65

## LIST OF FIGURES (Continued)

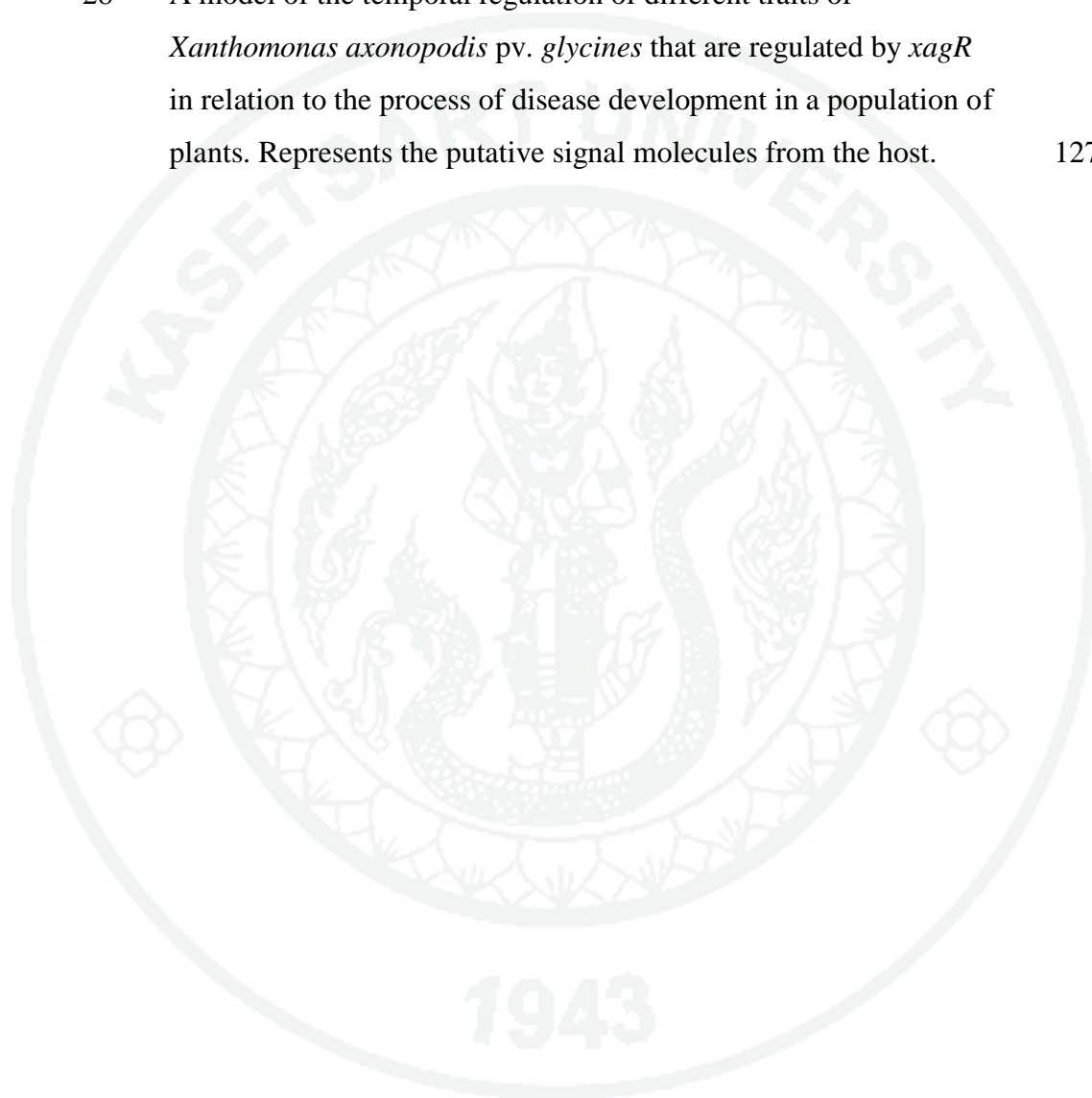
Figure		Page
19	The transcript abundance of a subset of the <i>xagR</i> -regulated genes in an XagR overexpressing strain compared with an <i>Xanthomonas axonopodis</i> pv. <i>glycines</i> wildtype were determined by RT-PCR analysis. The vertical bars represent the standard error of mean relative gene expression.	66
20	Visible halos of surfactant produced by various strains of <i>Xanthomonas axonopodis</i> pv. <i>glycines</i> (A) wildtype (B) <i>xagR</i> mutant (C) <i>pip</i> mutant (D) <i>xagR/pip</i> double mutant (E) XagR complementary and (F) XagR overexpressing strain as visualized by an atomized oil assay after growth on swarming media for 3 days.	75
21	The cells spread from the colony of XagR-overexpressing strain (A) and <i>Xanthomonas axonopodis</i> pv. <i>glycines</i> wildtype (B) grown on semi solid agar (0.3% LB) for 3 days.	75
22	Attachment of various strains of <i>Xanthomonas axonopodis</i> pv. <i>glycines</i> wildtype (red bar), <i>yapH</i> mutant (green bar), XagR overexpressing strain (light blue bar), <i>xagR</i> mutant (blue) and LB (spot bar) only to polystyrene wells assessed by crystal violet staining of adherent cells after 5 min, 7 hr and 24 hr of incubation. The vertical bars represent the standard error of mean absorbance value at 570 nm.	78
23	Attachment of various strains of <i>Xanthomonas axonopodis</i> pv. <i>glycines</i> wildtype (red bar), <i>yapH</i> mutant (green bar), XagR overexpressing strain (light blue) and <i>xagR</i> mutant (blue) to the surface of soybean leaves after topical application at 5 min, 3 hr and 7 hr of incubation. The vertical bars represent the standard error of mean log-transformed of bacterial cell.	79

## LIST OF FIGURES (Continued)

Figure		Page
24	Egression of the <i>Xanthomonas axonopodis</i> pv. <i>glycines</i> wildtype (red bar), <i>yapH</i> mutant (green bar), <i>xagR</i> mutant (light blue bar) and XagR overexpressing strain (blue bar) from the edges of discs of infected soybean leaves. The vertical bars represent the standard error of mean log- transformed of bacterial cell.	80
25	Incidence of bacterial pustule disease on soybean incited of <i>Xanthomonas axonopodis</i> pv. <i>glycines</i> wildtype, <i>yapH</i> mutant, <i>xagR</i> mutant and XagR overexpressing strain after spray inoculation when plants were allowed to dry slowly after inoculation (solid bars) or which were subjected to 30 minutes of simulated rain after inoculation (open bars). The vertical bars represent the standard error of mean disease incidence per plant.	82
26	Electropherogram summary of total RNA and mRNA from 3 replication of <i>Xanthomonas axonopodis</i> pv. <i>glycines</i> recovered from infected soybean. Total RNA of sample 1 (A), sample 2 (B) and sample 3 (C) from 2100 expert_EukaryoteTotal RNA Pico. mRNA of sample 1 (D), sample 2(E) and sample 3 (F) from 2100 expert_mRNA Pico chip.	84
27	The relationship between concentration and fold change across the genes compared between <i>Xanthomonas axonopodis</i> pv. <i>glycines</i> grown in plant and <i>X. axonopodis</i> pv. <i>glycines</i> in M9 minimal medium. The differentially expressed genes are colored red and the non-differentially expressed are colored black. The blue line is added at a log fold change of 2 to represent a level for biological significance.	87

**LIST OF FIGURES (Continued)**

<b>Figure</b>		<b>Page</b>
28	A model of the temporal regulation of different traits of <i>Xanthomonas axonopodis</i> pv. <i>glycines</i> that are regulated by <i>xagR</i> in relation to the process of disease development in a population of plants. Represents the putative signal molecules from the host.	127



## **THE ROLE OF *LuxR* HOMOLOG OF *Xanthomonas axonopodis* pv. *glycines* IS IMPORTANT FOR VIRULENT IN SOYBEAN**

### **INTRODUCTION**

As plant pathogenic bacteria engage in very intimate interactions with most host plants, there is growing evidence that they exploit chemical cues provided by the plant in order to coordinate their gene expression to orchestrate sequential expression of traits involved in the interaction. For example, phenolic glycosides and sugars are used as cues for the production of phytotoxins by different pathovars of *Pseudomonas syringae* (Mo *et al.*, 1991; Mo *et al.*, 1995). The expression of genes involved in type III secretion of effectors from many bacterial species into plants is likewise dependent on the presence of various plant-derived molecules as well as a low osmolarity environment and pH values typical of the plant apoplast (Arlat *et al.*, 1992; Huynh *et al.*, 1989; Rahme *et al.*, 1992; Schulte and Bonas, 1992; Wei *et al.*, 1992; Xiao *et al.*, 1992). Unknown compounds present in plant extracts also modulate extracellular enzyme production in soft-rotting plant pathogens (Hugouvieux-Cotte-Pattat *et al.*, 1996). There is a rich literature that demonstrates that the initial interactions of many rhizobia and *Agrobacterium tumefaciens* with host plants is dependent on recognition of specific plant compounds such as flavonoids and other phenolics (Bergman *et al.*, 1988; Caetano-Anolles *et al.*, 1988, Hawes and Smith, 1989; Parke *et al.*, 1987).

In addition to such extrinsic factors, many bacteria also coordinate gene expression in response to changes in intrinsic factors, often used to indicate local cell density in a process often called quorum sensing (QS). In most Gram-negative bacteria, the QS system is dependent on the production and perception of N-acyl homoserine lactones by two proteins belonging to the LuxI-LuxR families (Fuqua and Greenberg, 2002). While the signal is generated by a highly conserved N-acyl homoserine lactone synthase in the LuxI family of proteins, it is perceived by specific transcriptional regulators (LuxR homologs). The amino acid terminus of LuxR homologs contain an AHL binding region, which induces a multimerization and binding to promoters of a helix-turn-helix domain in the carboxyl terminus resulting

in activation of transcription of the target gene (Slock *et al.*, 1990; Choi and Greenberg, 1991; Stevens and Greenberg, 1994; Poellinger *et al.*, 1995; Stevens and Greenberg, 1997).

Numerous bacterial plant pathogens have been reported to carry so-called “orphan” LuxR homologs without an accompanying LuxI homolog, suggesting that they are not involved in classical cell density-dependent gene regulation. These LuxR homologs commonly regulate a variety of genes and/or functions involved in pathogenicity. For example, AviR and AvhR, LuxR homologs of *Agrobacterium vitis*, are associated with induction of the hypersensitive response on tobacco as well as necrosis in grape plants (Hao *et al.*, 2005). CepR2 positively regulates pyochelin production in *Burkholderia cenocepacia* by controlling transcription of one of the operons required for the biosynthesis of the siderophore (Malott *et al.*, 2009). Likewise, ExpR activates an RNA binding protein in *Erwinia carotovora* subsp. *carotovora* that functions as a negative regulator of extracellular enzymes and proteins as well as secondary metabolites (Cui *et al.*, 2005).

Curiously, recent work has shown that LuxR homologs in some plant-associated bacteria are responsive to plant signal molecules. PsoR, a LuxR homolog in the plant growth-promoting rhizobacterium *Pseudomonas fluorescens* is solubilized in the presence of macerated rice and wheat and regulates expression of target genes that contribute to its biocontrol activity (Subramoni *et al.*, 2011). Interestingly, LuxR homologs are required for full virulence of the vascular pathogens *Xanthomonas campestris* pv. *campestris* (*Xcc*) and *Xanthomonas oryzae* pv. *oryzae* (*Xoo*). The abundance of XccR, a LuxR homolog of *Xcc* was enhanced in the presence of the host plant cabbage and up-regulated the neighboring proline iminopeptidase gene (*pip*); both *xccR* and *pip* were required for full virulence of *X. campestris* pv. *campestris* to cabbage (Zhang *et al.*, 2007). Similarly, the abundance of OryR in *X. oryzae* pv. *oryzae* is elevated in the presence of a compound present in both healthy and infected rice and also regulates *pip*. Moreover, *cbsA* encoding 1,4- $\beta$ -cellobiosidase is positively regulated but the *oryR* promoter itself is negatively autoregulated by OryR, independent of the rice signal molecule. OryR also plays a role in *X. oryzae* pv.

*oryzae* virulence to rice since an *oryR* mutant incites less disease (Ferluga and Venturi, 2009).

Bacterial pustule caused by *Xanthomonas axonopodis* pv. *glycines* (*Xag*), is one of the most serious diseases of soybean in several parts of the world such as Thailand. The occurrence of bacterial pustule is strongly favored by high temperatures ( $\geq 30$  °C) and humidity (>60%RH) that typify such areas (Prathuangwong and Amnuaykit, 1987). Leaf lesions of bacterial pustule vary from minute specks to large, irregular, mottled brown areas that arise when smaller lesion coalesce in later stages of infection. Erumpent pustules, presumably favoring bacterial egress, typify lesions that are also surrounded by narrow yellow halos. Severe disease results in premature defoliation, resulting in decreased yield and seed quality (Weber *et al.*, 1966; Morgan 1963). Relatively little is known of the infection process in *X. axonopodis* pv. *glycines*. While *X. axonopodis* pv. *glycines* produces indole acetic acid and cytokinin, presumably contributing to pustule formation (Millar, 1955; Fett and Dunn, 1987), the role of a toxin (Hokawat and Rudolph, 1993) bacteriocins (Fett *et al.*, 1987), or a cellulase and protopectinase (Hokawat and Rudolph, 1993) in the process infection of soybean is less well established.

*X. axonopodis* pv. *glycines* has a very different lifestyle than the better studied vascular pathogens *X. campestris* pv. *campestris* and *X. oryzae* pv. *oryzae* since it infects through stomata and wounds on soybean leaves and causes hypertrophy of host cells. After invasion into the leaf through stomata large numbers of bacteria develop within the substomatal chambers and or intercellular spaces of the spongy mesophyll (Jones and Fett, 1985). This disease process is quite distinct from *X. campestris* pv. *campestris* and *X. oryzae* pv. *oryzae* which cause disease of cruciferous plants and rice, respectively, by invading the vascular system of these host plants. While *X. axonopodis* pv. *glycines* appears to harbor some regulators of virulence functions in common with *X. campestris* pv. *campestris* and *X. oryzae* pv. *oryzae*, such as a *luxR* homolog we term *xagR*, it seems likely that its distinct interactions with its host plant soybean will necessitate a different role for such regulators that is appropriate for this particular interaction.

In this study, we thus investigated the *X. axonopodis* pv. *glycines* strain 12-2 genome, plant up-regulatory genes and the role of *xagR* in the soybean pathosystem and elucidate its regulon to better understand the infection process. Evidence is provide for the contribution of host factors to the stabilization of XagR which in turn provides temporal control of a variety of traits involved in movement on and attachment to plants.



## OBJECTIVES

The objectives of this research were as follows:

1. To identify and characterize the *luxR* homolog gene in *Xanthomonas axonopodis* pv. *glycines*.
2. To study *luxR* homolog gene expression in *Xanthomonas axonopodis* pv. *glycines* that are dependent on soybean signal molecules.
3. To determine the expression pattern of the genes by *Xanthomonas axonopodis* pv. *glycines* during infection in soybean.

## LITERATURE REVIEW

### 1. Bacterial pustule disease

Bacterial diseases of soybean occur worldwide and limit production during years of high moisture. The most common bacterial incited diseases are bacterial blight and bacterial pustule. The prevalence and severity of these diseases vary considerably from year to year because of differences in weather patterns. Bacterial pustule, caused by *Xanthomonas axonopodis* pv. *glycines* is one of the most prevalent bacterial disease in most soybean growing areas of Thailand with warm temperatures and sufficient rainfall (Prathuangwong *et al.*, 1996). *X. axonopodis* pv. *glycines* is a motile Gram-negative rod within the range 0.5-0.9x1.4-2.3 micrometer, motile by a single polar flagellum. Colonies on beef infusion agar, nutrient agar and Wakimoto's agar are pale yellow, circular and smooth with an entire margin. The pathogen produces abundant, slimy, yellow growth on sugar-containing media (Hokawat, 1978). Optimum temperature for growth on potato dextrose agar is 25-30 °C maximum 35 °C and minimum 10 °C (Prathuangwong, 1983).

Bacterial pustule disease is important in many soybean-growing countries such as Argentina, Australia, Bolivia, Brazil, Cambodia, Canada, China, India, Japan, Malaysia, Nicaragua, Nigeria, Sudan, Taiwan, United states and Thailand (Sinclair and Dhingra, 1975). The disease can be damaging especially when the soybean is 30-40 days old (Sinclair and Dhingra, 1975). According to the investigation, the disease has been epidemic in the major soybean growing regions of Thailand and reduces yield significantly when the recommended local cultivars are grown under high humid and hot temperature in rainy season (Prathuangwong *et al.*, 2004). The disease causes premature defoliation that may decrease yield by reducing seed size and number (Laviolette *et al.*, 1976). In Thailand, Prathuangwong (1983) reported that yield losses due to natural dissemination in the susceptible soybean cultivar SJ4 were 20-35%. Early symptom of the disease is small, yellow to brown lesions with raised pustules in the center (Weber *et al.*, 1966). Spots of bacterial pustule vary from minute specks to large, irregular, mottled brown areas that arise when smaller lesion coalesce. In later

stages, dried, broken remnants of pustules seen on small brown necrotic are surrounded by narrow yellowing haloes. These symptoms are sometimes confused with those of soybean rust. This disease is sometimes more important in tropical areas than bacterial blight caused by *Pseudomonas syringae* pv. *glycinea* (Lelliott and Stead, 1987) and is one of the limiting factors in improvement of soybean production in Thailand (Hokawat, 1978).

There are no resistant varieties for soybean grown for marketing production. During 1976, the bacterial pustule outbreak was quite severe since the recommended varieties, namely SJ1, SJ2 and SJ4, were susceptible to this disease. The most widely used bactericides are copper-based, such as copper oxychloride and copper hydroxide to control phytopathogenic bacteria. Beside, copper is phytotoxic in various plants and should be used with caution (Prathuangwong *et al.*, 1996). There is general concern caused by rapid development of resistant strains of bacterial pathogens. There is a considerable decrease in chemical applications and the need for sustainable agriculture has never been greater. Recently, sustainable agriculture or organic farming systems with biological control have become more important. It is a strategy to decrease or replace chemical application. Research in Thailand is evaluating biological control agents primarily as new system of integrated disease management in several crops. New approaches are needed for management of important diseases such as bacterial pustule of soybean (Prathuangwong *et al.*, 2000).

## **2. Genome sequencing in Xanthomonads**

*Xanthomonas* is Gram-negative, rod-shaped phytopathogenic bacteria in the Gammaproteobacteria includes 420 species and more than hundreds of pathovars (Vauterin *et al.*, 2000). This genus is the causal agents of several economically important crops. The bacteria persist as epiphytes on the plant surface before they enter the plant via natural openings such as hydathodes, stomata or wounds. Inside the plant tissue, *Xanthomonas* spp. multiply either locally in the apoplast or colonize the vascular bundle especially xylem vessels and then spread systemically within the plant (Figure 1).

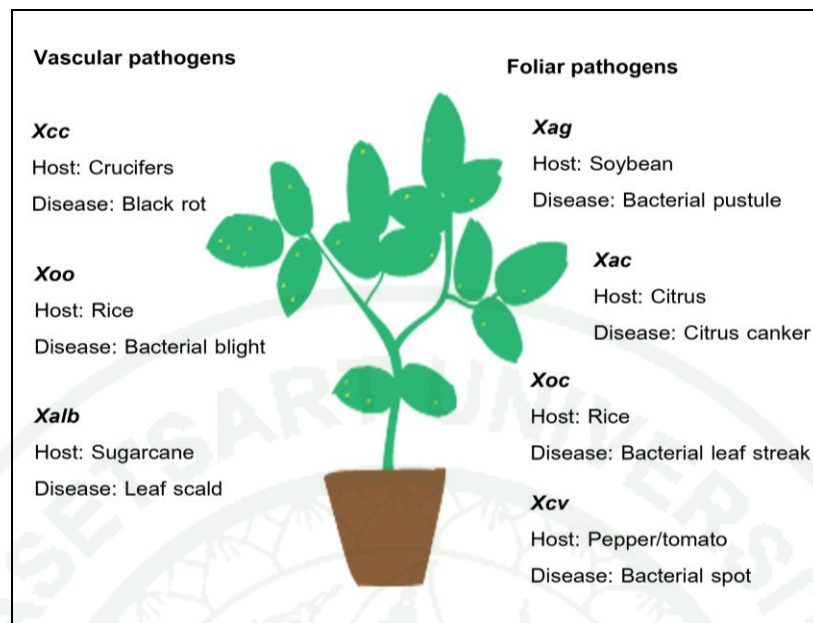


**Figure 1** The system of *Xanthomonas* spp. with published genome sequences, and the corresponding host plants on which they cause disease. *Xanthomonas campestris* pv. *campestris* (*Xcc*), *Xanthomonas oryzae* pv. *oryzae* (*Xoo*) and *Xanthomonas albilineans* (*Xalb*) spread in vascular system of the host plant, whereas *Xanthomonas axonopodis* pv. *glycines* (*Xag*), *Xanthomonas axonopodis* pv. *citri* (*Xac*), *Xanthomonas oryzae* pv. *oryzicola* (*Xoc*) and *Xanthomonas campestris* pv. *vesicatoria* (*Xcv*) either locally in the apoplast at the infection site.

The bacteria are hemibiotrophic pathogens that initially feed on living host tissue, but in later infection stages, cause the death of plant cells. *Xanthomonas* spp. are evolutionarily related to the opportunistic pathogen *Xanthomonas maltophilia*, (*Stenotrophomonas maltophilia*). *Stenotrophomonas maltophilia* is a human pathogen that associated with nosocomial infections and some strains are endophytic (Denton and Kerr, 1998). Members of the genus *Xanthomonas* were grouped into separate species on the basis of their host range, but according to the classical nomenclature, most species were later merged into the single species *Xanthomonas campestris* and subgrouped into different pathovars (Dye and Lelliott, 1974). The nomenclature of the currently approximately 19 species and 4140 pathovars is still under debate (Schaad *et al.*, 2000; Vauterin *et al.*, 2000; Rademaker *et al.*, 2005).

Complete genome sequences have been published for several members of the genus (Da Silva *et al.*, 2002; Lee *et al.*, 2005; Ochiai *et al.*, 2005; Qian *et al.*, 2005; Thieme *et al.*, 2005; Salzberg *et al.*, 2008; Vorholter *et al.*, 2008; Pieretti *et al.*, 2009; Moreira *et al.*, 2010) (Table 1). Thus, the genus is a compelling subject for comparative genomics, as such analyses should shed light on how this group of bacteria has adapted to exploit an extraordinary diversity of plant hosts and host tissues. Understanding pathogenic adaptations of *Xanthomonas* will foster the development of needed improvements in bacterial plant disease control and prevention.

**Table 1** *Xanthomonas* published genome sequences

<i>Xanthomonas</i> spp.	Strain	Reference
<i>X. axonopodis</i> pv. <i>citri</i> ( <i>Xac</i> )	306	(Da Silva <i>et al.</i> , 2002)
<i>X. campestris</i> pv. <i>campestris</i> ( <i>Xcc</i> )	8004	(Qian <i>et al.</i> , 2005)
	ATCC 33913	(Da Silva <i>et al.</i> , 2002)
	B100	(Vorholter <i>et al.</i> , 2008)
<i>X. campestris</i> pv. <i>vesicatoria</i> ( <i>Xcv</i> )	85-10	(Thieme <i>et al.</i> , 2005)
<i>X. oryzae</i> pv. <i>oryzae</i> ( <i>Xoo</i> )	KACC10331	(Lee <i>et al.</i> , 2005)
	MAFF311018	(Ochiai <i>et al.</i> , 2005)
	PXO99A	(Salzberg <i>et al.</i> , 2008)
<i>X. albilineans</i> ( <i>Xalb</i> )		(Pieretti <i>et al.</i> , 2009)
<i>X. fuscans</i> subsp. <i>aurantifolii</i>		(Moreira <i>et al.</i> , 2010)

### 3. Infection strategies of *Xanthomonas*

Important goal of research in molecular plant pathology is the identification of virulence factors that contribute to the host-pathogen interaction. To establish themselves successfully in host plants, bacteria should be able to attachment to the plant surface, invade the intercellular space of the host tissue, acquire nutrients and counteract plant defense responses. Bacterial protein secretion systems is necessary to

get successful infection of host plants. Bacteria secrete proteins into the extracellular environment or transport proteins and/or DNA directly into the host cell cytosol, a process referred to as translocation. Proteins that are translocated into the host cell are designated effector proteins.

### 3.1 Attachment to the plant surface

*Xanthomonas* spp. produce an extracellular polysaccharide (EPS) and xanthan, that leads to the mucoid appearance of the bacterial colonies. Xanthan is a polymer of repeating pentasaccharide units with consist of a cellulose and trisaccharide side chains (Jansson *et al.*, 1975; Becker *et al.*, 1998). The production of xanthan is directed by the *gum* gene cluster, which consists of 12 genes (*gumB* to *gumM*) and is highly conserved among *Xanthomonas* spp. (Katzen *et al.*, 1998; Vojnov *et al.*, 1998). Xanthan protects bacteria from environmental stresses such as dehydration and toxic compounds because of its highly hydrated and anionic consistency. In vascular pathogens, xanthan might block the water flow in xylem vessel led to cause wilting of host plants (Denny, 1995; Chan and Goodwin, 1999). Xanthan also suppresses basal plant defense responses such as callose deposition in the plant cell wall, presumably by chelation of divalent calcium ions that are present in the plant apoplast and are required for the activation of plant defense responses (Yun *et al.*, 2006; Aslam *et al.*, 2008).

Lipopolysaccharides (LPS) are major components of the bacterial outer membrane and protect the cell from environments. LPS in Gram-negative bacteria is a tripartite molecule consisting of membrane-anchored lipid A, a core oligosaccharide and polysaccharide side chains (O-antigen) (Raetz and Whitfield, 2002). Comparative sequence analysis revealed that LPS gene clusters of different *Xanthomonas* spp. are variable in number and identity of genes and were presumably subject to a strong diversifying selection (generation of multiple different alleles in different species, pathovars and even strains) (Lu *et al.*, 2008). Variations in the composition of LPS might allow the bacteria to evade recognition by the plant's immune system and

presumably also affect bacterial resistance to phage adsorption and/or infection (Ojanen *et al.*, 1993).

Adhesion of bacteria to biotic surfaces is key for the invasion of the host tissue. Bacterial attachment depends on specific adhesins that are anchored in the bacterial outer membrane and are classified into fimbrial and nonfimbrial adhesins. Fimbrial adhesins are filamentous proteinaceous structures such as type IV pili, which are structurally related to the predicted periplasmic pilus of type II secretion systems (Gerlach and Hensel, 2007). Nonfimbrial adhesins include trimeric autotransporters of type VI secretion systems (e.g. YadA from *Yersinia* spp.) and twopartner secretion substrates (e.g. filamentous hemagglutinin from *Bordetella pertussis* and YapH from *Yersinia* spp.) (Gerlach and Hensel, 2007).

Comparative genome sequence analysis revealed that plant pathogenic bacteria possess a number of adhesins that presumably mediate bacterial attachment to multiple host cell receptors and might contribute to different stages of the infection process (Das *et al.*, 2009). Adhesins from *Xanthomonas* spp. include XadA and XadB (both related to YadA from *Yersinia* spp.), homologs of the autotransporter adhesin, YapH from *Yersinia* spp., filamentous hemagglutinin-like proteins and proteins predicted to be involved in type IV pilus synthesis. Type IV pili were proposed to play a role in the attachment of *Xanthomonas campestris* pv. *hyacinthi* to the stomata of its host plant (van Doorn *et al.*, 1994). To date, adhesins from *X. oryzae* pv. *oryzae*, *X. axonopodis* pv. *citri* and *X. fuscans* ssp. *fuscans* were shown to be involved in bacterial virulence and attachment to leaves and/ or seeds (Ray *et al.*, 2002; Darsonval *et al.*, 2009; Das *et al.*, 2009; Gottig *et al.*, 2009). Mutational analyses of adhesin genes from *X. fuscans* ssp. *fuscans* revealed that adhesins contribute individually and in a complementary manner to different stages of the infection process (Darsonval *et al.*, 2009). In agreement with this is the finding that XadA and XadB from *X. oryzae* pv. *oryzae* are presumably required for bacterial attachment to the leaf surface, whereas the YapH homolog contributes to bacterial colonization of xylem vessels (Das *et al.*, 2009).

### 3.2 Establishment and multiplication of bacteria in the plant tissue

Pathogenicity of *Xanthomonas* and most other Gram-negative phytopathogenic bacteria depends on protein secretion systems and secreted virulence factors.

The type I secretion system is a heterotrimeric protein complex that consists of an ATP-binding cassette transporter in the inner membrane, a protein channel in the outer membrane and a membrane fusion protein that links the inner and the outer membrane components (Figure 2). Substrates of type I secretion system are secreted independent of the Sec system, presumably in a one-step process across both bacterial membranes, and include toxins, proteases and lipases (Gerlach and Hensel, 2007). The type I secretion system from *X. oryzae* pv. *oryzae* was shown to be required for the elicitation of a resistance response in rice plants that carry the disease resistance gene *Xa21* (Shen *et al.*, 2002; da Silva *et al.*, 2004).

The type II secretion system apparatus consists of 12-15 components, most of which are associated with the bacterial inner membrane (Sandkvist, 2001). A member of the secretin protein family forms a multimeric transmembrane channel in the outer membrane. It is assumed that secretion across the outer membrane depends on a predicted periplasmic pilus that is continuously assembled and disassembled and thus pushes type II secretion system substrates through the secretin channel (Johnson *et al.*, 2006). It secretes toxins and extracellular enzymes such as proteases, lipases and cell wall-degrading enzymes that might contribute to the host-pathogen interaction. Proteins secreted by the Xps- type II secretion system from *X. campestris* pv. *campestris*, *X. axonopodis* pv. *citri* and *X. oryzae* pv. *oryzae* include degradative enzymes such as cellulases, cellobiosidases, lipases, xylanases, endoglucanases, polygalacturonases and proteases (Dow *et al.*, 1987; Ray *et al.*, 2000; Schroter *et al.*, 2001; Furutani *et al.*, 2004; Rajeshwari *et al.*, 2005; Sun *et al.*, 2005; Jha *et al.*, 2007; Yamazaki *et al.*, 2008). A direct influence on the plant-pathogen interaction was shown for an endoglucanase and polygalacturonases from *X. campestris* pv. *campestris* as well as for a lipase/esterase, a cellulase, an endoglucanase and a

xylanase from *X. oryzae* pv. *oryzae* (Gough *et al.*, 1988; Rajeshwari *et al.*, 2005; Hu *et al.*, 2007; Jha *et al.*, 2007; Wang *et al.*, 2008).

Type III secretion system is the one of the key pathogenicity factors of most Gram-negative plant pathogenic bacteria (Ghosh, 2004). The type III secretion system is encoded by the chromosomal *hrp* (HR and pathogenicity) gene cluster, which contains more than 20 genes that are organized in several transcriptional units (Buttner and Bonas, 2002). *hrp* genes were first discovered by the analysis of transposon insertion mutants in *Pseudomonas syringae* pv. *phaseolicola* and were shown to be essential for bacterial pathogenicity and HR induction in host and nonhost plants (Lindgren *et al.*, 1986).

The type III secretion system from each *Xanthomonas* strains translocates the different effector proteins into the plant cell (Figure 2). Based on experimental and bioinformatic analyses, 24 effectors or effector candidates have been identified in *X. axonopodis* pv. *citri* strain 306, 30 in *X. campestris* pv. *vesicatoria* strain 85-10, 23 in *X. campestris* pv. *campestris* strains ATCC 33913 and 8004, respectively, 32 in *X. oryzae* pv. *oryzae* strain KACC10331 and 37 in *X. oryzae* pv. *oryzae* strains MAFF 311018 and PXO99A, respectively (<http://www.xanthomonas.org>). Inactivation of individual effector genes often does not significantly affect bacterial virulence, presumably due to functional redundancies among effector proteins. Comparative sequence analysis of type III effectors from *Xanthomonas* spp. revealed that several effectors belong to conserved protein families, members of which are present in different plant and animal pathogens. Furthermore, some effectors are homologous to proteins with known enzymatic activities such as cysteine proteases, phosphatases or transglutaminases. Despite the fact that a virulence function was shown only for a few effector proteins from plant pathogenic bacteria, accumulating experimental evidence suggests that individual effector proteins counteract the plant innate immune response that is triggered upon recognition of conserved pathogen-associated molecular patterns (PAMPs) such as flagellin, cell wall degradation products or LPS (Espinosa and Alfano, 2004; Keshavarzi *et al.*, 2004; Grant *et al.*, 2006; Jones and Dangl, 2006; Jha *et al.*, 2007; Block *et al.*, 2008). Suppression of PAMP-triggered immunity by

type III effectors might therefore be a major requirement for the successful establishment and multiplication of bacteria in the plant tissue.

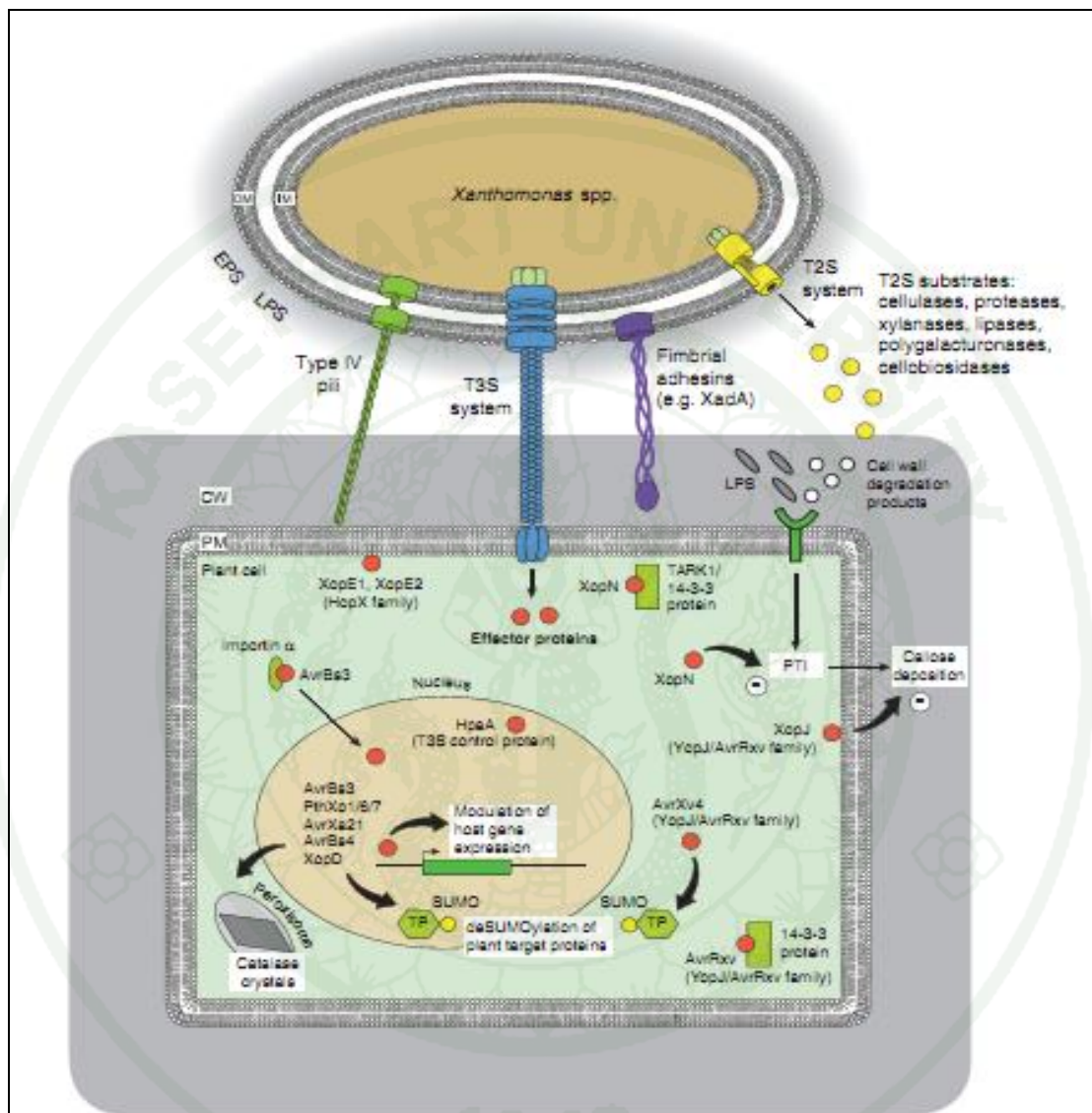


**Figure 2** Model of known virulence factors from Xanthomonads.

**Source:** Buttner and Bonas (2009)

For *X. axonopodis* pv. *glycines*, the successful infection of *X. axonopodis* pv. *glycines* including attachment of the pathogen by its extracellular polysaccharides (EPS) to the host cell wall, the ability of EPS to maintain a lesion in the intercellular spaces, the presence of appropriate bacterial auxin inducing hypertrophy, and the ability to overcome host defense reactions. Several works also reported that *X. axonopodis* pv. *glycines* produced indole acetic acid and cytokinin, toxin, bacteriocins, and exoenzymes including cellulase, protease, endo- $\beta$ -1,4-mannanase, and pectate lyases (Hokawat and Rudolph, 1993; Kaewnum *et al.*, 2006; Kasem *et al.*, 2007; Thowthampitak *et al.*, 2008) for a process of soybean-*X. axonopodis* pv. *glycines* interaction.

Transposon mutagenesis has identified many genes contributing to pathogenicity and virulence in *X. axonopodis* pv. *glycines*, including the presence of a type III secretion system (Kim *et al.*, 2003), secreted virulence factors such as pectate lyases (*xagP*) (Kaewnum *et al.*, 2006), phosphoenol pyruvate synthase (*ppsA*) gene (Kasem *et al.*, 2007) quorum sensing (Thowthampitak *et al.*, 2008) and an avirulence gene, *avrXg1*, that confers resistance in a gene for gene manner (Athinuwat *et al.*, 2009). The function of flagella; and pili associated genes, *flgC* and *flgK*, *fliC*, *fliD*; and *pilD* in the model motility, biofilm formation, and pathogenicity of *X. axonopodis* pv. *glycines* were demonstrated to play a role of colonization and virulence, and mediate a twitching for biofilm formation respectively (Athinuwat, 2009).

#### 4. Quorum sensing

The quorum-sensing bacteria produce, detect and respond to small signal molecules known as autoinducers or quorum-sensing signals ('quormones', a term proposed by Don Clewell at the American Society for Microbiology Conference on Cell-Cell Communication, July 2001, UT, USA). Quorum sensing (QS) refers to a bacterial cell-to-cell communication process. Rapid progress over the last few years has established that *N*-acylhomoserine lactones, known as autoinducers (AIs), are widely conserved signal molecules present in quorum-sensing systems of many Gram-negative bacteria. AIs were originally found in marine bacteria *Vibrio* species

in the regulation of bioluminescence (Eberhard *et al.*, 1981; Cao and Meighen, 1989). In recent years, several types of bacterial cell-cell communication signals have been identified in the last two decades, such as acylhomoserine lactone (AHL) (Eberhard *et al.*, 1981; Pearson *et al.*, 1994); cyclic thiolactone (AIP) (Ji *et al.*, 1995), hydroxyl-palmitic acid methyl ester (PAME) (Flavier *et al.*, 1997), furanosylborate (AI-2) (Chen *et al.*, 2002) and methyl dodecenoic acid (DSF) (Wang *et al.*, 2004). In this process, a bacterium synthesizes a signal molecule that is then released into the environment. Bacterial populations react to the accumulation of signal molecules by undergoing changes in their functions and characteristics if the signal molecule's concentration reaches a threshold level. In this manner, quorum sensing can coordinate behavior such as symbiosis, virulence, production of antibiotics, and formation of biofilm in bacteria. Among them, acyl homoserine lactones (AHLs) are one of the best characterized quormones, and they are found in many Gram-negative bacterial pathogens. More than 50 bacterial species are known to produce AHL quormones. AHL functions as a ligand to a LuxR-type transcription factor. In general, at the lower cell density stage, each cell in the bacterial population produces a basal level of AHL via an AHL synthase. At this stage, the function of LuxR proteins might or might not be required; a mutant lacking a LuxR type protein can produce a basal level of AHL molecules (Marketon *et al.*, 2002). At high population density, the concentration of AHL exceeds a threshold level and the accumulated AHL interacts with the LuxR-type transcription factor to trigger the expression of target genes.

Other bacterial groups use different types of compounds to regulate population density dependent behaviors. These include the furanosyl borate diester AI-2 signal of *Vibrio harveyi* (Chen *et al.*, 2002),  $\gamma$  butyrolactone in *Streptomyces* (Yamada and Nihira, 1998), oligopeptides in various Gram-positive species (Dunny and Winans, 1999; Kleerebezem and Quadri, 2001), cyclic dipeptides in several Gram-negative species (Holden *et al.*, 1999), and bradyoxetin in *Bradyrhizobium japonicum* (Loh *et al.*, 2002).

The plant pathogenic bacteria *Xanthomonas* spp. and *Xylella fastidiosa* use unique fatty acids as QS signals to regulate production of pathogenicity factors. The

*Xanthomonas* signalling system uses a novel in that diffusible signal factor (DSF). DSF is a fatty acid signal molecule involved in regulation of virulence in *X. campestris* pv. *campestris*, *X. oryzae* pv. *oryzae*, *X. axonopodis* pv. *citri* and *X. axonopodis* pv. *glycines* known to have the Rpf system for production and detection of DSF (Tang *et al.*, 1991; Barber *et al.*, 1997; Chatterjee and Sonti, 2002; Thowthampitak *et al.*, 2008 ). DSF from *X. campestris* pv. *campestris* has been characterized as *cis*-11-methyl-2-dodecenoic acid (Wang *et al.*, 2004). The DSF system also differs from a number of *N*-AHL systems in that the factor is present throughout growth and does not accumulate in later phases, the time at which extracellular enzyme synthesis occurs. DSF does not stimulate expression of *rpfF* and *rpfB* and thus does not behave in an auto-inductive fashion, as do some *N*-AHL systems (Tang *et al.*, 1991).

In *X. campestris* pv. *campestris*, DSF is required for the pathogenesis of this bacterium to plants. Nine *rpf* genes (*rpfA-I*) are linked within a 22.1-kb region, and transposon-induced mutations within this region abolish pathogenicity, exoenzyme production, and EPS synthesis (Tang *et al.*, 1991; Barber *et al.*, 1997). Several *rpf* genes are involved in the coordinate positive regulation of the production of virulence factors mediated by the small diffusible molecule DSF (for diffusible signal factor). RpfF directs the synthesis of DSF, and a two-component sensory transduction system comprising RpfC and RpfG has been implicated in the perception of the DSF signal and signal transduction. The *rpf* genes act to positively regulate the synthesis of extracellular enzymes, EPS, and pathogenicity (Tang *et al.*, 1991; Barber *et al.*, 1997; Dow *et al.*, 2000; Slater *et al.*, 2000).

Interestingly, *X. axonopodis* pv. *glycines* strain 12-2 from Thailand produced an DSF related to a well-characterized quorum sensing molecule produced by other *Xanthomonas* spp. Mutations in *rpfF* mutants of *X. axonopodis* pv. *glycines* strain 12-2 were defective in the production of DSF and reduce virulence on soybean plants because pathogenicity traits such as extracellular enzymes protease, cellulase and pectate lyase are no longer expressed in *rpfF* mutants (Thowthampitak *et al.*, 2008). Similarly, *rpfF* mutation in *X. fastidiosa*, which causes Pierce's disease of grapevine

and other important plant diseases, are also unable to produce the signal activity. In this pathogen a diffusible signal molecule is required for biofilm formation in the vector and for vector transmission to plants. In addition, *rpfF* mutants are more virulent than the wildtype when mechanically inoculated into plants. This signal therefore directs interaction of *X. fastidiosa* with both its insect vector and plant hosts (Newman *et al.*, 2004).

## 5. The *luxR* homolog genes

In Gram-negative bacteria, a typical QS system usually involve the production and response to an AHL. The AHL-dependent QS system is commonly mediated by two proteins belonging to the LuxI-LuxR families (Fuqua and Greenberg, 2002). *LuxI* is involved in the production of AHL autoinducers. On the other hand, LuxR binds to the AHL autoinducer, forming an LuxR-AI complex, which binds to the promoter of the enzyme responsible for fluorescence, and activates transcription of the gene at high bacterial concentrations. AHL autoinducers have increasing concentrations with increasing cell density and they can freely permeate bacterial cell membranes (Kaplan and Greenberg, 1985).

The amino acid terminus of LuxR homologs contain the AHL binding region, while the carboxyl terminus has the helix-turn-helix domain, which can multipolarize and bind to the promoter. The LuxR homolog binds to a 20 bp *lux* box, located 40 bp upstream of the transcription start, and activates transcription of the target gene (Slock *et al.*, 1990; Choi and Greenberg, 1991; Poellinger *et al.*, 1995; Stevens and Greenberg, 1997). LuxR-type proteins facilitate responses to acyl-HSLs through a series of recognizable steps including specific binding of cognate acyl-HSLs, conformational changes and alterations in multimerization of the protein following binding of the signal, binding or release of specific regulatory sequences upstream of target genes, and often activation of transcription.

It is now increasingly evident that naturally occurring QS-based cross-talk is more complicated than originally thought (Bassler and Losick, 2006). QS-mediated

communications between different bacterial species have been found. A furanosyl borate diester, called autoinducer 2 (AI-2) which is released by many groups of bacteria, may serve as a signal for interspecies communication (Xavier and Bassler, 2003). In another case, *Salmonella enterica* is unable to produce AHL signals, while its LuxR type protein SdiA can detect and respond to AHLs generated by other microbial species (Smith and Ahmer, 2003). Moreover, communications between bacteria and their eukaryotic hosts through signal molecules exist. For example, in *Agrobacterium tumefaciens*, the initiation of conjugation and the transfer of the Ti plasmid to a Ti-plasmidless recipient are regulated by the TraR/AHL complex, while the transcription of *traR* is relied on a derepression process via the action of opines derived from transformed plant tumour cells (Piper *et al.*, 1999). In addition, some higher plants have been demonstrated to secrete AHL activity-mimic compounds to interfere with the AHL-regulated bacterial behaviours (Teplitski *et al.*, 2000; Gao *et al.*, 2003). It is expected that more interkingdom communications will be discovered and new insights into bacterium-host interactions will be gained through such studies.

The plant-pathogenic *X. oryzae* pv. *oryzae* and *X.campestris* pv. *campestris* possess a LuxR homolog, designated OryR and XccR, which is required for full virulence to rice and cabbage, respectively. Both OryR and XccR do not bind or respond to AHLs and in their AHL-binding domain they lack two of the several conserved residues involved in AHL binding (Ferluga *et al.*, 2007; Zhang *et al.*, 2007). XccR regulates in planta the neighbouring proline iminopeptidase (*pip*) virulence gene. Orthologues of OryR and XccR are present in the genomes of several other plant-associated bacteria which are both beneficial and pathogenic, for example *Pseudomonas fluorescens* and *P. syringae* (Zhang *et al.*, 2007). Since some strains of these species do produce AHLs, it cannot be excluded that these solos can also respond to AHLs. It is postulated however that probably a subclass of LuxR solos are employed in interkingdom signaling between bacteria and plant; this is not so surprising, as bacteria have co-evolved with plants for many years. Plants have been reported to produce compounds that are able to act as agonists or antagonists to bacterial AHL QS systems and these have been called AHL mimics (Bauer and Mathesius, 2004). AHL mimics from several plants, including rice, are able to

stimulate gene expression via LuxR-family AHL sensors/regulators. To date the structures of these plant compounds are unknown and it cannot be excluded that similar molecules are involved in interkingdom signalling with the XccR/OryR subgroup of LuxR solos.

## 6. Expression of genes encoding LuxR-type proteins

Control of the expression or stability of the LuxR-type protein is a common mechanism for integrating quorum sensing into other aspects of cellular physiology. For example, the expression of the *V. fischeri luxR* gene is under the influence of the cyclic adenosine monophosphate receptor protein (CRP) (Dunlap and Greenberg, 1985). Another interesting example is the strict opine-dependence of *traR* gene expression in *A. tumefaciens*. Opines are unusual compounds produced by plants infected with *A. tumefaciens*, thereby restricting the function of this quorum sensor to the plant-associated environment (Fuqua and Winans, 1996; Piper *et al.*, 1999).

Expression of bacterial genes is often regulated by complex mechanisms, some of which involve host cues. Analysis of the *X. campestris* pv. *campestris* genome sequence revealed the presence of an *xccR/pip* locus. The upstream gene *xccR* is a *luxR* homolog, while *pip* codes for a proline iminopeptidase. A *lux* box-like element, named a *luxXc* box, is located in the *pip* promoter region. Disruption of either *xccR* or *pip* resulted in significantly attenuated virulence of *X. campestris* pv. *campestris* (Zhang *et al.*, 2007).

*X. oryzae* pv. *oryzae*, the causal agent of bacterial leaf blight in rice, contains a regulator that is encoded in the genome, designated OryR, which belongs to the N-acyl homoserine lactone (AHL)-dependent quorum-sensing LuxR subfamily of proteins. Disrupting *oryR* in three *X. oryzae* pv. *oryzae* strains resulted in a significant reduction of rice virulence. The wildtype *X. oryzae* pv. *oryzae* strains do not seem to produce AHLs and analysis of the *X. oryzae* pv. *oryzae* sequenced genomes did not reveal the presence of a LuxI-family AHL synthase. The OryR protein was shown to be induced by macerated rice and affected the production of two secreted proteins: a

cell-wall-degrading cellobiosidase and a 20-kDa protein of unknown function. By expressing and purifying OryR it was then observed that it was solubilized when grown in the presence of rice extract indicating that there could be a molecule(s) in rice which binds OryR (Ferluga and *et al.*, 2007). Three OryR target promoters which are regulated differently: (i) the neighboring proline iminopeptidase (*pip*) virulence gene, which is positively regulated by OryR in the presence of the rice signal molecule; (ii) the *oryR* promoter, which is negatively autoregulated independent of the rice signal molecule; and (iii) the 1, 4-beta-cellobiosidase *cbsA* gene, which is positively regulated by OryR independent of the rice signal molecule. The rice signal molecule for OryR is not related to AHLs, and is not able to activate the broad-range AHL biosensor *A. tumefaciens* NT1 (pZLQR). Furthermore, OryR does not regulate production of the quorum-sensing diffusible signal factor present in the genus *Xanthomonas*. Therefore, OryR has unique features and is an important regulator involved in interkingdom communication between the host and the pathogen for *X. oryzae* pv. *oryzae*.

## 7. Plant signals involved in plant-bacterial interactions

Over the course of a plant-microbe interaction, bacteria continue to monitor changes in the physiology of their host. These changes are often due to specific activities of the colonizing microbes, which in response continuously make adjustments to their own physiology. Thus, detection and response to various host signals in the plant-microbe interaction is a continuous process. In many cases, in addition to specific regulatory proteins, global regulators play a role in these interactions.

Foliar plant pathogens such as *Xanthomonas* spp. undergo different life stages and often colonize leaf surfaces as epiphytes before they invade the intercellular space. Like other pathogens, *Xanthomonas* spp. have evolved regulatory systems to adapt the expression of virulence factors to different extracellular stimuli such as population density, availability of nutrients, oxygen levels and the presence of plant-derived molecules. The interactions between plants and pathogens are monitored by receptor proteins in the host and effectors proteins delivered by the pathogens. The

ability of bacteria to respond to plant signals often depends on various additional regulatory elements, including QS systems and global environmental and physiological regulators.

*A. tumefaciens*-plant pathosystem and rhizobium-legume symbiosis are among the best-characterized plant-microbe systems available. Rhizobia detect flavonoid molecules released by plant roots via a transcriptional activator NodD. NodD in turn induces the bacterial *nod* genes responsible for the early formation of nodules (Geurts and Franssen, 1996). Several virulence (*vir*) genes in *A. tumefaciens* are transcriptionally activated by specific phenolic signal molecules such as acetosyringone. Phenolic-induced expression of *vir* genes is greatly enhanced by specific monosaccharides including arabinose, galactose, galacturonic acid, glucose, glucuronic acid, mannose, fucose, cellobiose, and xylose (Ankenbauer and Nester, 1990). Most of these sugars are monomers of plant cell wall polysaccharides or are otherwise involved in plant metabolism. Their effect on *vir* induction is especially pronounced at low concentrations of the inducing phenolic.

In *P. syringae* pv. *syringae*, syringomycin is one of the major virulence factors. Specific plant signal molecules are known to induce syringomycin production and expression of *syrBI*, a syringomycin synthetase gene. In a survey of 34 phenolic compounds, only specific phenolic glycosides exhibited *syrBI*-inducing activity. The phenolic glycosides that exhibited *syrBI*-inducing activity included arbutin, salicin, and esculin, which are abundant in the tissues of many plant species. Arbutin was shown to be an efficient signal molecule that induced the high expression of the *syrBI* synthetase gene (Mo and Gross, 1991).

The plant pathogen *Ralstonia solanacearum* senses the plant cell wall material by the membrane protein PrhA. Functional PrhA could induce expression of the *hrp* genes (Aldon *et al.*, 2000), contributing to a successful infection by the bacterium.

Various host factors capable of inducing expression of the bacterial genes including small diffusible plant signals, non-diffusible signals that present in the plant

cell wall and plant-derived metabolites such as the plant cell wall breakdown products arising from a direct bacterial infection (Newton and Fray, 2004).

Interestingly, in some bacteria, orphan LuxR regulators are responsive for exogenous signal molecules. For example, the orphan LuxR homologs XccR of *X. campestris* pv. *campestris* and OryR of *X. oryzae* pv. *oryzae* respond to host plant exudates in order to mediate virulence (Ferluga *et al.*, 2007). The interplay between host plant exudates and/or proteins and the bacterial effector proteins is complex that each effector appears to have a different role. They are probably most bind or modify different host proteins. But at least one has a passive role targeting the pathogen. These plant proteins govern interaction with symbiotic and pathogenic microbe and also disease process in development. Their recognition is highly specific and activates plant defense to effectively pathogen growth. This type of gene-for-gene recognition is typically overcome by structural alteration of the effector through mutation, while the presence of indispensable effectors may be masked by employing yet another effector to interfere with resistance (*R*) gene function (Jones and Dangl, 2006).

## MATERIALS AND METHODS

### 1. Bacterial strains, plasmids and recombinant techniques.

Bacterial strains and plasmids used in this study are described in Table 2. *X. axonopodis* pv. *glycines* strains were cultured at 28°C in Luria Bertani agar (LA) or in the minimal medium M9 (Sambrook *et al.*, 1989). Cells were also cultured on media containing soybean extracts including: 1) Fresh soybean medium consisting of 10 g of soybean leaves powdered in liquid nitrogen and added to 100 ml of sterilized distilled water. 2) Autoclaved soybean medium consisting of fresh soybean medium that was autoclaved. Bacterial growth was monitored by measuring the absorbance of cell suspensions at 600 nm. Antibiotics were added to media at the following concentrations: kanamycin, 50 µg/ml; chephalexin, 50 µg/ml and gentamycin, 40 µg/ml. All DNA manipulations, including DNA isolation, plasmid extraction, restriction digestion, ligation and gel electrophoresis were performed as described previously (Sambrook *et al.*, 1989).

**Table 2** Bacterial strains and plasmids

Bacterial strain or plasmid	Relevant characteristic <sup>a</sup>	Reference or source
<i>Xanthomonas axonopodis</i> pv. <i>glycines</i> 12-2	Wildtype, soybean pathogen	Thowthampitak <i>et al.</i> , 2008
<i>xagR</i> mutant	Km <sup>r</sup> , <i>xagR</i> ::Kan, <i>X. axonopodis</i> pv. <i>glycines</i> 12-2 derivative	This study
<i>pip</i> mutant	Km <sup>r</sup> , <i>pip</i> ::Kan, <i>X. axonopodis</i> pv. <i>glycines</i> 12-2 derivative	This study
<i>xagR/pip</i> double mutant	Km <sup>r</sup> , <i>xagR</i> and <i>pip</i> ::Kan, <i>X. axonopodis</i> pv. <i>glycines</i> 12-2 derivative	This study
XagID3706	Km <sup>r</sup> , homolog to XAC3964 from <i>Xac</i> ::Kan, 12-2 derivative	This study

Table 2 (Continued)

Bacterial strain or plasmid	Relevant characteristic <sup>a</sup>	Reference or source
XagID3707	Km <sup>r</sup> , homolog to XAC3965 from <i>Xac</i> -::Kan, 12-2 derivative	This study
XagID2132	Km <sup>r</sup> , <i>yapH</i> ::Kan, 12-2 derivative	This study
XagID0859	Km <sup>r</sup> , homolog to XAC0824 from <i>Xac</i> ::Kan, 12-2 derivative	This study
XagR+	<i>xagR</i> mutant complemented with pBBR:: <i>xagR</i>	This study
XagROX	Wildtype, containing pTrp:: <i>xagR</i>	This study
XagKI- <i>xagR</i>	Wildtype, containing <i>xagR</i> promoter cloned with <i>SacI</i> in pPROBE-KI	This study
XagKI- <i>pip</i>	Wildtype, containing <i>pip</i> promoter cloned with <i>SacI</i> in pPROBE-KI	This study
XagRKI- <i>xagR</i>	<i>xagR</i> mutant, containing <i>xagR</i> promoter cloned with <i>SacI</i> in pPROBE-KI	This study
XagRKI- <i>pip</i>	<i>xagR</i> mutant, containing <i>pip</i> promoter cloned with <i>SacI</i> in pPROBE-KI	This study
<b>Plasmids</b>		
pTok2	ColE1 replicon, suicide plasmid, Tc <sup>r</sup>	Kitten and Willis, 1996
pPROBE-KI	Broad-host-range plasmid with a transcriptional fusion cassette containing a promoterless <i>inaZ</i> reporter gene; Km <sup>r</sup>	Miller <i>et al.</i> , 2000
pJR4	<i>sacB</i> <sup>+</sup> and <i>flp</i> <sup>+</sup> (Cro promoter) from pFLP2 cloned into pUFR47. IncW, Mob <sup>+</sup> , <i>lacZ</i> $\alpha$ <sup>+</sup> , Par <sup>+</sup> , <i>sacB</i> <sup>+</sup> , <i>flp</i> <sup>+</sup> (Cro promoter), Gm <sup>r</sup> , Ap <sup>r</sup>	Castañeda <i>et al.</i> , 2005
pKD13	FRT-Km <sup>r</sup> -FRT, oriR6K, Ap <sup>r</sup> , Km <sup>r</sup>	Datsenko and Wanner, 2000
pBBR1MCS-5	Broad host range cloning vector, <i>lacZ</i> , Gm <sup>r</sup>	Kovach <i>et al.</i> , 1995
pTok2:: $\Delta$ <i>xagR</i>	$\Delta$ <i>xagR</i> ::Kan from overlapping PCR cloned into pTok2, Tc <sup>r</sup> , Km <sup>r</sup>	This study

**Table 2** (Continued)

<b>Bacterial strain or plasmid</b>	<b>Relevant characteristic <sup>a</sup></b>	<b>Reference or source</b>
pTok2:: $\Delta$ <i>pip</i>	$\Delta$ <i>pip</i> ::Kan from overlapping PCR cloned into pTok2, Tc <sup>r</sup> , Km <sup>r</sup>	This study
pTok2:: $\Delta$ <i>xagR</i> and <i>pip</i>	$\Delta$ <i>xagR</i> and <i>pip</i> ::Kan from overlapping PCR cloned into pTok2, Tc <sup>r</sup> , Km <sup>r</sup>	This study
pTok2:: $\Delta$ homolog to XAC3964	$\Delta$ homolog to XAC3964::Kan from overlapping PCR cloned into pTok2, Tc <sup>r</sup> , Km <sup>r</sup>	This study
pTok2:: $\Delta$ homolog to XAC3965	$\Delta$ homolog to XAC3965::Kan from overlapping PCR cloned into pTok2, Tc <sup>r</sup> , Km <sup>r</sup>	This study
pTok2:: $\Delta$ <i>yapH</i>	$\Delta$ <i>yapH</i> ::Kan from overlapping PCR cloned into pTok2, Tc <sup>r</sup> , Km <sup>r</sup>	This study
pTok2:: $\Delta$ homolog to XAC0824	$\Delta$ homolog to XAC0824::Kan from overlapping PCR cloned into pTok2, Tc <sup>r</sup> , Km <sup>r</sup>	This study
pXagR-KI	<i>xagR</i> promoter cloned with <i>SacI</i> in pPROBE-KI	This study
pPip-KI	<i>pip</i> promoter cloned with <i>SacI</i> in pPROBE-KI	This study
pTrp:: <i>xagR</i>	<i>xagR</i> gene fusion with <i>trp</i> promoter cloned into pBBR1MCS-5, <i>lacZ</i> , Gm <sup>r</sup>	This study
pBBR:: <i>xagR</i>	<i>xagR</i> gene with native promoter cloned into pBBR1MCS-5, <i>lacZ</i> , Gm <sup>r</sup>	This study

## 2. Genomic sequencing and annotation

### 2.1 Genomic DNA extraction and library preparation

Genomic DNA was prepared from a culture of *X. axonopodis* pv. *glycines* strain 12-2 grown in NYGB (Nitrogen Yeast Glycerol Broth) medium using a QIAGEN genomic DNA purification kit (QIAGEN Inc., Valencia). Genomic DNA library were prepared following protocol provided for illumina sequencing system. Briefly, 100  $\mu$ g of genomic DNA were fragmented using ultrasonic bath for 5 min. Fragmented DNA were purified following the instructions in the QIAquick PCR

Purification Kit to purify on one QIAquick column and converts the overhangs resulting from fragmentation into blunt ends, using T4 DNA polymerase and *E. coli* DNA polymerase I Klenow fragment. An 'A' base was added to the 3' end of the blunt phosphorylated DNA fragments, using the polymerase activity of Klenow fragment (3' to 5' exo minus). This prepares the DNA fragments for ligation to the adapters, which have a single 'T' base overhang at their 3' end. Adapters were ligated to the ends of the DNA fragments, prepared them to hybridized to a flow cell. The products of the ligation reaction on a gel were purified to remove all unligated adapters, remove any adapters that may have ligated to one another, and select a size-range of templates to go on the cluster generation platform. Enrich the Adapter-Modified DNA Fragments by PCR. PCR reaction mix were prepared following: DNA (1  $\mu$ l), Phusion DNA polymerase (Finnzymes Oy) (25  $\mu$ l), PCR primer 1.1 (1  $\mu$ l), PCR primer 2.1 (1  $\mu$ l), Water (22  $\mu$ l) in total volume 50  $\mu$ l. Amplify using the following PCR protocol: A) 30 seconds at 98°C B) 18 cycles of 10 seconds at 98°C 30 seconds at 65°C and 30 seconds at 72°C, C) 5 minutes at 72°C, and D) Hold at 4°C. Determine the concentration of the library by load 10% of the volume of the library on a gel and check that the size range is about 200 bp (Figure3).

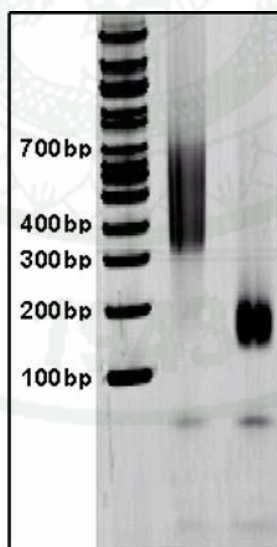


**Figure 3** Sequencing gel. The left lane shows a marker ladder. The smear on the middle lane shows a long insert library and the smear on the right shows a short insert library.

## 2.2 Whole genome sequencing

Whole genome sequencing was performed on a 454 GS-FLX Titanium sequencer in accordance with the manufacturer's protocol at Kansas State University, and Illumina Solexa GA sequencing at the Functional Genomics Laboratory at the University of California, Berkeley. Paired-end reads (ca. 400 bp and 100 bp, respectively) were generated in both cases. All reads were mapped to the genome of *X. axonopodis* pv. *citri* strain 360 as a reference to obtain a *X. axonopodis* pv. *glycines* consensus sequence. All short reads that were not mapped to the reference genome were assembled *de novo* using CLCbio Genomics Workbench version 4.0, with length fraction and similarity set at 0.8 and all other parameters using default values. The *X. axonopodis* pv. *glycines* consensus sequence and contigs were submitted to the RAST server (Rapid Annotations using Subsystems Technology) (Aziz *et al.*, 2008) to identify protein-encoding, rRNA and tRNA genes and to assign functions to these genes.

## 3. Knockout of genes regulated by XagR.

Individual targeted disruptions of *xagR*, *pip*, *yapH*, and the genes homologous to *X. axonopodis* pv. *citri* strain 360 loci 3964 and 3965 were accomplished using overlap extension mutagenesis. The upstream and downstream regions flanking target genes in *X. axonopodis* pv. *glycines* 12-2 were amplified using primers unique to these regions, with one having an extension complementary to the kanamycin resistance cassette from pKD13 to generate two amplicons with ends overlapping those of the resistance cassette (Datsenko and Wanner, 2000) (Table 3). Overlap extension PCR was used to link the two PCR amplicons and the resistance cassette; this larger fragment was then cloned into the destination vector pTok2 using the quick ligation protocol (New England Biolabs Inc.) and introduced into the mobilizing strain *E. coli* S17-1 by transformation, and then transferred to *X. axonopodis* pv. *glycines* via conjugation, selecting for transconjugants on LA containing kanamycin and cephalixin. Because pTok2 is non-replicative in *Xanthomonas* spp., kanamycin-resistant but tetracycline-sensitive colonies of *X. axonopodis* pv. *glycines* were expected to have undergone a double-crossover event between the DNA cloned in

pTok2 and the corresponding sequence in the *X. axonopodis* pv. *glycines* chromosome, resulting in deletion of the target gene. Gene disruption was confirmed using PCR with primers specific to the sequences flanking each gene.

#### 4. Complementation of *xagR* mutant.

To complement the *xagR* mutant, the 1.4-kb sequence of *xagR* containing the native promoter was amplified using primers XagRcom-F (*SalI*) and XagRcom-R (*HindIII*) (Table 3) and the amplicon was then digested with both *SalI* and *HindIII* and ligated into the multiple cloning site of vector pBBR1MCS-5 to yield pBBR::*xagR*, which was then introduced into *xagR* mutant by electroporation.

#### 5. Generation of XagR over-expressing strain.

The XagR-overexpressing strain, XagROX was constructed by placing the coding region of *xagR* downstream of the strong *E. coli trp* operon promoter in pBBR1MCS-5 and introducing it into *X. axonopodis* pv. *glycines* strain 12-2. *xagR* was amplified using *X. axonopodis* pv. *glycines* genomic DNA as the template with primers Ptp-F-1, Ptp-F-2, Ptp-F-blunt and XagR-R-blunt (Table 3) and cloned into the *SmaI* site of pBBR1MCS-5 to yield pTrp::*xagR* which was then introduced into *X. axonopodis* pv. *glycines* strain 12-2 by electroporation.

**Table 3** Polymerase chain reaction primers

Primer	Sequence <sup>a</sup>	Description
Ptp-F-1	5' TAGTAACTAGTACGAAAGTTCACA TGAGAAGGAGGACAGCTTCTAGAAT GTTTCGACATTCTGGCCAGCC 3'	For placing <i>trp</i> operon promoter upstream of start codon of <i>xagR</i> gene for construct <i>xagR</i> -overexpressing strain

**Table 3** (Continued)

<b>Primer</b>	<b>Sequence<sup>1</sup></b>	<b>Description</b>
Ptp-F-2	5' GGCAAATATACTGAAATAGGTGTTGA CATTATCCATCGAACTAGTTAACTAGT ACGAAAGTTC 3'	For second round of placing <i>trp</i> operon promoter upstream of <i>xagR</i> this primer overlapping with Ptp-F-1
Ptp-F-blunt	5' TAAAGTTATGTCATGTACATCATAA CGGTCCGGCAAATATACTGAAATA GGTGTGAC 3'	For third round of placing <i>trp</i> operon promoter upstream of <i>xagR</i> this primer overlapping with Ptp-F-2
XagR-R-blunt	5' TTATGTCTCCAACAACCGATAGTG 3'	Amplification of <i>xagR</i> gene for construct <i>xagR</i> overexpressing strain
XagRPRO-F ( <i>SacI</i> )	5' TTGTAGTAGAGCTCCCTCGGACAT GGTGGAGATTG 3'	Amplification of promoter region of <i>xagR</i>
XagRPRO-R ( <i>SacI</i> )	5' TTGTAGTAGAGCTCAAACCGAGCG CACAGACATCGC 3'	.....
PipPRO-F ( <i>SacI</i> )	5' TTGTAGTAGAGCTCACTACCAACA TGACCCTGTTCAG 3'	Amplification of promoter region of <i>pip</i>
PipPRO-R ( <i>SacI</i> )	5' TTGTAGTAGAGCTCACCGCCGTGC AGCACCAGTAG 3'	.....
XagRKO-F1-F	5' TTCCTCGGACATGGTGGAGATTG 3'	Amplification of upstream region of <i>xagR</i> for generate <i>xagR</i> mutant
XagRKO-F1-R	<b>5' GAAGCAGCTCCAGCCTACACA</b> TGGCCAGAATGTCTGAACATGGTG 3'	.....
XagRKO-F2-F	5' <u>GGTCGACGGATCCCCGGAAT</u> TATGCACTATCGGTTGTTGGAGAC 3'	Amplification of downstream region of <i>xagR</i> for generate <i>xagR</i> mutant
XagRKO-F2-R	5' CTGCGCGTAGAACACCTGACTG 3'	.....
PipKO-F1-F	5' TACTACCAACATGACCCTGTTCAG 3'	Amplification of upstream region of <i>pip</i> for generate <i>pip</i> mutant
PipKO-F1-R	<b>5' GAAGCAGCTCCAGCCTACACA</b> CATGACCTGCGCCTGCCTAC 3'	.....

**Table 3** (Continued)

<b>Primer</b>	<b>Sequence<sup>1</sup></b>	<b>Description</b>
PipKO-F2-F	5' <u>GGTCGACGGATCCCCGGAAT</u> TGTTTGAGCGTGCAGGGTGC 3'	Amplification of downstream region of <i>pip</i> for generate <i>pip</i> mutant .....
PipKO-F2-R	5' GACCGCTGTCTTGTGCCGCC 3'	.....
MemKO-F1-F	5' CATTCTCTCGAAGCGATGGA 3'	Amplification of upstream region of the genes homologous to <i>Xac</i> loci 3964 for generate XagID3706 mutant .....
MemKO-1-R	5' <b>GAAGCAGCTCCAGCCTACACA</b> TTCCGTAAAGGGACTTGCG 3'	.....
MemKO-2-F	5' <u>GGTCGACGGATCCCCGGAAT</u> TGACAACAATGAGTACATCGC 3'	Amplification of downstream region of the genes homologous to <i>Xac</i> loci 3964 for generate XagID3706 mutant .....
MemKO-2-R	5' CGCATCGATGGACTTGTAC 3'	.....
RtcbKO-1-F	5' ACGCAAGTCCCTTTACGG 3'	Amplification of upstream region of the genes homologous to <i>Xac</i> loci 3965 for generate XagID3707 mutant .....
RtcbKO-1-R	5' <b>GAAGCAGCTCCAGCCTACACA</b> AACAACTCGTCCAGCGTC 3'	.....
RtcbKO-2-F	5' <u>GGTCGACGGATCCCCGGAAT</u> GCAATGCAGTGCACAGTTC 3'	Amplification of downstream region of the genes homologous to <i>Xac</i> loci 3965 for generate XagID3707 mutant

**Table 3** (Continued)

<b>Primer</b>	<b>Sequence<sup>1</sup></b>	<b>Description</b>
RtcbKO-2-R	5' GAGAAGACCGCAGATTAGTCG 3'	.....
YapHKO-1-F	5' ATCTGTTGCTCAACGCAGT 3'	Amplification of upstream region of <i>yapH</i> homolog for generate <i>yapH</i> mutant
YapHKO-1-R	<b>5' GAAGCAGCTCCAGCCTACACA</b> AGGTCAATGCATGACATCG 3'	.....
YapHKO-2-F	<u>5'GGTCGACGGATCCCCGGAATATAG</u> GCGAATCAATCAGCC 3'	Amplification of downstream region of <i>yapH</i> homolog for generate <i>yapH</i> mutant
YapHKO-2-R	5' CGCGTCAACACATAGCTG 3'	.....
XagRcom-F ( <i>Sal</i> I)	5'TTGTAGTAGTCGACCAGCCCGTAG ATCAACAGATCC 3'	Amplification of 1.4 kb of <i>XagR</i> for generate <i>XagR</i> complementary strain
XagRcom-R ( <i>Hind</i> III)	5'TTGTAGTAAAGCTTCAAATTCAC AGGTTTGGGCGCG 3'	.....

<sup>a</sup>Bold sequence= Reverse complementary priming for pKD13 site, Underline sequence= pKD13 priming site

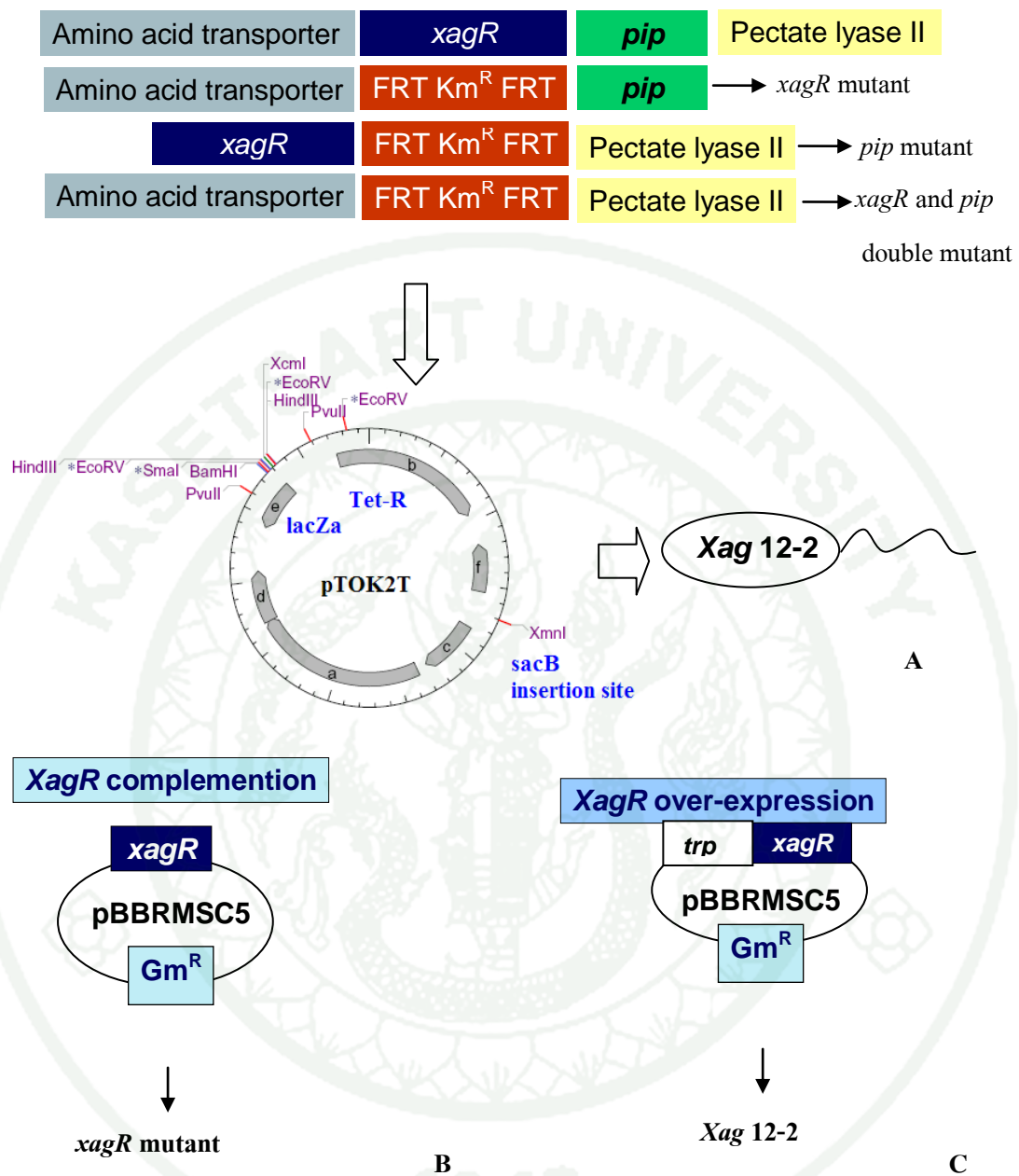


**Figure 4** Overlap extension PCR was used to create constructs in the suicide-delivery vector pTOK2 to create site-directed mutants in *Xanthomonas axonopodis* pv. *glycines* 12-2 by recombination (A). An XagR-complementary strain, the 1.4-kb sequence of *xagR* containing the native promoter was amplified and ligated into the multiple cloning site of vector pBBR1MCS-5(B). XagR-overexpressing strain was constructed by placing the coding region of *xagR* amplified as a 765 bp fragment from *Xag12-2* genomic DNA with *Sma*I sites downstream of the *E. coli* *trp* operon promoter pBBR1MCS-5 to yield pTrp::*xagR* (C).

## 6. *inaZ*-reporter gene fusion assays.

### 6.1 Reporter gene construction

The promoter-containing sequences upstream of *xagR* and *pip* were amplified from genomic DNA of *X. axonopodis* pv. *glycines* 12-2 using primers XagRPRO-F(*Sac*I) and XagRPRO-R(*Sac*I); PipPRO-F (*Sac*I) and PipPRO-R (*Sac*I) respectively (Table 3). Each amplicon was digested with *Sac*I (New England BioLabs, MA, USA) and purified using a QIAEX II gel extraction kit (QIAGEN, CA, USA) and cloned immediately 5' to the promoterless *inaZ* ice nucleation reporter gene in the broad-host-range vector pPROBE-KI (Miller *et al.*, 2000). The resulting plasmids, designated pXagR-KI and pPip-KI, were transformed into competent cells of *E. coli* DH5 $\alpha$  (Sambrook *et al.*, 1989) and introduced into *X. axonopodis* pv. *glycines* 12-2 as well as the *xagR* mutant of *X. axonopodis* pv. *glycines* by electroporation with a BioRad GenePulser Xcell electroporation system (Hercules, CA).

### 6.2 The ice nucleation activity assay

The ice nucleation activity of cells harboring pXagR-KI and pPip-KI *in vitro* was determined after growth for 2 days at 25°C in M9 medium with or without addition of fresh or autoclaved soybean extract (10%) after suspension in 10 mM potassium phosphate buffer, pH 7.4. *In planta* ice nucleation activity was assessed in cells recovered at various times from inoculated plants. Cells were harvested from LA and re-suspended to a final density of approximately 10<sup>8</sup> cells/ml and infiltrated under vacuum into the intercellular spaces of soybean plants (3-4 weeks old). Plants were incubated under light (12 hour photoperiod) at 25°C and replicate samples of individual leaves were macerated in buffer. The ice nucleation activity of serial dilutions of either bacterial cell suspensions or leaf macerates was measured by a droplet freezing assay performed at -5 °C as described previously (Loper and Lindow, 1996). Ice nucleation activity was normalized for the number of viable cells present in

a sample as determined by dilution plating on LA amended with kanamycin. The experiments were repeated three to five times with similar results.

## **7. *X. axonopodis* pv. *glycines* recovery from infected soybean**

### *7.1 X. axonopodis* pv. *glycines* endophyte harvesting

Bacteria cells from infected soybean plant were harvested in hot phenol solution. Briefly, 300 infected leaves were cut and made into confetti directly over the 600 ml hot phenol stop solution and sonicated for 10 minutes. Bacterial cell in hot phenol solution were enriched. The plant slurry was passed through cheesecloth using a side-arm-flask setup. The filtered liquids were spined at 8,000 rpm for 10 minutes in 200 ml conical polycarbonate tubes from Nalgene. The most of the phenol liquid were discarded and keep a small amount (3 ml) in each tube for resuspended calls along with the visible green plant debris. The suspension were poured into a syringe packed with cheesecloth, and fitted with a Millipore millex-sv 25 mm durapore PVDF 5 um filter unit and then centrifuge in eppendorf tubes. The pellets were flash frozen and stored at -80 °C until RNA extraction process.

### *7.2 RNA extraction of X. axonopodis* pv. *glycines* endophyte

The cell pellet were resuspended into 1 ml Trizol reagent and incubated for 10 minutes at 65 °C. The 200 ml of chloroform were added and shaken for 15 seconds followed by vortex for 15 second. The samples were incubated for 15 minutes at room temperature and then centrifuge the samples at 14,000 rpm for 15 minutes at 4 °C. The upper aqueous phases were collected and transfer to the new tube and then the 500 ml of isopropanol were added and frozen at -80 °C for 30 minutes. The frozen pellets were centrifuged at 14000 rpm for 30 minutes at 4 °C, the supernatant were discarded and the pellets were washed 3 times with 1 ml of 75% EtOH. The pellets were air dried at room temperature and kept at -80 °C for future experiment.

### 7.3 Ribosomal RNA depleted

Since the total RNA of *X. axonopodis* pv. *glycines* endophyte sample contaminated with plant ribosomal RNA. The ribosomal RNA were removed from total RNA using Ribo-Zero™ rRNA Removal Kit (Gram-Negative Bacteria) combined with Ribo-Zero™ rRNA Removal Kit (Plant Leaf) (Epicentre) according to the manufacturer's protocol, with 5 µg total RNA treated per depletion reaction.

## 8. RNA isolation and quantitative RT-PCR analysis

Total RNA of *X. axonopodis* pv. *glycines* *in vitro* was extracted using the Qiagen RNA/DNA Mini Kit, and DNA was removed using an on-column DNase treatment (RNeasy Mini Kit with DNase I; Qiagen). RNA samples were analyzed for quality using a BioAnalyzer 2100 (Agilent, CA, USA). cDNA was generated from 1 µg of RNA using SuperScript II (Invitrogen, CA, USA) and random hexamers. To confirm that DNA was removed, samples processed in parallel without reverse transcriptase served as negative controls in quantitative PCR experiments (Q-PCR) described below. Q-PCR was performed on 1 µg of the cDNA using LightCycler FastStart DNA MasterPLUS SYBR Green I (Roche, Indianapolis, IN) on a Roche Lightcycler II (Roche) following manufacturer's specifications. An external standard curve was generated using purified *ihfA* (integration host factor A) DNA (Champoiseau *et al.*, 2006). Melting curve analysis was used to verify amplification of a single product. The concentration of amplification products from negative controls (RNA samples to which no superscript was added) was undetectable in all cases, indicating a lack of interference from contaminating DNA.

## 9. mRNA sequencing

Sequencing was performed on mRNA isolated from *X. axonopodis* pv. *glycines* strain 12-2 and *XagR*-overexpressing strain (XagROX) for *xagR* regulon experiment and from mRNA isolated from *X. axonopodis* pv. *glycines* cells recovery from plant for plant inducible gene experiment. Total RNA was isolated with TRIZOL

(Invitrogen, CA, USA) from cells grown in M9 minimal medium using the method of (Santiago-Vazquez *et al.*, 2006). Contaminating DNA was removed using the Turbo DNA-free kit (Ambion) and was cleaned using the RNeasy mini kit (Qiagen, CA, USA). 16S and 23S rRNA were removed from total RNA using Ribo-Zero™ rRNA Removal Kit (Gram-Negative Bacteria) (Epicentre, WI, USA) according to the manufacturer's protocol, with 5 µg total RNA treated per depletion reaction. Enriched mRNA samples were assessed with a 2100 Bioanalyzer (Agilent, CA, USA) to confirm the removal of 16S and 23S rRNA. Quantification of remaining mRNA prior to preparation of cDNA fragment libraries was performed using the qBit RNA assay (Invitrogen, CA, USA). Ambion RNA fragmentation reagents (Ambion, #AM8740) were used to generate 60-200 nucleotide RNA fragments with an input of 100 ng of mRNA. Fragmented RNA was purified using ethanol precipitation in the presence of glycogen and precipitated RNA was resuspended in RNase free water. First strand cDNA synthesis was performed using random primers (Invitrogen, CA, USA) and Superscript II Reverse Transcriptase, followed by second strand cDNA synthesis using RNaseH and DNA pol I (Invitrogen, CA, USA). Double stranded cDNA was purified using AMPure XP beads (Beckman Coulter) with PEG 6000 added to a final concentration of 6.5% (w/v). cDNA end repair was performed using the Klenow DNA polymerase, T4 DNA polymerase, and T4 polynucleotide kinase (all New England Biolabs, ). An A tail was added to DNA fragments using Klenow exo minus and 250 µM (final concentration) dATP. Illumina adapters were ligated to the DNA fragments using T4 DNA ligase, with PEG 6000 addition (5.0% final concentration) (New England Biolabs, MA, USA). Fragments were amplified using Illumina barcoded primers and Phusion DNA polymerase (New England Biolabs, MA, USA). Amplified fragments were purified similarly as above, except without PEG addition. Fragment sizes of 200 to 300 nucleotides were confirmed using the 2100 Bioanalyzer. Sequencing was performed by running 36 cycles on the Illumina HiSeq 2000. Amplified material from each of 3 replicate samples were assigned distinct bar-coded linkers and loaded onto independent flow cells. All short reads of cDNA sequence were mapped to *X. axonopodis* pv. *glycines* ORFs using Bowtie 0.12.7 (Langmead *et al.*, 2009). Differential gene expression was assessed with edgeR: a Bioconductor package (Gentleman *et al.*, 2004; Robinson *et al.*, 2010).

## 10. Western blot analysis

Bacterial cells from 10 ml overnight shake cultures were pelleted by centrifugation for 10 minutes at 14,000 rpm and then re-suspended in 0.75 ml lysis buffer (50 mM Tris pH 8.0, 10% glycerol, 0.1% Triton X-100 and Complete Mini protease inhibitors cocktail (Roche)). Cells were disrupted by sonication (Vibracell, Sonics Materials Inc) and 6 µg of total protein (as determined by a Bradford protein assay) were mixed 4:1 with sample buffer (0.1 M Tris pH 8.3, 50% glycerol, 10% sodium dodecyl sulphate (SDS), 25% β-Mercaptoethanol and traces of bromophenol blue) and separated by SDS polyacrylamide gel electrophoresis (SDS-PAGE; 15% (w/v) polyacrylamide). Bacterial cells were also recovered from infected soybean plants. Individual leaves of plants vacuum infiltrated were harvested at different times after inoculation and macerated in phosphate buffer. Total protein content of the plant macerate was performed by boiling the protein suspension in sample buffer for 10 min. Equal amounts of total protein (ca. 6 ug) were then separated by SDS-PAGE as previously outlined. In both cases, proteins were transferred to a PVDF membrane (Immobilon-P; Millipore) using a tank system according to the manufacturer's instructions. The membrane was subjected to Western blot analysis using polyclonal antibodies (1:5000 dilution) against OryR, the LuxR homolog of *X. oryzae* pv. *oryzae* provided by Vittorio Venturi (Ferluga *et al.*, 2007; Ferluga and Venturi, 2009) and a HRP conjugated goat anti-rabbit secondary antibody (Promega, WI, USA). The membrane was developed using SuperSignal West Pico chemiluminescent substrate (Pierce) and blue x-ray film (Phenix Research Products).

## 11. Biosurfactant detection.

Biosurfactant production of *X. axonopodis* pv. *glycines* was assessed on semi-solid LA plates containing 0.4% technical agar as described previously (Burch *et al.*, 2010). Cells were grown overnight on LA medium and then harvested and washed in potassium phosphate buffer. Cells were resuspended in buffer to a concentration of  $10^8$  cells/ml and then were spotted (10 ul) onto a plate and incubated for 3 days at room temperature. The biosurfactant was detected by an atomized oil assay in which

biosurfactant halos are visualized with an indirect source of bright light (Burch *et al.*, 2010). The radii of biosurfactant spreading was measured (from the leading edge of the bacterial colony to the edge of the surfactant halo). The swarming distance was calculated as the average diameter of spreading colonies initiated from point sources as above.

## 12. Bacterial adhesion assays

To assess bacterial adhesion to abiotic surfaces, cells of overnight cultures in LB were resuspended to a concentration of  $10^7$  cells/ml in M9 minimal medium and 100  $\mu$ l incubated individually in wells of 96-well flat-bottom polystyrene tissue culture plates and incubated at 28°C for different lengths of times before the medium was removed using a pipette. The wells were washed gently three times with 150  $\mu$ l of sterile distilled water, and the plates were transferred to a 60°C incubator for 20 min. The abundance of the surface-attached biofilm was determined by crystal violet staining as in other studies (Davey and O'Toole, 2000). Dye abundance was measured by absorption at 570 nm using a microtiter plate reader. Readings from 36 replicate wells were averaged. The experiments were repeated three times with similar results.

Bacterial adhesion to soybean leaves was assessed by immersing six individual leaves into 500 ml of a suspension of a given bacterial strain ( $10^7$  cells/ml) at 28 °C. After 5 min, 3 hr and 7 hr, the leaves were removed and rinsed gently with distilled water for 30 sec. To enumerate the attached bacteria a single 2 cm diameter disc was cut from a portion of each leaf in an area lacking major veins using a cork borer, the discs homogenized using a mortar and pestle, and cells enumerated by dilution plating.

## 13. Bacterial egression assay.

Bacterial suspensions ( $10^7$  cells/ml) in 10 mM phosphate buffer were vacuum infiltrated into soybean plants and incubated at 28 °C for 4 days. Six leaves from plants in each treatment were then detached and surface sterilized using UV

irradiation (254 nm, with flux of ca. 1,000 ergs/ m<sup>2</sup>/ s for 30 minutes each side). A 2 cm disc was cut from each leaf as above and was placed into a tube containing 1 ml of sterile distilled water and incubated at 28°C for 30 minutes without agitation and the egressing bacteria enumerated by dilution plating.

#### 14. Virulence and bacterial growth in soybean

The virulence of *X. axonopodis* pv. *glycines* was assessed on soybean cv. Spencer following topical spray application (Kaewnum *et al.*, 2005). Briefly, cell suspensions of a given strain (OD<sub>600</sub> = 0.2; ca. 10<sup>8</sup> cells/ml) in 1 mM buffer were sprayed onto leaves of plants (ca. 6 weeks old) maintained in a greenhouse (average temperature ca. 25°C). For the first 24 hours after inoculation, plants were held in an enclosed plastic tent to maintain high humidity and moisture on leaves before being returned to the greenhouse bench. In an experiment designed to simulate rainfall, plants were sprinkled with distilled water (ca. 500 ml/plant) over a period of about 30 minutes immediately after spray inoculation. At 7 to 10 days after inoculation, disease severity was assessed by counting the number of lesions on each leaf. Three trifoliolate leaves, collected each from the top, middle and basal portion of three plants from each of 5 replicate pots, were evaluated for each strain. The experiments were repeated three times with similar results.

Bacterial growth was assessed within leaves in which bacteria had been infiltrated under vacuum. Briefly, cells of a given strain were re-suspended in phosphate buffer, their concentrations determined from their optical density at 600 nm, and then were diluted to a final density of approximately 10<sup>6</sup> cells/ml and infiltrated under vacuum into soybean plants (3-4 weeks old). Leaves were collected daily for 7 days after infiltration (three leaves at each sample time for each strain). Samples were periodically removed and macerated in 5 ml (final volume) of 0.1 M potassium phosphate buffer and the number of viable cells was determined by dilution plating on LA. The experiments were repeated three times with similar results.

## RESULTS AND DISCUSSION

### Results

#### 1. *X. axonopodis* pv. *glycines* genome description

The draft genome sequence of *X. axonopodis* pv. *glycines* strain 12-2 was determined using a combination of 454 GS-FLX pyrosequencing (paired-end) and paired-end Illumina/Solexa sequencing. The reads from 454 and Illumina were mapped against the finished genome sequence of *X. axonopodis* pv. *citri* strain 306 as a scaffold to create a *X. axonopodis* pv. *glycines* consensus sequence. Those reads that could not be mapped onto the reference strain were assembled *de novo* to produce contigs unique to *X. axonopodis* pv. *glycines*. The combined *X. axonopodis* pv. *glycines* consensus sequences and unmapped contigs were used to identify most of the functional genes in *X. axonopodis* pv. *glycines*. The combined Illumina and 454 platforms generated a total of 41,792,635 high-quality filtered sequence reads with an average read length of 71.43 bp. Average coverage was more than 400-fold. This yielded 489 contigs with a N50 value of 20,859 bp. A total of 5,062 putative coding genes (ORFs) were identified in the *X. axonopodis* pv. *glycines* genome.

##### 1.1 Draft genome comparative analysis

For comparative analyses, the short read of *X. axonopodis* pv. *glycines* 12-2 obtained from both 454 and illumina sequencing were mapped with the complete sequences of *Xanthomonas* spp. including *X. axonopodis* pv. *citri* 306 (GenBank accession no. NC\_003919), *X. campestris* pv. *vesicatoria* 85-10 (GenBank accession no. NC\_007508), *X. campestris* pv. *campestris* ATCC 33913 and *X. oryzae* pv. *oryzae* KACC10331 using CLCbio Genomics Workbench version 4.0. The genome of *X. axonopodis* pv. *glycines* 12-2 closest relatives to *X. axonopodis* pv. *citri* str. 306, *X. campestris* pv. *vesicatoria* str. 85-10, *X. campestris* pv. *campestris* ATCC 33913 and *X. oryzae* pv. *oryzae* KACC10331 with the size of consensus 4,720,705, 4,487,830, 3,845,356 and 3,774,556 bp respectively. The dot blot comparison between draft

genome of *X. axonopodis* pv. *glycines* 12-2 and other *Xanthomonads* above were also analyzed. Sequence similarity is shown as red dots in the graph. The dot blot comparison show a strong similarity between draft genome of *X. axonopodis* pv. *glycines* 12-2 and complete genome of *X. axonopodis* pv. *citri* 306, *X. campestris* pv. *vesicatoria* str. 85-10 and *X. campestris* pv. *campestris* ATCC 33913, while show low similarity with *X. oryzae* pv. *oryzae* KACC10331 (Figure 5).

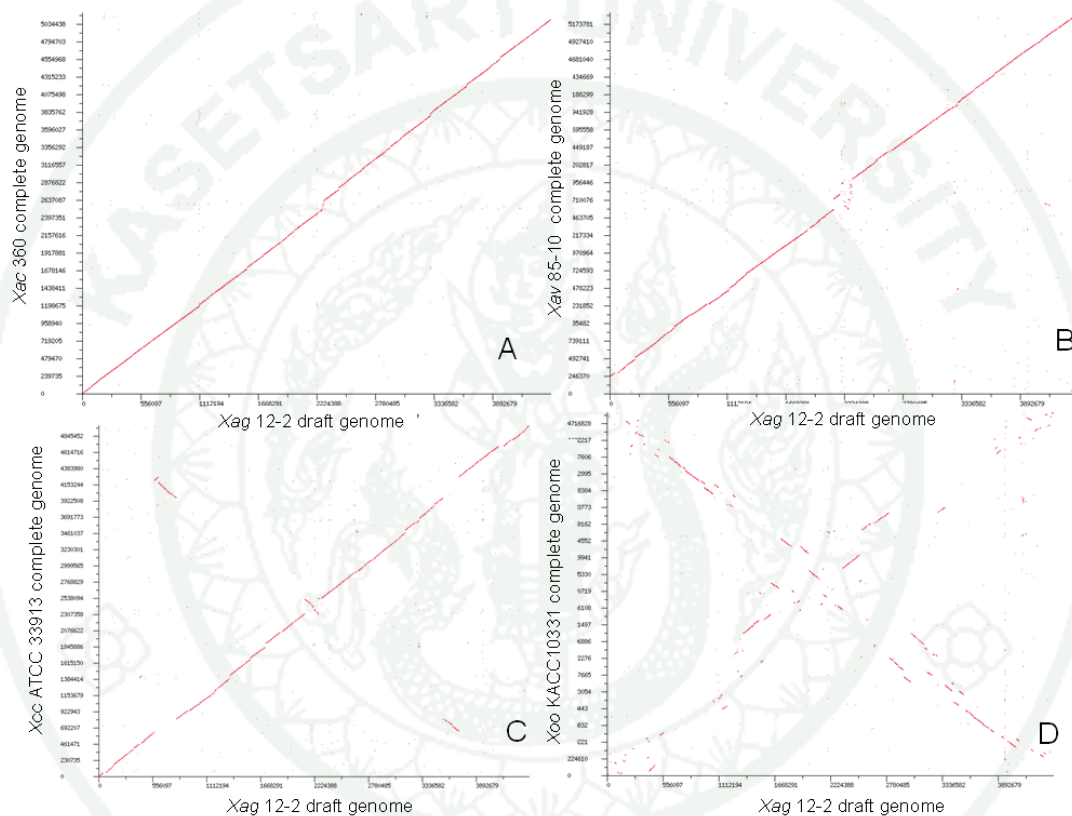


**Figure 5** Dot blot comparison between draft genome of *Xanthomonas axonopodis* pv. *glycines* 12-2 and complete genomes of *Xanthomonas axonopodis* pv. *citri* 306 (A), *Xanthomonas campestris* pv. *vesicatoria* 85-10 (B), *Xanthomonas campestris* pv. *campestris* ATCC 33913 (C) and *Xanthomonas oryzae* pv. *oryzae* KACC10331 (D) using RAST subsystem technology.

## 1.2 Unique genes in *X. axonopodis* pv. *glycines* 12-2

We also analysis the unique genes in *X. axonopodis* pv. *glycines* 12-2 were obtained from the contig of the reads that were not mapped to the published complete genomes of *X. axonopodis* pv. *citri* str. 306, *X. campestris* pv. *vesicatoria* str. 85-10, *X. campestris* pv. *campestris* ATCC 33913, *X. oryzae* pv. *oryzae* KACC10331, *X. oryzae* pv. *oryzicola* and *X. albilineans* GPE PC73. All unmapped read were assembly to the contig and submit to RAST subsystem to predict its functions. All 500 unique genes and its functions were shown in the additional table 1 (see appendix). Of these, 62% of the unique genes were predicted as hypothetical protein. Interestingly, we found some genes that might be related with the pathogenicity and virulence factors. The genes predicted as filamentous hemagglutinin-related protein, adhesin HecA family and hemagglutinin/hemolysin-related protein located in the same cluster that this cluster might be play a specific role of adhesion in *X. axonopodis* pv. *glycines* 12-2. The genes predicted as avirulence protein, beta-lactamase and 1,4-beta-cellobiosidase were also found in the unique genes list. Moreover, we also found the several gene that predicted to be flagella operon including RNA polymerase sigma factor for flagellar operon, flagellar biosynthesis protein FliP, hook protein FlgE, basal-body rod modification protein FlgD, flagellum-specific ATP synthase FliI, M-ring protein FliF, basal-body rod proteins FlgC and FlgG, P-ring protein FlgI, L-ring protein FlgH, putative flagellar basal-body rod protein flgF, flagellar biosynthesis protein FlhA, FlhB and FliQ and flagellar biosynthesis pathway, component FliR.

## 1.3 The predicted pathogenicity genes of *X. axonopodis* pv. *glycines* 12-2

In *Xanthomonas* spp., the type III secretion system (T3SS) encoded by a cluster of hypersensitive response and pathogenicity (*hrp*) genes is one critical pathogenicity factor. In this study, we found the *hrp* gene cluster that encoded the several Hrp protein including HrpF, HrpE, HrpD6, HrpD5, HrpB1, HrpB2, HrpB4 and HrpB7 at the same operon and HrpG and HrpX protein in different operon.

Moreover, we found several gene including type III secretion inner membrane protein YscS, which homologous to flagellar export components and YscR, SpaR, HrcR, EscR, homologous to flagellar export components, type III secretion inner membrane channel protein (LcrD, HrcV, EscV, SsaV), type III secretion inner membrane protein (YscU, SpaS, EscU, HrcU, SsaU, homologous to flagellar export components), type III secretion bridge between inner and outer membrane lipoprotein (YscJ, HrcJ, EscJ, PscJ), type III secretion inner membrane protein SctL, type III secretion cytoplasmic ATP synthase (EC 3.6.3.14, YscN, SpaL, MxiB, HrcN, EscN), type III secretion inner membrane protein (YscT, HrcT, SpaR, EscT, EpaR1, homologous to flagellar export components), type III secretion outer membrane pore forming protein (YscC, MxiD, HrcC, InvG). Interestingly, the candidate type III effector HolPtoQ, Hop protein, putative type III effector HopPtoH like protein that was found in *Pseudomonas syringae*, were also found in *X. axonopodis* pv. *glycines* 12-2 draft genome.

## 2. Presence of *xagR* and *pip*

The sequenced *X. axonopodis* pv. *glycines* 12-2 genome revealed the presence of a putative *luxR* homolog that we termed *xagR*. XagR is a protein of 254 amino acids with a molecular mass of 29.7 kDa. Analysis of XagR with Conserved Domain Architecture Retrieval Tool revealed (CDART) that it contains an autoinducer-binding domain (pfam03472) located in residues 17 to 177 and a helix-turn-helix DNA-binding domain from residues 189 to 246, characteristic of the LuxR family of proteins (Figure 6A). XagR shared the highest level of identity (99%) to the AhyR/AsaR family transcriptional regulator from *X. axonopodis* pv. *citri* 306, while it exhibited 96, 93, 92 and 86% identity to a homolog in *X. campestris* pv. *vesicatoria* 85-10 and *X. oryzae* pv. *oryzicola* BLS256, as well as OryR from *X. oryzae* pv. *oryzae* and XccR from *X. campestris* pv. *campestris*, respectively (Table 4). *xagR* is located upstream of and in the same orientation as a homolog of *pip* in *X. oryzae* pv. *oryzae* and *X. campestris* pv. *campestris*, with an intergenic sequence of 384 bp. Within the 384 bp intergenic region, a 20 bp palindromic sequence centered -70.5 bp from the translation start site of *pip* (Figure 6B) was found that is highly similar to the *lux* box

sequences located in a similar position in *X. campestris* pv. *campestris* and *X. oryzae* pv. *oryzae* (Figure 6C) (Ferluga *et al.*, 2007; Zhang *et al.*, 2007).

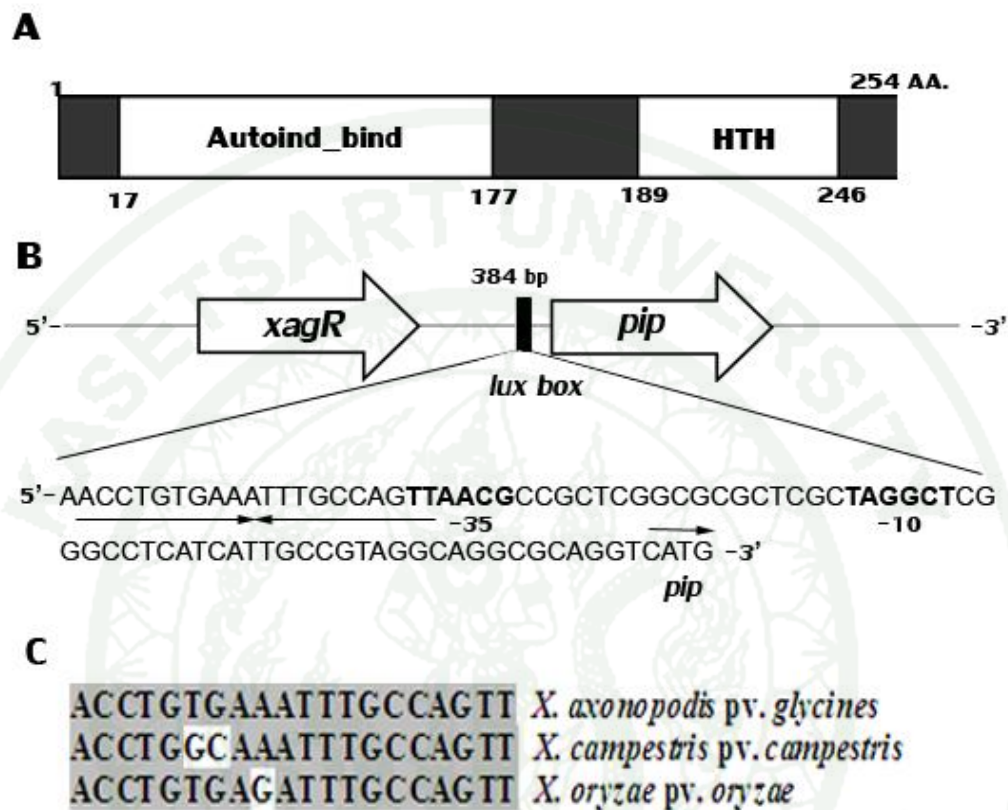


**Figure 6** Structure of XagR from *Xanthomonas axonopodis* pv. *glycines* with schematic representation of the positions of the AHL-binding and the helix-turn-helix-DNA binding domains typical of quorum sensing LuxR family regulators (A). Analysis of the *pip* promoter locus within the 384-bp intergenic region upstream from the *pip* gene and location of a putative palindromic *lux box* sequence (B). Alignment of the putative *lux boxes* associated with *pip* genes in *X. axonopodis* pv. *glycines*, *Xanthomonas campestris* pv. *campestris* and *Xanthomonas oryzae* pv. *oryzae* (C).

**Table 4** The *luxR* homolog/*pip*-like loci found in other bacterial species

Strains containing the <i>luxR</i> homolog/ <i>pip</i> -like locus	Percentage sequence identity with the proteins from <i>Xag 12-2</i>		Position of the putative <i>lux</i> box in the promoter
	LuxR	Pip	
<i>Xanthomonas axonopodis</i> pv. <i>citri</i> 306	99	99	2-bp overlapping the -35 element
<i>X. campestris</i> pv. <i>vesicatoria</i> 85-10	96	98	2-bp overlapping the -35 element
<i>X. oryzae</i> pv. <i>oryzicola</i> BLS256	93	94	2-bp overlapping the -35 element
<i>X. oryzae</i> pv. <i>oryzae</i> KACC10331	92	94	2-bp overlapping the -35 element
<i>X. campestris</i> pv. <i>vasculorum</i> NCPPB702	91	96	2-bp overlapping the -35 element
<i>X. campestris</i> pv. <i>campestris</i> str. 8004	86	91	2-bp overlapping the -35 element
<i>X. campestris</i> pv. <i>campestris</i> str. ATCC 33913	85	91	2-bp overlapping the -35 element
<i>Pseudomonas syringae</i> pv. <i>syringae</i> B728a	50	65	2-bp overlapping the -35 element
<i>Pseudomonas fluorescens</i> Pf-5	49	52	No <i>lux</i> box was found
<i>Rhizobium leguminosarum</i> bv. <i>trifolii</i> WSM2304	43	64	2-bp overlapping the -35 element
<i>Sinorhizobium meliloti</i> 1021	43	62	2-bp overlapping the -35 element
<i>Rhizobium leguminosarum</i> bv. <i>viciae</i> 3841	42	64	2-bp overlapping the -35 element

### 3. *XagR* and *pip* contribute to virulence of *X. axonopodis* pv. *glycines* to soybean.

Disruption of *xagR* significantly reduced the incidence of infection of soybean leaves when cells were sprayed onto a susceptible soybean cultivar (Figure 7). Since *pip* is regulated by a *luxR* homolog in both *X. campestris* pv. *campestris* and *X. oryzae* and contributes to their virulence to cabbage and rice, respectively, we assessed the virulence of a *pip* mutant and a *xagR/pip* double mutant of *X. axonopodis* pv. *glycines*; both exhibited similarly reduced virulence as the *xagR* mutant alone. A *xagR* mutant complemented with *xagR in trans* on a low copy number vector (*XagR*<sup>+</sup>) exhibited similar virulence to soybean as the wildtype strain (Table 5). Curiously, the virulence of the *XagR*-over-expressing strain (*XagROX*) was less than that of the *Xag* 12-2 wildtype strain (Table 5). In order to determine if the virulence deficiency of the *xagR* and *pip* mutants was associated with decreased bacterial growth *in planta*, we monitored the growth of cells infiltrated into soybean leaves.

The population size of the mutants was similar to that of the wildtype strain at a given time after infiltration into soybean (Figure 8). It was noteworthy that the numbers of cells of *X. axonopodis* pv. *glycines* increased progressively in the plant for up to 7 days, when symptom development was readily apparent. The population dynamics of *X. axonopodis* pv. *glycines* is thus quite distinct from that seen with many other foliar pathogens such as *Pseudomonas syringae*, in which bacterial multiplication in the plant typically ceases 2 or 3 days after inoculation. These results indicated that *XagR* and *Pip* are required for full virulence of *X. axonopodis* pv. *glycines* to soybean and that much of the contribution of *XagR* might be via any effect it might have on expression of *pip*.

**Table 5** Virulence of *Xanthomonas axonopodis* pv. *glycines* mutants on soybean<sup>a</sup>

<b>Bacterial strains</b>	<b>Lesions per plant</b>
<i>X. axonopodis</i> pv. <i>glycines</i> 12-2	254 +/- 80
<i>xagR</i> mutant	97 +/- 29
<i>pip</i> mutant	102 +/- 32
<i>xagR/pip</i> double mutant	96 +/- 45
XagR <sup>+</sup>	297 +/- 84
XagROX	86 +/- 32
XagID3706 mutant	183 +/- 24
XagID3707 mutant	137 +/- 22
<i>yapH</i> mutant	433 +/- 57

<sup>a</sup> Data shown are the averages +/- standard deviations



**Figure 7** Disease severity on susceptible soybean cv. Spencer caused by *Xanthomonas axonopodis* pv. *glycines* 12-2 (A), *xagR* mutant (B), *pip* mutant (C), *xagR/pip* double mutant (D), XagR overexpressing strain (E) and *xagR* complementary strain (F).

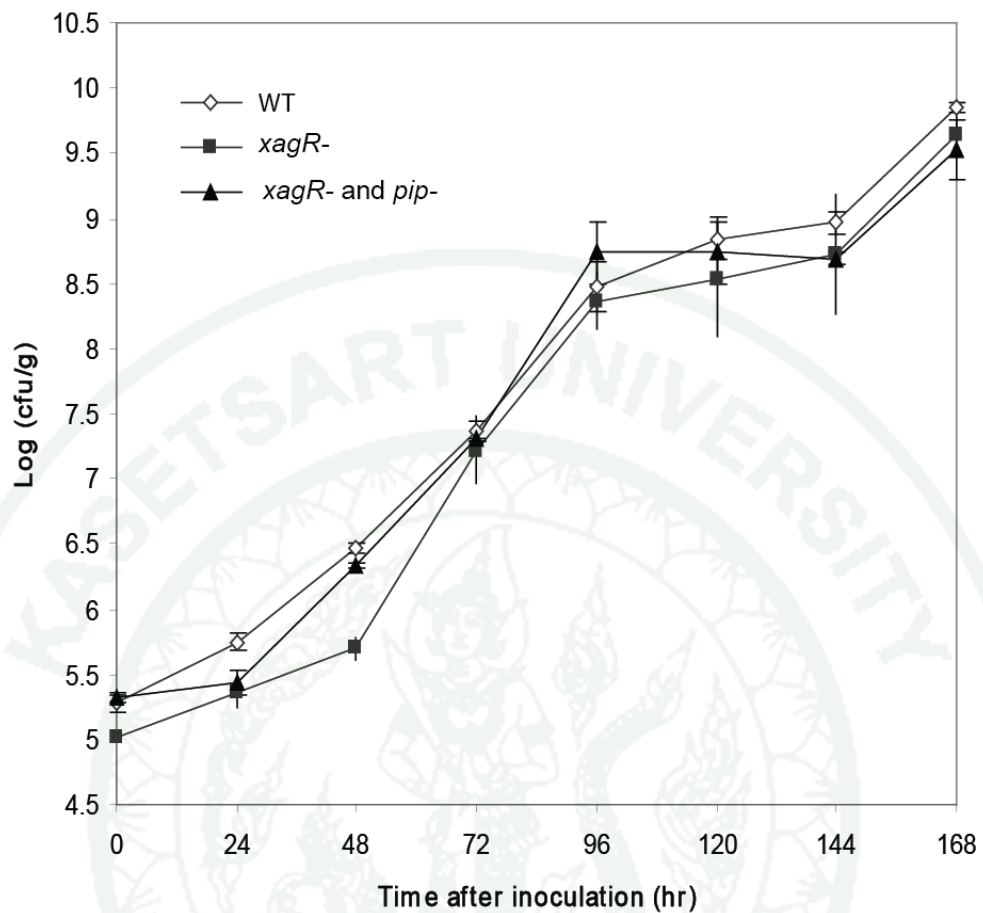


**Figure 8** Population size of the wildtype strain of *Xanthomonas axonopodis* pv. *glycines* (diamonds), a *xagR* mutant (squares) and a *xagR/pip* double mutant (triangles) in soybean at various times after infiltration. The vertical bars represent the standard error of mean log-transformed population sizes.

#### 4. XagR of *X. axonopodis* pv. *glycines* is required for *pip* induction in *planta*.

##### 4.1 *inaZ* reporter gene analysis

Since the *pip* genes are expressed in a *luxR* homolog-dependent manner in both *X. campestris* pv. *campestris* and *X. oryzae* pv. *oryzae*, and are induced in host plants in *X. campestris* pv. *campestris* and by rice extracts in *X. oryzae* pv. *oryzae* (Ferluga *et al.*, 2007; Ferluga and Venturi 2009; Zhang *et al.*, 2007) we explored the context-dependent expression of *pip* in *X. axonopodis* pv. *glycines*. The expression of *pip* was assessed using a promoterless ice nucleation (*inaZ*) reporter gene cloned downstream of the *pip* promoter-containing region in pPip-KI (Figure 9). The ice nucleation activity of the *X. axonopodis* pv. *glycines* wildtype strain and a *xagR* mutant carrying pPip-KI were compared when grown under different conditions including LB medium, M9 minimal medium, M9 minimal medium containing macerates of either healthy or *X. axonopodis* pv. *glycines* -infected soybean, as well as in cells recovered from infiltrated soybean 2 days after inoculation. The ice nucleation activity of cells of the *X. axonopodis* pv. *glycines* wildtype strain, but not a *xagR* mutant was markedly increased after inoculated into susceptible soybean. No induction of *pip* was seen in either strain when grown in media containing soybean macerates nor in the resistant soybean cultivar Williams 82 (Figure 10). XagR thus appears to regulate the expression of at least *pip* and assessment of *pip* expression thus provides a convenient means by which the activity of XagR can be monitored.

Given that XagR has the characteristic signatures of an AHL-dependent response regulator we tested whether its regulatory ability was responsive to the presence of AHLs. No induction of *pip* was observed when structurally different AHLs (C4, C6, C8, C10, C12, C14-, oxoC6 and oxoC8) were added to the culture medium at a final concentration of 1  $\mu$ M.

Since the accumulation of OryR and XccR in *X. oryzae* pv. *oryzae* and *X. campestris* pv. *campestris*, respectively, was found to be responsive to signal molecules present in their compatible hosts, we assessed whether XagR function was

as responsive to these plant species as it was in soybean. The ice nucleation activity of *X. axonopodis* pv. *glycines* wildtype harboring a *pip:inaZ* fusion but not the *xagR* mutant was increased when infiltrated into rice, cabbage and soybean, but not into tobacco (Figure 12). This result suggests that the signal molecule that interacts with XagR might be common to all of the plants, although the fact that macerates of rice could induce OryR but soybean extracts could not would argue otherwise.

#### 4.2 RT-PCR analysis

Quantitative reverse transcription polymerase chain reaction (RT-PCR) was performed to determine whether *pip* transcript abundance, in addition to its rate of production was elevated in *X. axonopodis* pv. *glycines* after inoculation into soybean. The levels of *pip* transcript in wildtype *X. axonopodis* pv. *glycines* cells recovered from infected soybean plants was 18-fold higher than that in either cells grown in culture or in a *xagR* mutant (Figure 11). As observed with reporter gene fusions, there was no increased accumulation of *pip* transcript in wildtype cells grown on media containing soybean macerates, and little *pip* transcript in the *xagR* mutant in most conditions. The induction of *pip* thus is dependent on XagR and appears to require specific molecule(s) in living soybean plants that are not easily extracted or are labile.

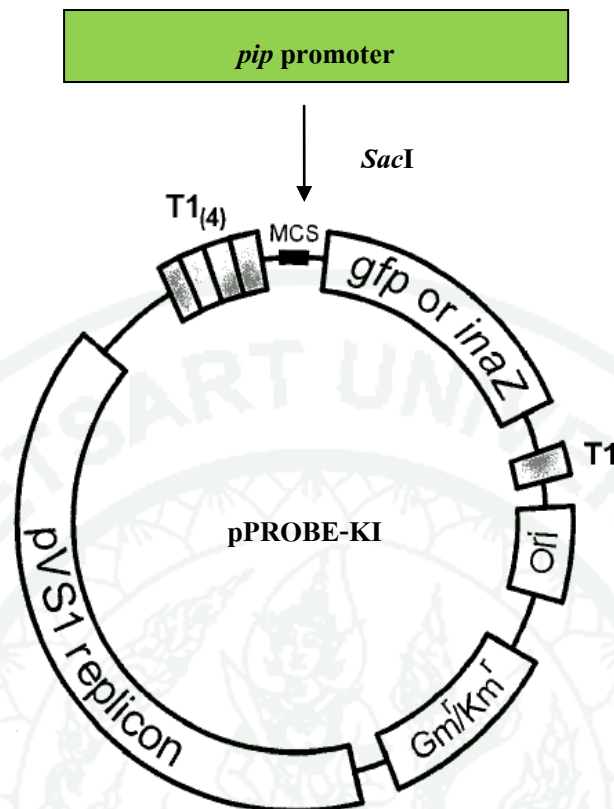


**Figure 9** pKI- *pip* promoter-probe vectors contain a common cassette that has four tandem copies of the T1 terminator (T1<sub>(4)</sub>; shaded boxes), a multicloning site (solid box) containing *pip* promoter was cutted with *SacI*, *inaZ* reporter genes (including optimally placed ribosome binding sites and a single *rrnB* T1 terminator (T1; shaded box) (Miller and Lindow, 1997).

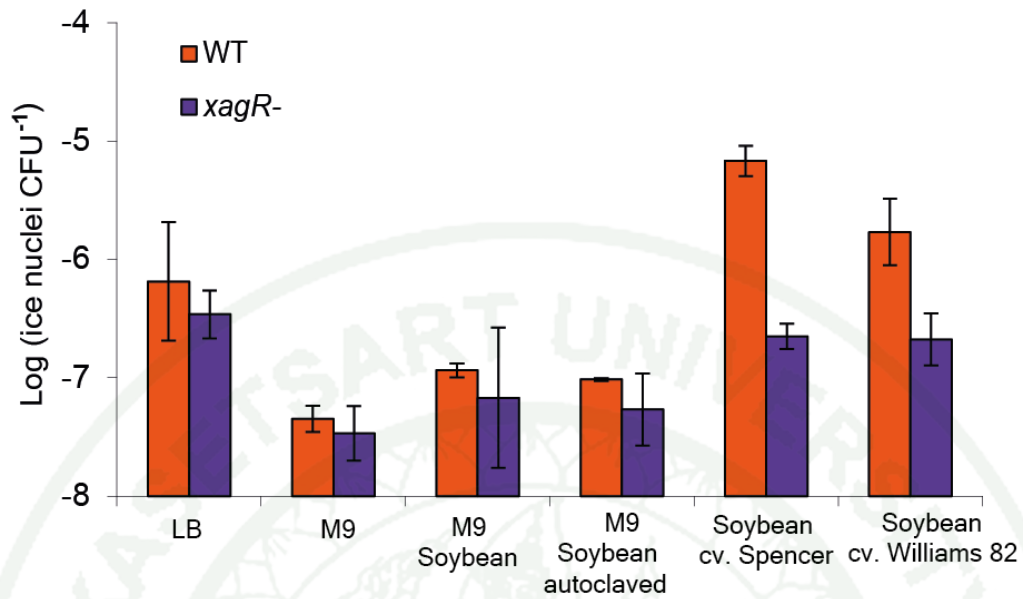


**Figure 10** Ice nucleation activity indicative of *pip* promoter activity in a wildtype strain of *Xanthomonas axonopodis* pv. *glycines* (orange bars) and a *xagR* mutant (purple bars) harboring a *pip:inaZ* fusion when grown in various culture media including LB, M9 minimal medium, M9 minimal medium added with fresh macerated soybean, M9 minimal medium added with autoclaved soybean and when inoculated into soybean plants. Vertical bars represent the standard error of mean log-transformed ice nucleation activity.

1943

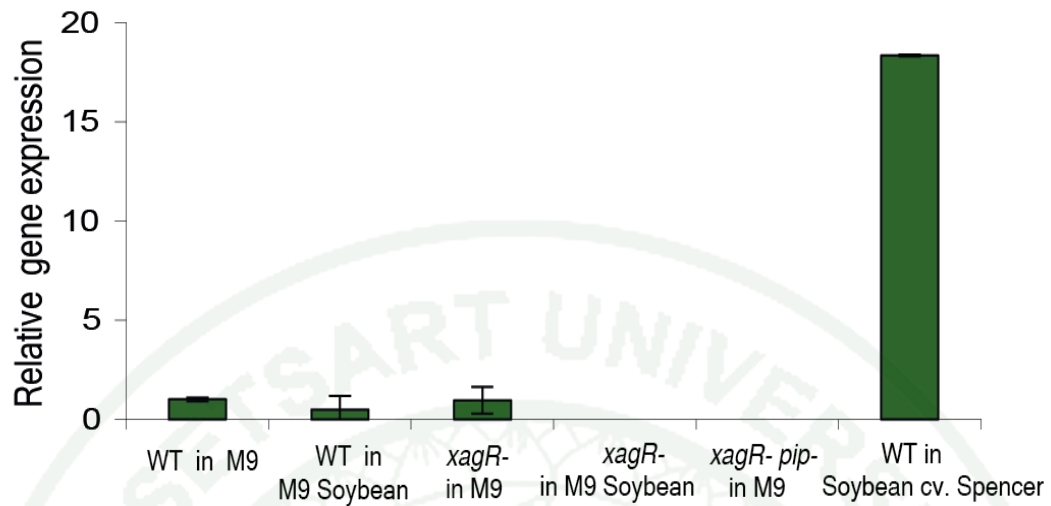


**Figure 11** Relative abundance of *pip* transcripts in a wildtype and *xagR* mutant of *Xanthomonas axonopodis* pv. *glycines* grown in M9 minimal media, M9 minimal media containing fresh soybean leaf macerates, or in cells *in planta* as determined by RT-PCR. The vertical bars represent the standard error of mean relative gene expression.

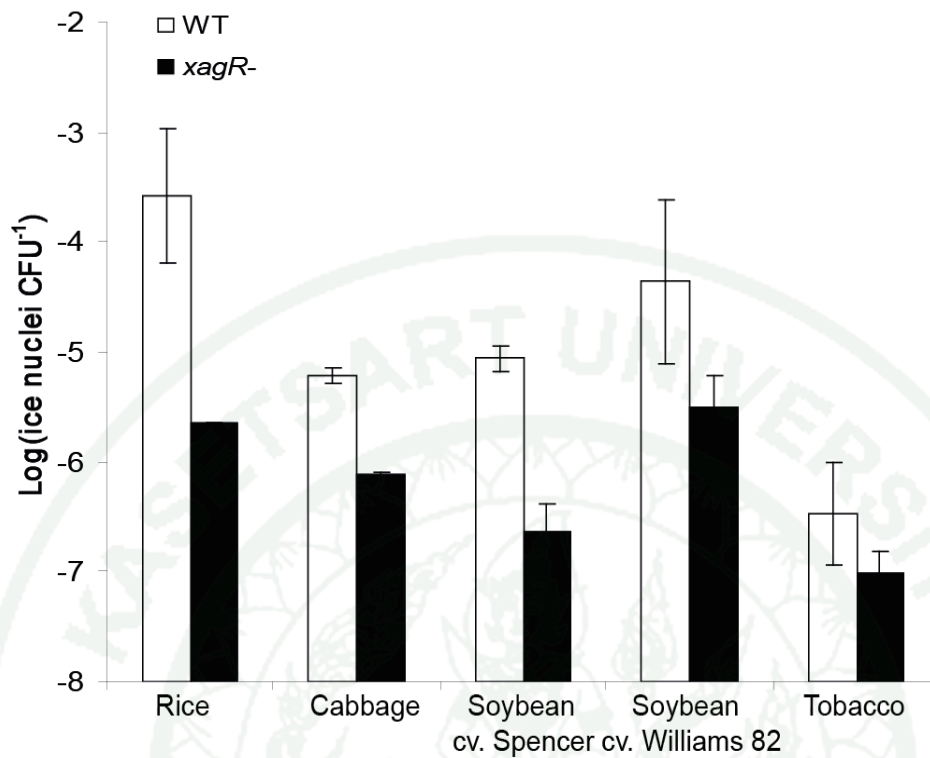


**Figure 12** Ice nucleation activity indicative of *pip* promoter activity in a wildtype strain of *Xanthomonas axonopodis* pv. *glycines* (open bars) and a *xagR* mutant (solid bars) harboring a *pip:inaZ* fusion when recovered from rice, cabbage, soybean cv. Spencer (susceptible), soybean cv. Williams 82 (resistant) and tobacco two days after inoculation. The vertical bars represent the standard error of mean log-transformed ice nucleation activity.

## 5. Temporal expression of *pip* during an infection event.

While *pip* expression increased by two days after inoculation of *X. axonopodis* pv. *glycines* into soybean, suggesting that a molecule(s) present in soybean was responsible for altering XagR function we lacked information whether such a factor was pre-formed in the plant or whether it increased after plant infection, as was suggested for the factor found in *X. oryzae* pv. *oryzae* -infected rice (Ferluga *et al.*, 2007; Ferluga and Venturi, 2009). We thus measured the expression of *pip* as a function of time after inoculation into soybean. The ice nucleation activity of wildtype *X. axonopodis* pv. *glycines* cells harboring a *pip:inaZ* fusion increased only slowly after inoculation of into soybean and the highest expression was observed 72 hr after inoculation and then decreased slowly with time (Figure 13A). The ice nucleation activity of cells of a *xagR* mutant harboring the reporter gene remained low at all times after inoculation (Figure 13A). Considerable and similar growth of the *X. axonopodis* pv. *glycines* wildtype strain and *xagR* mutant occurred during this time interval, indicating that they both progressively colonized the plant and that the lack of induction of *pip* was not due to a deficiency of the *xagR* mutant to grow in soybean (Figure 13B). These results suggest that the plant factor that enhances XagR function, and thus *pip* expression, is low in healthy plants but increases during the infection process.

1943

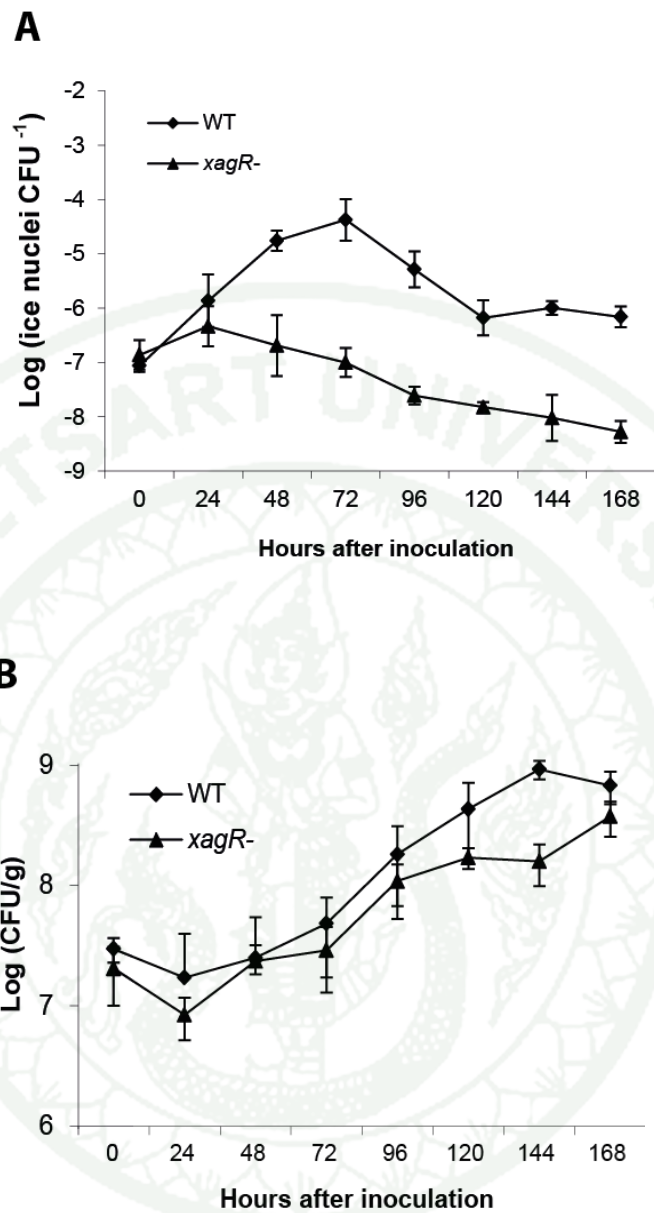


**Figure 13** Ice nucleation activity indicative of *pip* promoter activity in a wildtype strain of *Xanthomonas axonopodis* pv. *glycines* (circles) and a *xagR* mutant (triangles) harboring a *pip:inaZ* fusion at various times after infiltration into soybean leaves (A). Population size of the wildtype strain of *X. axonopodis* pv. *glycines* (circles) and a *xagR* mutant (triangles) at various times after infiltration (B). The vertical bars represent the standard error of mean log-transformed ice nucleation activity or population sizes.

## 6. XagR expression analysis

### 6.1 The *xagR* transcription analysis

Since *pip* transcription is induced by specific molecule(s) in living soybean plants and is dependent on *xagR*, we determined if the transcription of *xagR* is also enhanced by the signal molecule(s). The *xagR* promoter was cloned upstream of the promoterless *inaZ* reporter gene to yield pXagR-KI which was introduced into both the *X. axonopodis* pv. *glycines* wildtype and the *xagR* mutant strains (Figure 14).

The ice nucleation activity of both strains was similar in all culture media and *in planta*, indicating that *xagR* was constitutively expressed, even in soybean plants (Figure 15). The levels of *xagR* transcript measured by RT-PCR also did not differ under any condition (Figure 16). The constitutive expression of *xagR* differs from that of its homologs in *X. campestris* pv. *campestris* and *X. oryzae* pv. *oryzae* in that signal molecules from cabbage increased transcription of *xccR* (Furluga *et al.*, 2007; Furluga and Venturi, 2009) while *oryR* negatively regulated its own expression and functioned as a transcriptional regulator in the absence of rice signal molecules (Zhang *et al.*, 2007).

### 6.2 XagR protein level analysis

The abundance of XagR was determined by Western blot analysis using anti-OryR antibodies to which it also could bind. XagR could not be detected in cells of either the *X. axonopodis* pv. *glycines* wildtype or the *xagR* mutant when grown in minimal media with or without added macerated soybean (Figure 17). XagR was also over-expressed by placing it under the control of the *trp* promoter in pBBRMCS-5 and introducing it into *X. axonopodis* pv. *glycines* to create strain, XagROX. XagR was readily detected in XagROX when grown in minimal media (Figure 17). Importantly, abundant XagR was detected in *X. axonopodis* pv. *glycines* 12-2 wildtype cells recovered from soybean plants 72 hours or more after infiltration (Figure 17). XagR was not detected in cells harvested from plants at either 24 or 48

hours after inoculation. While the numbers of cells present in plants 48 hours after inoculation were 2-to 5-fold less than those present after 72 hours (Figure 13B) the presence of XagR in such cells should have been easily detected had it been produced at the concentrations seen in cells later in the infection process, suggesting that XagR accumulation increased substantially 48 hours or more after inoculation, much like the induction of *pip* (Figure 13A). These results indicated that some component(s) in soybean that increased during the infection process facilitated accumulation of XagR, possibly by preventing its proteolytic degradation, and thus that the modulation of XagR levels is a post-transcriptional process.

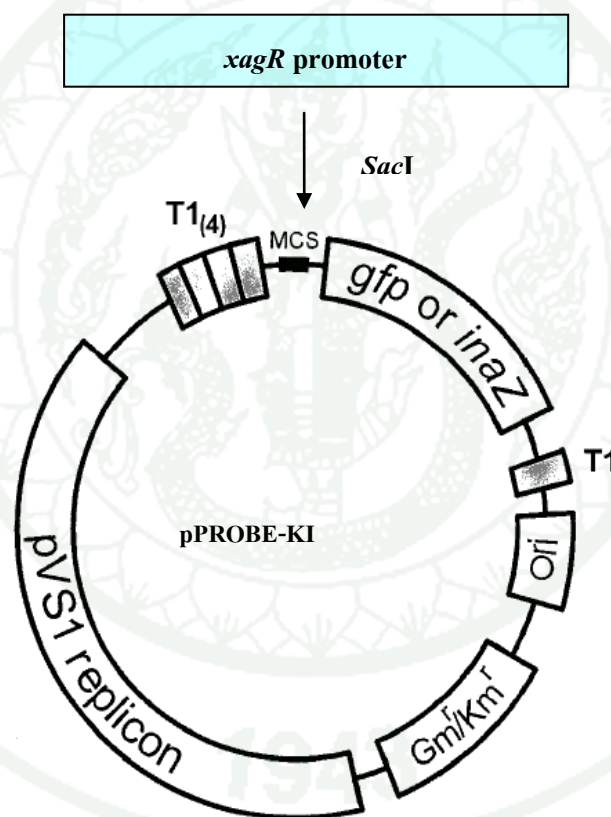


**Figure 14** pXagR-KI contain a common cassette that has four tandem copies of the T1 terminator (T1<sub>(4)</sub>; shaded boxes), a multicloning site (solid box) containing *XagR* promoter was cutted with *SacI* *inaZ* reporter genes (including optimally placed ribosome binding sites and a single *rrmB* T1 terminator (T1; shaded box) (Miller and Lindow, 1997).

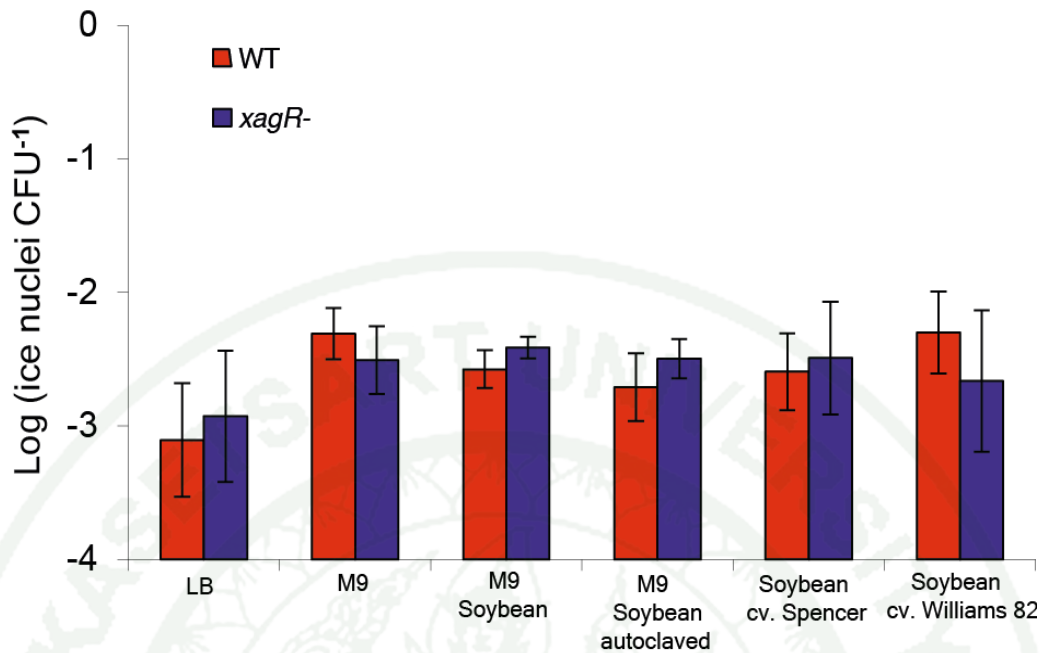


**Figure 15** Ice nucleation activity indicative of *xagR* promoter activity in a wildtype strain of *Xanthomonas axonopodis* pv. *glycines* (red bars) and a *xagR* mutant (blue bars) harboring a *xagR:inaZ* fusion when grown in various culture media including LB, M9 minimal medium, M9 minimal medium added with fresh macerated soybean, M9 minimal medium added with autoclaved soybean and when inoculated into soybean plants. The vertical bars represent the standard error of mean log-transformed ice nucleation activity or population sizes.

1943

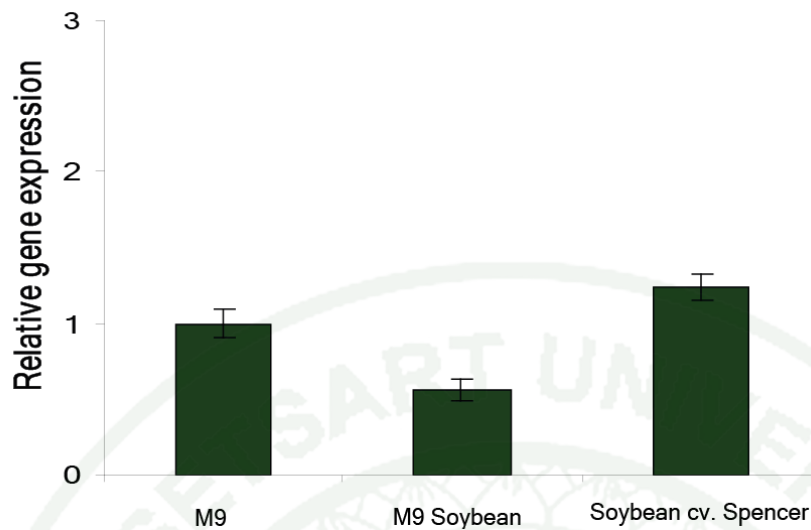


**Figure 16** Relative abundance of *xagR* transcripts in a wildtype strain of *Xanthomonas axonopodis* pv. *glycines* grown in M9 minimal media, M9 minimal media containing fresh soybean leaf macerates, or in cells *in planta* as determined by RT-PCR. The vertical bars represent the standard error of mean relative gene expression.

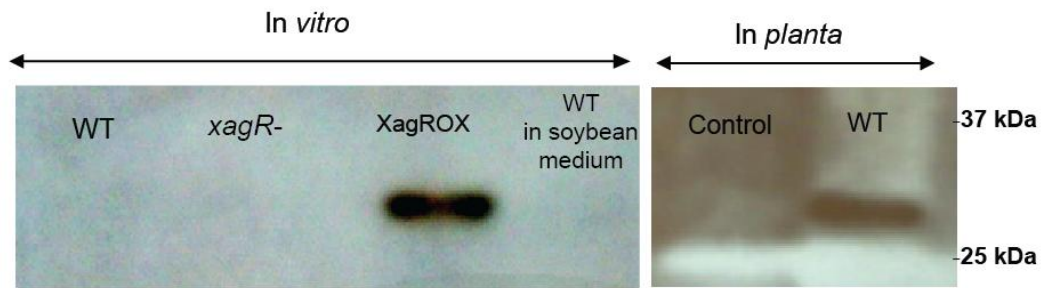


**Figure 17** Western blot analysis of XagR in different strains of *Xanthomonas axonopodis* pv. *glycines* including wildtype strain, *xagR* mutant and XagR overexpressing strain grown in minimal medium (left three lanes) or in media containing fresh soybean leaf macerates (left panel) or in uninoculated soybean leaves or leaves inoculated with the *X. axonopodis* pv. *glycines* wildtype strain 72 hours after inoculation (right panel).

## 7. The *xagR* regulon in *X. axonopodis* pv. *glycines* 12-2

To better understand the number and type of genes in *X. axonopodis* pv. *glycines* that are dependent on XagR for expression, the transcriptome of a wildtype (in which XagR does not accumulate in culture) was compared with that of the XagR-overexpressing strain, XagROX in which XagR does accumulate. The abundance of transcripts of both *xagR* and *pip* as measured by RT-PCR were significantly higher in XagROX than in the *Xag* wildtype strain, probably accounting for the higher accumulation of XagR in XagROX. RNA-Seq analysis was performed on three independent replicate RNA samples collected from each strain grown to stationary phase in M9 minimal medium. cDNA was generated from mRNA-enriched total RNA preparations from each strain and sequenced using an Illumina Genome Analyzer, with a minimum of 16,589,895 reads assignable to genes other than those in the ribosomal RNA operon (an average of 41 % of the total reads) for each replicate. As the *X. axonopodis* pv. *glycines* 12-2 genome was not completely closed, the sequence reads were aligned to ORFs present in a *X. axonopodis* pv. *glycines* 12-2 draft genome that was created for this study (see Material and Methods for details).

Transcript levels of 79 ORFs differed significantly and by at least 4 fold change and p value cut off = 0.01 between the *Xag* wildtype strain and XagROX (Figure 18). Of these, 61 genes were more highly expressed in XagROX while 18 genes were expressed at a lower level compared to the wildtype strain (Table 6). The transcript abundance of a subset of the XagR-regulated genes was also assessed using RT-PCR; very similar relative levels of transcript abundance to that observed by mRNA sequencing was seen for a given gene (Figure 19) providing evidence that RNA sequencing yielded reliable quantitative estimates of transcript abundance in this study.

The gene showing the highest induction in XagROX (9.86- $\log_2$  fold change) was *xagR* itself, confirming that in our experimental conditions XagR was indeed over-expressed. Likewise, as expected from the results of ice nucleation reporter gene assays and RT-PCR analysis, *pip* transcripts were 7.52- $\log_2$  fold change higher in

XagROX than in the wildtype strain. Other genes highly up-regulated in XagROX included those encoding membrane protease subunits (homolog XAC3964 from *X. axonopodis* pv. *citri* strain 306) and a protein similar to RtcB (homolog to XAC3965), as well as several genes with unknown function. Among the genes strongly down-regulated in XagROX was a gene encoding a homolog of a *Yersinia* autotransporter protein H (YapH) (-6.06 log<sub>2</sub> fold change). YapH is predicted to be an autotransported adhesin that contributes to leaf attachment and virulence of *X. oryzae* pv. *oryzae* to rice (Das *et al.*, 2009). Gene encoding a GAF/GGDEF/EAL domain protein and proteins involved in general stress response were also negatively regulated by XagR.

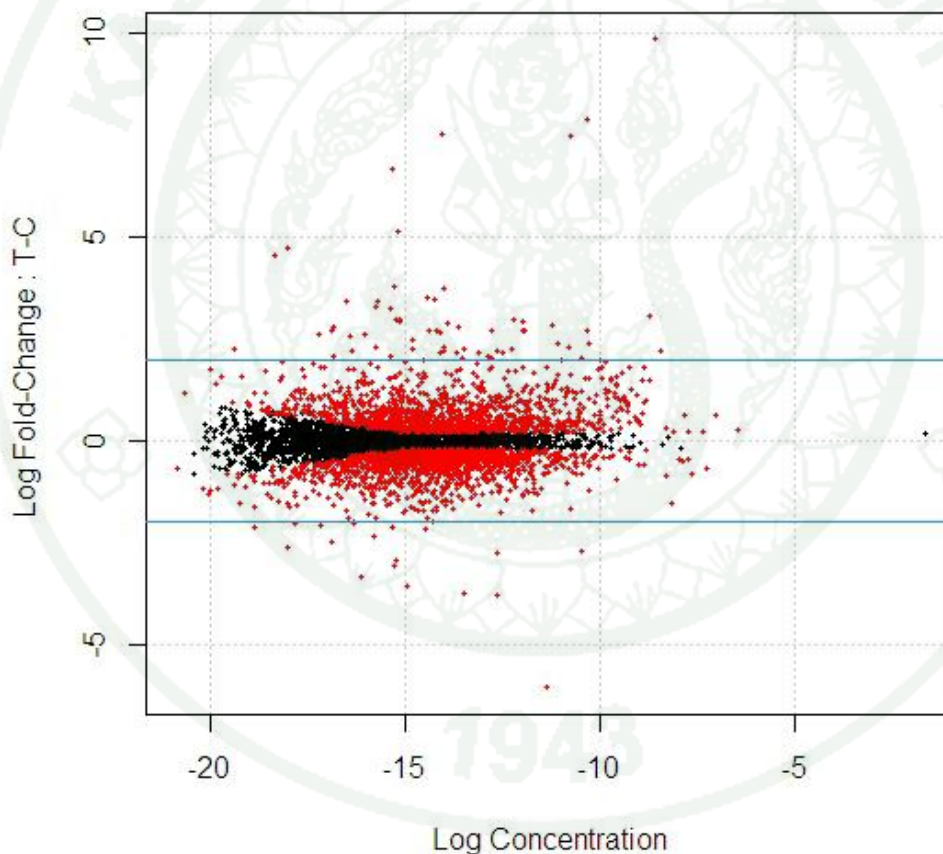


**Figure 18** The relationship between concentration and fold-change across the genes compared between XagR overexpressing strain and *X. axonopodis* pv. *glycines* wildtype. The differentially expressed genes are colored red and the non-differentially expressed are colored black. The blue line is added at a log fold change of 2 to represent a level for biological significance.

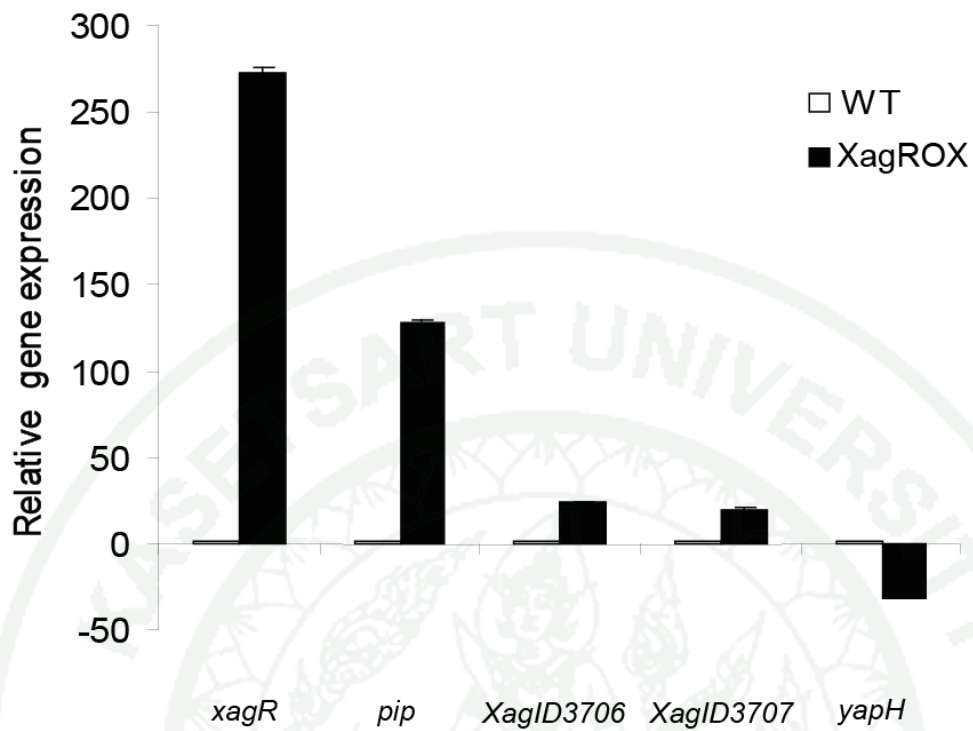


**Figure 19** The transcript abundance of a subset of the *xagR*-regulated genes in an XagR overexpressing strain compared with an *Xanthomonas axonopodis* pv. *glycines* wildtype were determined by RT-PCR analysis. The vertical bars represent the standard error of mean relative gene expression.

**Table 6** Transcriptional analysis of *Xanthomonas axonopodis* pv. *glycines* 12-2 genes controlled by *xagR*

Locus ID	Function	Log <sub>2</sub> fold change <sup>a</sup>	P_value <sup>a</sup>
XagROX/Wildtype			
<b>Genes up-regulated by <i>xagR</i></b>			
Xag2825	XagR protein (transcriptional regulator <i>ahyR/asaR</i> family)	9.865	0
Xag3706	Membrane protease subunits, stomatin/prohibitin homologs (XagID3706)	7.883	0
Xag2823	PIP (proline iminopeptidase)	7.520	0
Xag3707	Protein RtcB (XagID3707)	7.471	0
Xag2822	FIG01212123: hypothetical protein	6.665	0
Xag(1)_490	Hypothetical protein	5.123	0
Xag0399	FIG01211031: hypothetical protein	3.744	3.97E-281
Xag0914	Protocatechuate 4,5-dioxygenase alpha chain (EC 1.13.11.8)	3.798	4.42E-254
Xag0913	Protocatechuate 3,4-dioxygenase beta chain (EC 1.13.11.3)	3.489	5.97E-248
Xag2827	Amino acid transporter	3.498	1.52E-247
Xag0229	FIG01209870: hypothetical protein	3.084	2.76E-209

**Table 6** (Continued)

<b>Locus ID</b>	<b>Function</b>	<b>Log<sub>2</sub> fold change<sup>a</sup></b>	<b>P_value<sup>a</sup></b>
<b>XagROX/Wildtype</b>			
Xag0165	TRAP-type C4-dicarboxylate transport system, periplasmic component	3.439	2.80E-205
Xag3396	FIG01210979: hypothetical protein	2.956	3.55E-192
Xag0166	TRAP-type transport system, small permease component, predicted N-acetylneuraminate transporter	3.230	3.16E-191
Xag(1)_558	Hypothetical protein	2.930	1.21E-189
Xag2146	FIG024214: transcriptional regulator, AraC family	2.986	9.50E-180
Xag0915	Transcriptional regulator, LysR family	2.889	1.80E-179
Xag3054	Membrane-bound lytic murein transglycosylase B precursor (EC 3.2.1.-)	2.828	5.27E-179
Xag0167	TRAP-type C4-dicarboxylate transport system, large permease component	2.930	1.03E-174
Xag2817	Renal dipeptidase family protein	2.781	6.47E-169

**Table 6** (Continued)

<b>Locus ID</b>	<b>Function</b>	<b>Log<sub>2</sub> fold change<sup>a</sup></b>	<b>P_value<sup>a</sup></b>
<b>XagROX/Wildtype</b>			
Xag0573	2-keto-3-deoxy-D-arabino- heptulosonate-7-phosphate synthase I alpha (EC 2.5.1.54)	2.720	1.39E-167
Xag0574	Hypothetical protein	2.697	7.96E-164
Xag(1)_438	Hypothetical protein	2.685	1.51E-162
Xag(1)_559	Patatin	2.697	1.63E-162
Xag2145	FIG002283: isochorismatase family protein	2.699	1.37E-157
Xag2590	Metallopeptidase	2.678	7.11E-156
Xag1307	tRNA (guanine37-N1) - methyltransferase (EC 2.1.1.31)	2.692	8.03E-156
Xag(1)_437	Hypothetical protein	2.384	2.76E-132
Xag(1)_435	2-keto-3-deoxy-D-arabino- heptulosonate-7-phosphate synthase I alpha (EC 2.5.1.54)	2.377	3.06E-131
Xag1319	Wall associated protein	2.469	6.15E-130
Xag(1)_436	Hypothetical protein	2.279	1.21E-121
Xag1740	Regulatory protein RecX	2.273	2.14E-117
Xag3392	ATP-dependent RNA helicase RhIE	2.245	3.65E-117
Xag0779	FIG01209811: hypothetical protein	2.281	2.25E-116

**Table 6** (Continued)

<b>Locus ID</b>	<b>Function</b>	<b>Log<sub>2</sub> fold change<sup>a</sup></b>	<b>P_value<sup>a</sup></b>
<b>XagROX/Wildtype</b>			
Xag3442	Outer membrane protein W precursor	2.197	2.70E-114
Xag1481	Phospholipase A1 precursor (EC 3.1.1.32, EC 3.1.1.4); outer membrane phospholipase A	2.209	3.46E-113
Xag2826	FIG01214912: hypothetical protein	3.279	4.53E-112
Xag0789	Potassium-transporting ATPase A chain (EC 3.6.3.12) (TC 3.A.3.7.1)	3.419	2.69E-111
Xag0750	Betaine aldehyde dehydrogenase (EC 1.2.1.8)	2.225	3.80E-111
Xag0300	FIG01211436: hypothetical protein	2.161	5.41E-109
Xag2988	Type I antifreeze protein	2.238	2.50E-108
Xag(1)_466	Hypothetical protein	2.152	4.86E-107
Xag0749	Choline dehydrogenase (EC 1.1.99.1)	2.160	6.53E-105
Xag1143	FIG01212197: hypothetical protein	2.142	1.25E-104
Xag(1)_439	Hypothetical protein	2.970	2.32E-101

**Table 6** (Continued)

<b>Locus ID</b>	<b>Function</b>	<b>Log<sub>2</sub> fold change<sup>a</sup></b>	<b>P_value<sup>a</sup></b>
<b>XagROX/Wildtype</b>			
Xag2698	Cysteine protease	2.053	1.62E-98
Xag1627	SSU ribosomal protein S18p	2.019	1.93E-97
Xag(1)_560	FIG01197816: hypothetical protein	2.009	9.27E-95
Xag2149	Methyl-accepting chemotaxis protein	2.020	3.02E-94
Xag0787	Hypothetical protein	4.751	3.67E-76
Xag2657	RNA polymerase ECF-type sigma factor	2.594	1.40E-72
Xag3316	FIG01210843: hypothetical protein	2.285	3.92E-61
Xag0790	Potassium-transporting ATPase B chain (EC 3.6.3.12) (TC 3.A.3.7.1)	2.800	1.09E-55
Xag0788	FIG01212092: hypothetical protein	4.568	1.69E-52
Xag2658	FIG01210863: hypothetical protein	2.052	4.52E-51
Xag2144	Membrane protein 2, distant similarity to thiosulphate:quinone oxidoreductase DoxD	2.561	1.17E-49
Xag2821	Hypothetical protein	2.698	4.53E-41

**Table 6** (Continued)

<b>Locus ID</b>	<b>Function</b>	<b>Log<sub>2</sub> fold change<sup>a</sup></b>	<b>P_value<sup>a</sup></b>
<b>XagROX/Wildtype</b>			
Xag2143	Exoenzymes regulatory protein AepA precursor	2.221	1.06E-38
Xag0791	Potassium-transporting ATPase C chain (EC 3.6.3.12) (TC 3.A.3.7.1)	2.594	7.64E-31
Xag0168	Beta-xylosidase (EC 3.2.1.37)	2.065	8.80E-26
Xag3720	Hypothetical protein	2.270	4.62E-09
<b>Genes down-regulated by XagR</b>			
Xag2132	YapH protein	-6.070	0
Xag2137	General stress protein	-3.800	3.34E-293
Xag2133	GAF domain/GGDEF domain/EAL domain protein	-3.743	2.72E-282
Xag3507	Protein yciF	-3.560	6.27E-247
Xag3506	FIG01214889: hypothetical protein	-3.350	4.60E-111
Xag3508	Mn-containing catalase	-3.077	2.13E-186
Xag2953	N-acetylglucosamine-regulated TonB-dependent outer membrane receptor	-2.924	1.29E-170
Xag3933	Cytochrome C biogenesis protein	-2.765	8.59E-170
Xag3934	FIG01212148: hypothetical protein	-2.727	3.41E-168

**Table 6** (Continued)

<b>Locus ID</b>	<b>Function</b>	<b>Log<sub>2</sub> fold change<sup>a</sup></b>	<b>P_value<sup>a</sup></b>
<b>XagROX/Wildtype</b>			
Xag2025	Hypothetical protein	-2.637	6.63E-18
Xag2952	Predicted N-acetylglucosamine kinase, glucokinase-like (EC 2.7.1.59)	-2.497	1.57E-35
Xag(1)_907	Alpha-1,2-mannosidase	-2.342	2.87E-61
Xag1183	Glycosyl hydrolase	-2.158	3.35E-102
Xag3932	Hypothetical protein	-2.138	8.81E-10
Xag1186	Alpha-1,2-mannosidase	-2.108	3.23E-92
Xag(1)_41	Hypothetical protein	-2.094	8.41E-13
Xag3509	FIG01210612: hypothetical protein	-2.049	7.36E-12
Xag(1)_42	Hypothetical protein	-2.012	2.50E-25

<sup>a</sup>Fold change values (Log<sub>2</sub>) and adjusted P values are indicated for pairwise comparison of the differential gene expression between XagROX and wildtype using edgeR: a Bioconductor package.

## 8. XagR regulates the expression of a biosurfactant that contributes to swarming

In addition to identifying genes regulated by XagR, we explored XagR-dependent phenotypes in culture that might not be easily linked to particular genes. XccR and Pip have been shown to be virulence factors in *X. campestris* pv. *campestris* that control the production of extracellular proteases, amylases, and the ability to spread and grow in the vascular system (Zhang *et al.*, 2007). To explore whether XagR might also regulate such virulence factors, these traits were compared in the *Xag* wildtype, *xagR* mutant, *pip* mutant, *xagR/pip* double mutant, XagR complementary and XagROX strains in vitro. While the expression of these traits did not differ between the *Xag* wildtype and all mutants strains, over-production of a biosurfactant was apparent in XagROX (Figure 20). This was also associated with a concomitant increased ability of cells to spread over semisolid agar surfaces (Figure 21).

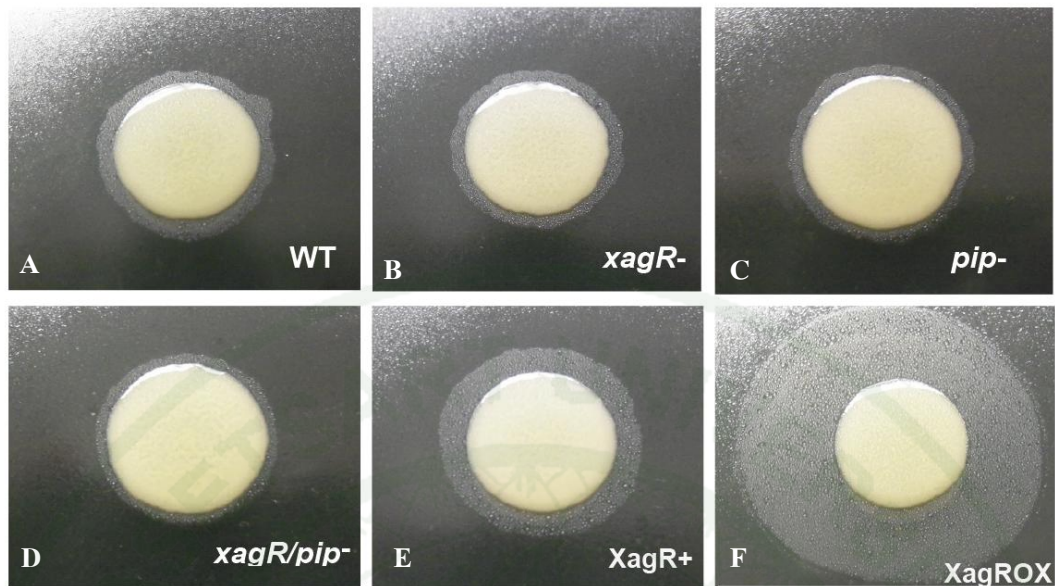


**Figure 20** Visible halos of surfactant produced by various strains of *Xanthomonas axonopodis* pv. *glycines* (A) wildtype (B) *xagR* mutant (C) *pip* mutant (D) *xagR/pip* double mutant (E) XagR complementary and (F) XagR overexpressing strain as visualized by an atomized oil assay after growth on swarming media for 3 days.

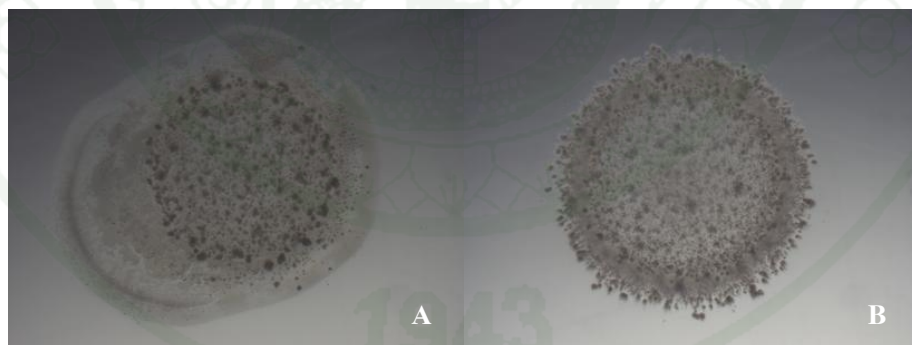


**Figure 21** The cells spread from the colony of XagR-overexpressing strain (A) and *Xanthomonas axonopodis* pv. *glycines* wildtype (B) grown on semi solid agar (0.3% LB) for 3 days.

## 9. Contribution of XagR-regulated genes to the virulence of *X. axonopodis* pv. *glycines*

While we had found that *pip*, which is regulated by XagR, is required for full virulence of *X. axonopodis* pv. *glycines* we also determined the contributions of other XagR-regulated genes. We thus disrupted the genes encoding the putative membrane protease subunit, the RtcB homolog, and the YapH homolog (designated XagID3706, XagID3707, and XagID2132 respectively) in *Xag*. The XagID3707 mutant was significantly less virulent than the wildtype strain while the incidence of disease incited by the RtcB homolog mutant was similar to that of the wildtype strain. Interestingly, the incidence of disease caused by the *yapH* mutant was significantly greater than that incited by the wildtype strain on plants incubated in the greenhouse after inoculation (Table 5).

## 10. The role of *xagR* on bacterial attachment to plants and egression from lesions

### 10.1 Attachment to abiotic surface

Given that mutants of *yapH*, which was down-regulated in cells of XagROX in which XagR had accumulated, were hyper-virulent to soybean, we addressed whether this trait was due to contributions of this protein to the adhesiveness of *X. axonopodis* pv. *glycines*. In principle, cells with low adhesiveness might more readily invade leaves and initiate infection events than cells that were more adhesive. To quantify the role of XagR and YapH in attachment to abiotic surfaces, the adhesion of cells to polystyrene microtiter plates was assessed. The number of adherent cells of the *yapH* mutant and XagROX as measured by crystal violet staining after 7 h of incubation were significantly lower than the wildtype strain; the differences in adhesion were largest when observed 24 h after inoculation (Figure 22).

## 10.2 Attachment to soybean leaf surface

The adhesion of the *yapH* mutant and XagROX strains to the surface of soybean leaves also was studied by quantifying those cells remaining on leaves after they were dipped into bacterial cell suspensions. The number of cells of the *yapH* mutant and of XagROX that remained attached after gentle washing of the inoculated leaves was significantly lower than that of both the wildtype strain and the *xagR* mutant (Figure 23). Thus XagR accumulation apparently reduces the amount of YapH available to participate in the adhesion of the cells to the surface of soybean leaves.

## 10.3 Bacterial egression assay

Since YapH contributes to attachment of *X. axonopodis* pv. *glycines* to the surface of soybean leaves, we reasoned that it might also cause it to be retained within the apoplast of infected leaves. We assessed the ability of *X. axonopodis* pv. *glycines* to egress from the apoplast by measuring the number of cells released from the edges of leaf discs cut from surface-sterilized, infected leaves. While the number of cells of the *yapH* mutant and XagROX released from the tissue were consistently higher than that of the wildtype strain, due to the high variability of these experiments these differences were not statistically significant. However, significantly fewer cells of the *xagR* mutant escaped the discs compared to the wildtype strain (Figure 24). These results suggest that XagR plays a role in the disease process by suppressing YapH expression and thus promoting *X. axonopodis* pv. *glycines* egression from the apoplast onto leaf surface where it could be spread to initiate new infections.

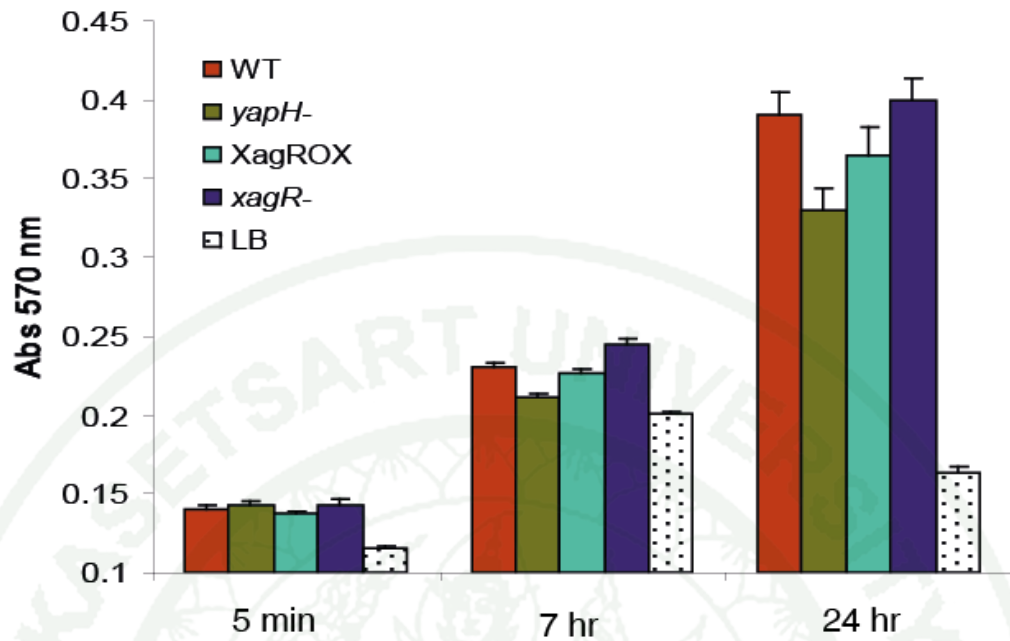


**Figure 22** Attachment of various strains of *Xanthomonas axonopodis* pv. *glycines* wildtype (red bar), *yapH* mutant (green bar), XagR overexpressing strain (light blue bar), *xagR* mutant (blue) and LB (spot bar) only to polystyrene wells assessed by crystal violet staining of adherent cells after 5 min, 7 hr and 24 hr of incubation. The vertical bars represent the standard error of mean absorbance value at 570 nm.

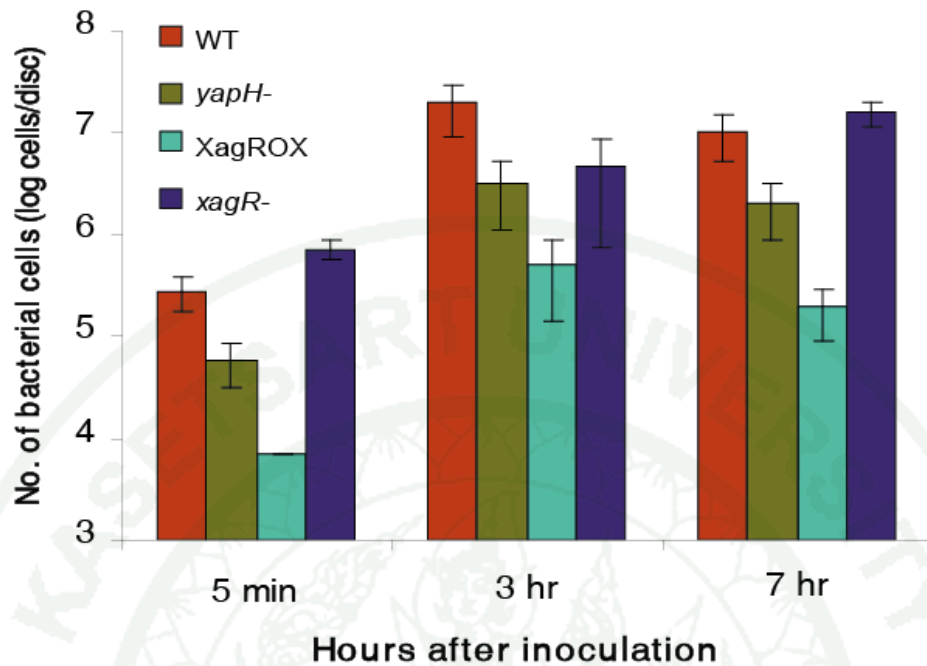


**Figure 23** Attachment of various strains of *Xanthomonas axonopodis* pv. *glycines* wildtype (red bar), *yapH* mutant (green bar), XagR overexpressing strain (light blue) and *xagR* mutant (blue) to the surface of soybean leaves after topical application at 5 min, 3 hr and 7 hr of incubation. The vertical bars represent the standard error of mean log-transformed of bacterial cell.

1943

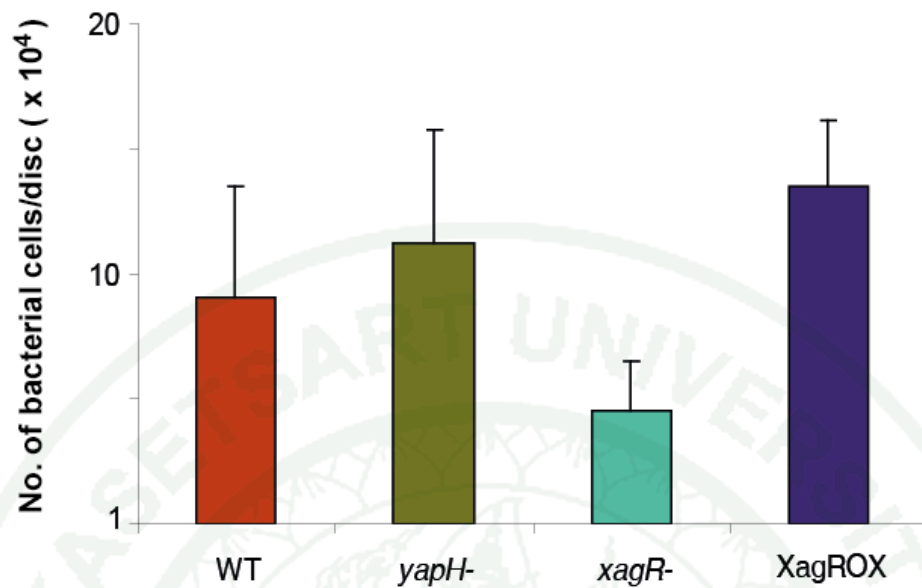


**Figure 24** Egression of the *Xanthomonas axonopodis* pv. *glycines* wildtype (red bar), *yapH* mutant (green bar), *xagR* mutant (light blue bar) and XagR overexpressing strain (blue bar) from the edges of discs of infected soybean leaves. The vertical bars represent the standard error of mean log-transformed of bacterial cell.

## 11. The role of XagR to contribute virulent on soybean under rainfall condition

While YapH-mediated cell adhesion affected the apparent virulence of *X. axonopodis* pv. *glycines*, such an effect would be expected to be context dependent. Under conditions when removal of cells from a leaf by rainfall would not be expected (such as in our initial greenhouse experiments), cells of lower adhesiveness might more easily invade leaves, while loss of adhesiveness would be expected to lead to removal of cells from leaf surfaces during rainfall events, thus lowering infection events. We thus compared the role of XagR-mediated changes in adhesiveness on virulence of *X. axonopodis* pv. *glycines* under conditions of artificial rain following topical inoculation compared with dry conditions in greenhouse experiments. Strains XagROX and the *yapH* mutant, which were less adherent to soybean leaves, both incited significantly fewer lesions than the wildtype strain when leaves were exposed to simulated rainfall 30 minutes after inoculation (Figure 25). As observed previously, the *yapH* mutant was somewhat more virulent while XagROX was less virulent than the wildtype strain when rainfall was not applied after inoculation (Figure 25).

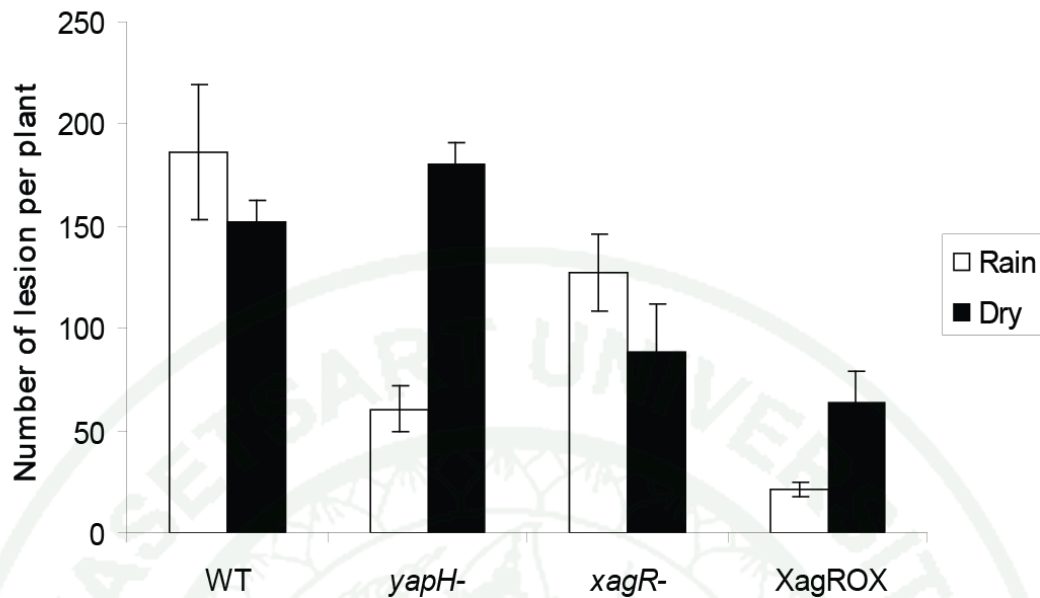


**Figure 25** Incidence of bacterial pustule disease on soybean incited of *Xanthomonas axonopodis* pv. *glycines* wildtype, *yapH* mutant, *xagR* mutant and XagR overexpressing strain after spray inoculation when plants were allowed to dry slowly after inoculation (solid bars) or which were subjected to 30 minutes of simulated rain after inoculation (open bars). The vertical bars represent the standard error of mean disease incidence per plant.

## 12. Plant-upregulated genes of *X. axonopodis* pv. *glycines* 12-2

### 12.1 Bacterial recovery from plant tissues and RNA isolation

The suspension of *Xag* 12-2 at  $10^8$  colony-forming units (cfu/ml) were vacuum infiltration into the 3-4 weeks soybean plants and incubated for 2, 3 and 4 day before used for endophyte extraction. The population of bacterial cell that obtained from 4 days infected soybean plant show the good result for bacterial cell recover and total RNA yield at 10-15  $\mu\text{g}$  of total RNA whereas the soybean infected plant at 2 or 3 days after inoculation show low quantity and quality of total RNA product at 1-3  $\mu\text{g}$ . Due to the total RNA samples from endophyte contaminated with total RNA of the soybean plants. The 18S and 28S plant rRNA and 16S and 23S bacterial rRNA were remove using Ribo-Zero rRNA Removal Kit (Plant leaf mix with Gram negative bacteria solution) and determine the mRNA quality using Bioanalyzer (Figure 26).

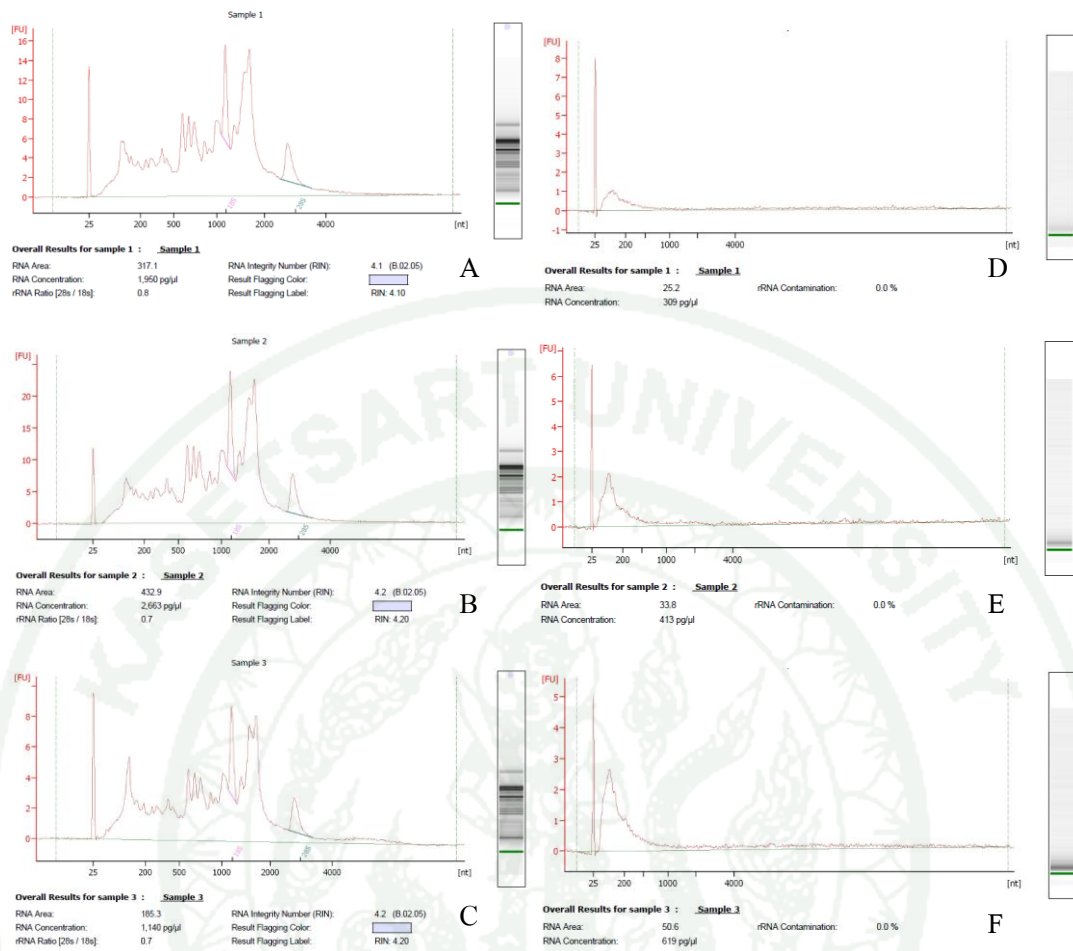


**Figure 26** Electropherogram summary of total RNA and mRNA from 3 replication of *Xanthomonas axonopodis* pv. *glycines* 12-2 recovered from infected soybean. Total RNA of sample 1 (A), sample 2 (B) and sample 3 (C) from 2100 expert\_Eukaryote Total RNA Pico. mRNA of sample 1 (D), sample 2 (E) and sample 3 (F) from 2100 expert\_mRNA Pico chip.

## 12.2 Identification of differentially expressed genes

Deep RNA sequencing technology was used to identify genes in *X. axonopodis* pv. *glycines* 12-2 that were specifically upregulated in soybean compared with growth in a laboratory culture medium. RNA-Seq analyses were performed on three independent replicate RNA samples collected from *X. axonopodis* pv. *glycines* cell recovered from soybean infected plant and compared with *X. axonopodis* pv. *glycines* strain grown to stationary phase in M9 minimal medium. cDNA was generated from mRNA-enriched total RNA preparations from each strain and sequenced using an Illumina Genome Analyzer, with a minimum of 23,452,348 (57.76%) assignable to genes other than those in the ribosomal RNA operon for each replicate. The sequence reads were aligned to ORFs present in a *X. axonopodis* pv. *glycines* 12-2 draft genome that was created for this study.

Transcript levels of 823 ORFs differed significantly by at least 4 fold change between the *X. axonopodis* pv. *glycines* recovery from soybean and *X. axonopodis* pv. *glycines* grown in M9 minimal medium. Of these, 534 genes were more highly expressed in *X. axonopodis* pv. *glycines* recovered from infected soybean plant while 289 genes were expressed in a lower level compared to the *X. axonopodis* pv. *glycines* wildtype strain grown in M9 minimal medium (Figure 27).

Among these plant-upregulated genes, several known or new putative virulence factor homologs of *Xanthomonas* spp. and other pathogens were identified (Table 7). These include the type III secretion genes *hrpB*, *hrpD*, *hrpE*, *hrpF* and *hrpX* which also have been found in *X. campestris* pv. *campestris*. Type III secretion proteins and avirulent protein were also plant-upregulated genes. In addition, the gene predicted to candidate type III effector HolPtoQ were also upregulated in *X. axonopodis* pv. *glycines* infected plant. For virulent factor of *Xanthomonas*, the secretes toxins and extracellular enzymes such as proteases, lipases and cell wall-degrading enzymes that might contribute to the host–pathogen interaction. In this study, the type II secretion proteins including polygalacturonase, xylanase precursor, halogenase, alpha-amylase, xylosidase/arabinosidase, hydrolase, endoglucanase

precursor, catalase and cysteine protease were highly expression when *X. axonopodis* pv. *glycines* grown in soybean. In addition, many chemotaxis genes, gene related to stress respond such as choline dehydrogenase, the gene involed in quorum sensing system such as RpfN protein of *X. axonopodis* pv. *glycines* 12-2 were also high expressed *in planta*. Moreover, various other genes encoding proteins with unknown function or showing no similarity to other proteins were also induced.

Several genes involved in adhesion were found to be downregulated in the host plant from our RNA sequencing data (Table 8). Bacterial attachment depends on specific adhesins that are anchored in the bacterial outer membrane and are classified into fimbrial and nonfimbrial adhesins. These include YapH protein, Sigma-fimbriae tip adhesion, putative hemolysin activation protein, Type IV fimbrial biogenesis protein FimT, PilV, PilX, PilW and PilY1. Also, the flagella cluster genes were found lower expression *in planta*. These include flagellar basal-body rod protein FlgB and FlgG, flagellar motor switch protein FliM, FliN and FliG, flagellar biosynthesis protein FliL, FliQ, FliP, FliR, FliO and FlhF, flagellar hook-basal body complex protein FliE, flagellar M-ring protein FliF, flagellar L-ring protein FlgH, flagellar hook-associated protein FliD, flagellar basal-body rod modification protein FlgD, and flagellar basal-body P-ring formation protein FlgA. Some enzyme that might be related to virulent factor were down regulated in plant included endo-1,3-beta-glucanase precursor, protease, extracellular protease precursor, 1,4-beta-cellobiosidase, cellulose and pectate lyase II.

1943

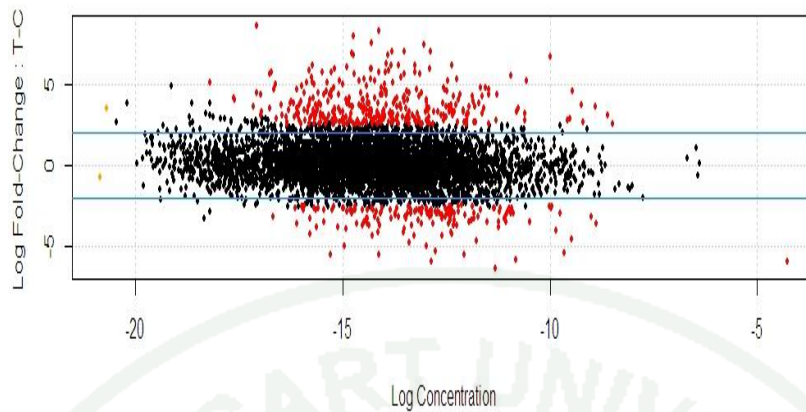


**Figure 27** The relationship between concentration and fold change across the genes compared between *Xanthomonas axonopodis* pv. *glycines* grown in plant and *X. axonopodis* pv. *glycines* in M9 minimal medium. The differentially expressed genes are colored red and the non-differentially expressed are colored black. The blue line is added at a log fold change of 2 to represent a level for biological significance.

**Table 7** The differentially plant upregulated genes in *Xanthomonas axonopodis* pv. *glycines* 12-2

Locus ID	Function	Log2 fold change <sup>a</sup>	P_value <sup>a</sup>
Xag(1)_828	hypothetical protein RND efflux system, membrane fusion	8.778194	0
Xag2689	protein CmeA	8.210077	0
Xag1076	FIG01210384: hypothetical protein	8.074402	0
Xag82	TonB-dependent receptor	7.503834	0
Xag430	HrpB1 protein	7.403575	0
Xag3780	Endonuclease	7.014861	0
Xag2620	FIG01210188: hypothetical protein	7.005384	0
Xag3924	hypothetical protein	6.97996	0
Xag1156	TonB-dependent receptor	6.919602	0
Xag3779	hypothetical protein RND efflux system, inner membrane	6.878332	0
Xag2688	transporter CmeB	6.760051	0
Xag439	Hpa1 protein Phosphate-specific outer membrane porin OprP ; Pyrophosphate-specific outer	6.725706	0
Xag3277	membrane porin OprO	6.312293	0
Xag691	Polygalacturonase (EC 3.2.1.15)	6.201521	0
Xag431	HrpB2 protein	6.198904	0
Xag3279	Acetoacetyl-CoA reductase (EC 1.1.1.36)	6.191828	0
Xag422	HrpD5 protein	6.149256	0
Xag3914	Alkaline phosphatase D Type III secretion inner membrane protein	6.098163	0
Xag434	SctL	5.974232	0
Xag3916	Phosphodiesterase/alkaline phosphatase D	5.942663	0
Xag523	FIG00401076: hypothetical protein Phosphate-specific outer membrane porin OprP ; Pyrophosphate-specific outer	5.939962	0
Xag1584	membrane porin OprO	5.935141	0
Xag81	FIG01210380: hypothetical protein	5.900601	0
Xag(1)_913	Transcriptional regulator, TetR family	5.881715	0
Xag3127	hypothetical protein RND efflux system, outer membrane	5.85923	1.36E-53
Xag2687	lipoprotein CmeC	5.794152	0
Xag1077	Glycosyltransferase RND efflux system, outer membrane	5.759589	0
Xag(1)_914	lipoprotein CmeC	5.747151	0
Xag3278	Mg <sup>++</sup> /citrate complex transporter	5.743687	0
Xag433	HrpB4 protein	5.735345	0
Xag4127	TonB-dependent receptor	5.732979	0
Xag3156	FIG01210744: hypothetical protein	5.678812	0
Xag427	HpaP protein Phosphate ABC transporter, periplasmic phosphate-binding protein PstS (TC	5.628872	0
Xag1583	3.A.1.7.1)	5.608086	0

Table 7 (Continued)

Locus ID	Function	Log2 fold change <sup>a</sup>	P_value <sup>a</sup>
	Type III secretion bridge between inner and outer membrane		
Xag432	lipoprotein(YscJ,HrcJ,EscJ,)	5.605998	0
Xag3923	peptidyl-prolyl cis-trans isomerase	5.577089	0
Xag421	HrpD6 protein	5.577052	0
Xag(1)_25	hypothetical protein	5.417946	0
Xag2127	possible serine protease homolog	5.417043	0
Xag(1)_780	Transposase	5.370671	0
Xag(1)_547	hypothetical protein	5.276028	0
Xag(1)_26	Avirulence protein	5.259792	0
Xag582	proteinase	5.2332	0
Xag723	FIG01211281: hypothetical protein	5.219275	0
	Type III secretion cytoplasmic ATP synthase (EC 3.6.3.14,		
Xag435	YscN,SpaL,MxiB,HrcN,EscN)	5.205513	0
Xag426	HrcQ protein	5.204053	0
Xag460	VirK protein	5.203294	0
Xag1060	TonB-dependent receptor	5.136185	0
Xag3875	ECF sigma factor	5.128822	0
Xag419	HpaB protein	5.072129	0
Xag725	General secretion pathway protein C	5.049016	0
	Adenine-specific methyltransferase (EC		
Xag(1)_783	2.1.1.72)	5.040171	0
Xag2260	Polygalacturonase (EC 3.2.1.15)	4.975121	0
Xag(1)_785	hypothetical protein	4.959977	3.37E-197
Xag3742	FIG01210544: hypothetical protein	4.952556	0
	Type III secretion inner membrane protein (YscU,SpaS,EscU,HrcU,SsaU, homologous to flagellar export		
Xag429	components)	4.945019	0
Xag1681	cytochrome like B561	4.940611	0
Xag2990	TonB-dependent receptor	4.932786	0
Xag476	FIG01209887: hypothetical protein	4.921502	0
	Type III secretion inner membrane protein (YscS,homologous to flagellar export		
Xag424	components)	4.80576	0
Xag3614	FIG01212471: hypothetical protein	4.77631	0
Xag3615	FIG01210406: hypothetical protein	4.762954	0
Xag2686	Transcriptional regulator, TetR family	4.759726	0
Xag(1)_100	candidate type III effector HolPtoQ	4.740154	0
Xag3509	FIG01210612: hypothetical protein	4.7106	0
Xag233	FIG01211399: hypothetical protein	4.7102	0
Xag416	HrpF protein	4.696114	0
	Putative metal chaperone, involved in Zn		
Xag(1)_37	homeostasis, GTPase of COG0523 family	4.681312	0
	Periplasmic chorismate mutase I precursor		
Xag3425	(EC 5.4.99.5)	4.674324	0

Table 7 (Continued)

Locus ID	Function	Log2 fold change <sup>a</sup>	P_value <sup>a</sup>
Xag(1)_546	hypothetical protein	4.614095	0
Xag3876	FecR protein	4.588007	0
Xag1362	FIG01209923: hypothetical protein	4.587986	0
Xag2677	FIG01210140: hypothetical protein	4.582277	0
Xag1679	Cytochrome c2	4.550983	0
Xag2621	hypothetical protein	4.532698	0
Xag1784	Alkaline phosphatase	4.525326	0
Xag1062	hypothetical protein	4.524221	0
Xag93	FIG01214754: hypothetical protein	4.519396	0
Xag3626	FIG01211117: hypothetical protein	4.504275	0
Xag381	Aerobic glycerol-3-phosphate dehydrogenase (EC 1.1.5.3)	4.480418	0
Xag3157	TonB-dependent receptor	4.459209	0
Xag3915	hypothetical protein	4.440605	0
Xag1157	Glycerophosphoryl diester phosphodiesterase (EC 3.1.4.46)	4.413053	0
Xag107	AtsE	4.402702	0
Xag291	hypothetical protein	4.352453	0
Xag(1)_36	FIG01211022: hypothetical protein	4.328929	0
Xag(1)_824	hypothetical protein	4.32648	0
Xag437	Type III secretion inner membrane protein (YscT,HrcT,SpaR,EscT,EpaR1,homologous to flagellar export components)	4.322039	0
Xag(1)_490	hypothetical protein	4.32188	0
Xag3637	FIG01209726: hypothetical protein	4.311157	0
Xag2698	Cysteine protease	4.309433	0
Xag3462	hypothetical protein	4.297122	0
Xag353	FIG01211796: hypothetical protein	4.296966	0
Xag1690	FIG01210266: hypothetical protein	4.288329	0
Xag2676	extracellular serine protease	4.286031	0
Xag423	HpaA protein	4.277699	0
Xag1161	Peroxiredoxin	4.266253	0
Xag1158	hypothetical protein	4.248689	0
Xag773	FIG01210793: hypothetical protein	4.243888	0
Xag(1)_549	Halogenase	4.235128	0
Xag(1)_804	Chemotaxis protein	4.188324	0
Xag1680	Cytochrome C	4.170594	0
Xag3001	hypothetical protein	4.165878	0
Xag438	Type III secretion outer membrane pore forming protein (YscC,MxiD,HrcC, InvG)	4.140625	0
Xag1177	Serine/threonine kinase	4.134851	0
Xag(1)_51	hypothetical protein	4.113141	0
Xag1179	hypothetical protein	4.108524	0
Xag594	Phosphoribosyl-dephospho-CoA transferase (EC 2.7.7.-)	4.032814	0
Xag436	HrpB7 protein	4.018182	0

**Table 7** (Continued)

<b>Locus ID</b>	<b>Function</b>	<b>Log2 fold change<sup>a</sup></b>	<b>P_value<sup>a</sup></b>
Xag2632	FIG01209996: hypothetical protein	4.017341	0
Xag570	FIG01212041: hypothetical protein	4.011607	0
Xag3467	hypothetical protein	4.011391	0
Xag726	General secretion pathway protein D	3.993841	0
Xag4077	putative; ORF located using Glimmer/Genemark	3.989577	0
Xag(1)_548	hypothetical protein	3.982765	0
Xag425	Type III secretion inner membrane protein (YscR, SpaR, HrcR, EscR, homologous to flagellar export components)	3.977748	0
Xag2679	FIG01210140: hypothetical protein	3.961199	0
Xag2590	Metallopeptidase	3.952725	0
Xag1061	Non-hemolytic phospholipase C	3.906412	0
Xag2988	Type I antifreeze protein	3.9032	0
Xag3000	putative cytochrome P450 hydroxylase	3.901907	0
Xag(1)_68	hypothetical protein	3.89826	0
Xag1682	FIG01210424: hypothetical protein	3.89123	0
Xag2393	FIG01209769: hypothetical protein	3.88717	0
Xag1160	Bacterioferritin	3.867096	0
Xag590	Malonate decarboxylase alpha subunit	3.854962	0
Xag615	FIG01212332: hypothetical protein	3.836405	0
Xag428	Type III secretion inner membrane channel protein (LcrD, HrcV, EscV, SsaV)	3.833124	0
Xag2257	hypothetical protein	3.827769	0
Xag(1)_53	hypothetical protein	3.820076	0
Xag1639	hypothetical protein	3.819374	7.86E-225
Xag1357	FIG01210025: hypothetical protein	3.798468	0
Xag1745	Pirin	3.793493	0
Xag1273	HrpX protein	3.790771	0
Xag2112	Alpha/beta hydrolase fold	3.777754	0
Xag2376	FIG01210040: hypothetical protein	3.728667	0
Xag3749	Protein yjbJ Phosphate transport ATP-binding protein	3.720359	0
Xag1578	PstB (TC 3.A.1.7.1)	3.719259	0
Xag2046	hypothetical protein	3.718423	0
Xag2379	TonB-dependent receptor	3.714151	0
Xag102	putative metalloprotease	3.702571	0
Xag2045	Oxidoreductase (EC 1.1.1.-)	3.700436	0
Xag1684	FIG01214411: hypothetical protein	3.68212	0
Xag595	Triphosphoribosyl-dephospho-CoA synthetase (EC 2.7.8.25)	3.676379	0
Xag1697	FIG01211473: hypothetical protein	3.669633	0
Xag628	putative; ORF located using Glimmer/Genemark	3.66909	0

Table 7 (Continued)

Locus ID	Function	Log2 fold change <sup>a</sup>	P_value <sup>a</sup>
Xag(1)_815	aklaviketone reductase	3.66771	1.01E-163
Xag1382	FIG01210130: hypothetical protein	3.652379	0
Xag2258	general stress protein	3.651729	0
Xag2678	extracellular serine protease	3.646462	0
Xag3528	FIG01212232: hypothetical protein	3.624355	0
Xag(1)_895	Serine/threonine kinase	3.614404	0
Xag3551	endonuclease precursor	3.591711	0
Xag3625	FIG01211687: hypothetical protein	3.587803	0
	Dehydrogenases with different specificities (related to short-chain alcohol dehydrogenases)		
Xag1185		3.583872	0
Xag3521	Oxidoreductase	3.579134	0
Xag1882	chemotaxis protein	3.57715	0
	Phosphoenolpyruvate-protein phosphotransferase of PTS system (EC 2.7.3.9)		
Xag2365		3.572391	0
Xag(1)_890	Urea carboxylase (EC 6.3.4.6)	3.57159	0
Xag(1)_689	hypothetical protein	3.565541	0
Xag(1)_434	hypothetical protein	3.546322	0
Xag919	Transcriptional regulator, MarR family	3.546125	0
Xag(1)_179	hypothetical protein	3.546005	2.02E-55
Xag3284	NonF-related protein	3.542948	0
	Methyl-accepting chemotaxis protein I (serine chemoreceptor protein)		
Xag(1)_23		3.539902	0
	Organic hydroperoxide resistance		
Xag295	transcriptional regulator	3.532294	0
Xag3714	FIG01211718: hypothetical protein	3.525326	0
Xag1459	Transcriptional regulator, MarR family	3.521117	0
Xag2423	hypothetical protein	3.504091	0
Xag25	FIG01209898: hypothetical protein	3.459931	0
	Xanthomonapepsin precursor (EC 3.4.21.101)		
Xag830		3.45113	0
Xag1691	Methyltransferase	3.437349	0
Xag(1)_805	FIG01214082: hypothetical protein	3.432538	0
	Predicted sucrose-specific TonB-dependent receptor		
Xag3282		3.423169	0
Xag2715	Endonuclease V (EC 3.1.21.7)	3.408261	0
Xag1285	TonB-dependent receptor	3.397361	0
Xag3708	FIG01210460: hypothetical protein	3.388142	0
Xag1582	FIG01209815: hypothetical protein	3.380665	0
	Phosphate transport system permease protein PstA (TC 3.A.1.7.1)		
Xag1579		3.375953	0
	N-formylglutamate deformylase (EC 3.5.1.68)		
Xag1642		3.373656	0
Xag3466	FIG01209884: hypothetical protein	3.368073	0
	Trehalose-6-phosphate phosphatase (EC 3.1.3.12)		
Xag3037		3.357552	0

Table 7 (Continued)

Locus ID	Function	Log2 fold change <sup>a</sup>	P_value <sup>a</sup>
Xag4081	Allophanate hydrolase (EC 3.5.1.54)	3.352548	0
Xag301	avirulence protein	3.347997	0
Xag1693	biotin synthesis protein	3.33999	0
Xag2898	predicted N-acetylglucosamine kinase, glucokinase-like (EC 2.7.1.59)	3.337222	0
Xag2765	ThiJ/PfpI family protein	3.336244	0
Xag972	Xylanase	3.332291	0
Xag40	FIG01210731: hypothetical protein	3.328993	0
Xag3530	FIG01211002: hypothetical protein	3.326345	0
Xag2467	Transposase	3.324496	0
Xag1145	Methylisocitrate lyase (EC 4.1.3.30)	3.319111	0
Xag914	Protocatechuate 4,5-dioxygenase alpha chain (EC 1.13.11.8)	3.31392	0
Xag1500	aklaviketone reductase	3.312745	0
Xag593	Malonate decarboxylase gamma subunit	3.312144	0
Xag913	Protocatechuate 3,4-dioxygenase beta chain (EC 1.13.11.3)	3.298306	0
Xag342	RND efflux system, membrane fusion protein CmeA	3.29687	0
Xag2366	1-phosphofructokinase (EC 2.7.1.56)	3.28623	0
Xag2113	2-keto-gluconate dehydrogenase	3.274409	0
Xag(1)_466	hypothetical protein	3.261741	0
Xag2411	D-amino-acid oxidase (EC 1.4.3.3)	3.259792	0
Xag2136	Protein yciE	3.259506	0
Xag592	Malonate decarboxylase beta subunit	3.24455	0
Xag1698	Radical SAM domain protein	3.241936	0
Xag591	Malonate decarboxylase delta subunit	3.241476	0
Xag2330	Succinate-semialdehyde dehydrogenase [NAD] (EC 1.2.1.24); Succinate-semialdehyde dehydrogenase [NADP+] (EC 1.2.1.16)	3.240716	0
Xag3283	alpha-amylase (EC 3.2.1.1)	3.239193	0
Xag98	FIG01211857: hypothetical protein	3.238389	0
Xag1692	chlorohydrolase family protein	3.236688	0
Xag609	FIG01210848: hypothetical protein	3.222701	0
Xag(1)_64	FIG01211857: hypothetical protein	3.212557	0
Xag138	FIG01211329: hypothetical protein	3.212262	0
Xag3396	FIG01210979: hypothetical protein	3.201526	0
Xag440	Hpa2 protein	3.194552	0
Xag2410	Hypothetical, similar to sarcosine oxidase alpha subunit, 2Fe-2S domain	3.194255	0
Xag2729	FIG01210249: hypothetical protein	3.183414	0
Xag3054	Membrane-bound lytic murein transglycosylase B precursor (EC 3.2.1.-)	3.182441	0
Xag(1)_52	FIG00964775: hypothetical protein	3.162999	0
Xag3522	UDP-glucose 4-epimerase (EC 5.1.3.2)	3.154222	1.41E-144
Xag751	High-affinity choline uptake protein BefT	3.142987	0

**Table 7** (Continued)

<b>Locus ID</b>	<b>Function</b>	<b>Log2 fold change<sup>a</sup></b>	<b>P_value<sup>a</sup></b>
Xag1197	Periplasmic aromatic aldehyde oxidoreductase, iron-sulfur subunit YagT	3.128386	0
Xag1082	Phosphate regulon transcriptional regulatory protein PhoB (SphR)	3.120047	0
Xag1764	TonB-dependent receptor	3.112238	0
Xag2392	Xylosidase/arabinosidase	3.106815	0
Xag1676	serine protease	3.101804	0
Xag1700	ABC transporter ATP-binding protein	3.100836	0
	Phosphate ABC transporter, periplasmic phosphate-binding protein PstS (TC 3.A.1.7.1)		
Xag1581		3.098377	0
Xag234	FIG01211960: hypothetical protein	3.093808	0
Xag(1)_410	hypothetical protein	3.091643	0
Xag420	HrpE protein	3.082441	0
	Phosphate transport system permease protein PstC (TC 3.A.1.7.1)		
Xag1580		3.082224	0
Xag927	FIG01214762: hypothetical protein	3.072586	0
Xag1274	FIG01213369: hypothetical protein	3.053846	0
Xag3490	Putative cytoplasmic protein	3.050362	0
Xag1438	Sigma-fimbriae chaperone protein	3.048618	0
Xag2306	FIG01210490: hypothetical protein	3.041482	0
Xag3308	hypothetical protein	3.040171	7.01E-142
Xag4128	Phosphatase	3.038431	0
Xag3263	C4-dicarboxylate transport protein	3.037983	0
Xag3159	ErfK/YbiS/YcfS/YnhG family protein	3.03094	0
Xag270	hypothetical protein	3.023112	0
Xag2377	hypothetical protein	3.007268	0
Xag3225	FIG01211035: hypothetical protein	3.007197	0
Xag3125	TonB-dependent receptor	2.984765	0
Xag(1)_733	Flagellar motor rotation protein MotB	2.969323	0
Xag646	GGDEF family protein	2.967194	0
Xag(1)_675	hypothetical protein	2.94862	0
Xag915	Transcriptional regulator, LysR family	2.948107	0
	Malonyl CoA acyl carrier protein		
Xag596	transacylase (EC 2.3.1.39)	2.945507	0
Xag979	FIG01211925: hypothetical protein	2.938084	0
	Periplasmic aromatic aldehyde oxidoreductase, FAD binding subunit		
Xag1196	YagS	2.9345	0
	DNA topoisomerase IB (poxvirus type)		
Xag39	(EC 5.99.1.2)	2.934424	0
Xag1644	Imidazolonepropionase (EC 3.5.2.7)	2.93298	0
Xag(1)_65	hypothetical protein	2.932394	0
Xag3715	FIG01210952: hypothetical protein	2.932022	0
Xag3636	putative transmembrane protein	2.928896	0
Xag101	FIG01211055: hypothetical protein	2.925707	0
Xag1678	hypothetical protein	2.919814	0

**Table 7** (Continued)

<b>Locus ID</b>	<b>Function</b>	<b>Log2 fold change<sup>a</sup></b>	<b>P_value<sup>a</sup></b>
Xag788	FIG01212092: hypothetical protein	2.918196	1.17E-90
Xag3880	Phosphoanhydride phosphohydrolase	2.91297	6.50E-139
Xag3922	FIG01211021: hypothetical protein	2.912418	0
Xag(1)_335	hypothetical protein	2.910484	0
Xag1187	short chain dehydrogenase	2.904762	0
Xag709	Putative exported protein	2.899633	0
Xag3716	Cell division inhibitor	2.899527	0
Xag1699	FIG01211092: hypothetical protein	2.898219	0
Xag2378	putative phytase precursor	2.886427	0
Xag271	Isocitrate lyase (EC 4.1.3.1)	2.881902	0
Xag2915	FIG01210781: hypothetical protein	2.876883	0
Xag3529	Uncharacterized zinc-type alcohol dehydrogenase-like protein ybdR	2.865725	0
Xag2409	Putative oxidoreductase in 4-hydroxyproline catabolic gene cluster	2.861578	0
Xag3316	FIG01210843: hypothetical protein	2.854854	0
Xag2334	Outer membrane component of tripartite multidrug resistance system	2.849676	0
Xag727	General secretion pathway protein E	2.846072	9.12E-301
Xag1806	Biofilm PGA synthesis deacetylase PgaB (EC 3.-)	2.835232	9.88E-144
Xag2418	hypothetical protein	2.828897	0
Xag980	Transcriptional regulator	2.818428	0
Xag1202	FIG01210841: hypothetical protein	2.817592	0
Xag391	hypothetical protein	2.816773	4.12E-204
Xag4108	FIG01212194: hypothetical protein	2.812404	0
Xag(1)_468	hypothetical protein	2.804847	0
Xag973	Xylanase	2.801358	0
Xag3973	FIG01212617: hypothetical protein	2.80024	0
Xag3972	hypothetical protein	2.799061	0
Xag1805	Biofilm PGA synthesis N-glycosyltransferase PgaC (EC 2.4.-.-)	2.798843	7.29E-152
Xag3160	Membrane proteins related to metalloendopeptidases	2.795839	0
Xag352	hypothetical protein	2.794851	0
Xag1683	transferase, putative	2.792125	0
Xag1081	Phosphate regulon sensor protein PhoR (SphS) (EC 2.7.13.3)	2.791446	0
Xag3527	FIG01212552: hypothetical protein	2.781256	0
Xag887	TonB-dependent receptor	2.775097	0
Xag(1)_912	Aldo-keto reductase	2.762954	0
Xag637	FIG01211260: hypothetical protein	2.761512	0
Xag2394	TonB-dependent receptor	2.758832	1.53E-162
Xag(1)_395	hypothetical protein	2.758803	0
Xag1894	Methyl-accepting chemotaxis protein I (serine chemoreceptor protein)	2.753132	0
Xag307	FIG01210121: hypothetical protein	2.750884	0

**Table 7** (Continued)

<b>Locus ID</b>	<b>Function</b>	<b>Log2 fold change<sup>a</sup></b>	<b>P_value<sup>a</sup></b>
Xag2083	Peptide synthetase	2.749927	5.40E-238
Xag(1)_827	Saccharopine dehydrogenase and related proteins	2.746355	0
Xag1686	Aminotransferase	2.742699	0
Xag216	lactoylglutathione lyase	2.738156	0
Xag4026	Putative oxidoreductase SMc00968	2.737423	0
Xag2367	PTS system, fructose-specific IIB component (EC 2.7.1.69) / PTS system, fructose-specific IIC component (EC 2.7.1.69)	2.736002	0
Xag1694	FIG01214060: hypothetical protein	2.734426	9.19E-297
Xag3953	Quino(hemo)protein alcohol dehydrogenase, PQQ-dependent (EC 1.1.99.8)	2.733049	0
Xag296	Organic hydroperoxide resistance protein	2.728519	0
Xag2128	Cobalt/zinc/cadmium efflux RND transporter, membrane fusion protein, CzcB family	2.722884	2.87E-219
Xag1638	Uncharacterized dehydrogenase [pyrroloquinoline-quinone]	2.72235	0
Xag364	hypothetical protein	2.719914	0
Xag1250	FIG01212698: hypothetical protein	2.717067	0
Xag1695	Glycosyltransferase	2.716601	5.21E-289
Xag1501	RND efflux system, membrane fusion protein CmeA	2.705331	0
Xag1696	Glycosyltransferase (EC 2.4.1.-)	2.700963	0
Xag1671	C-type cytochrome biogenesis protein	2.698109	0
Xag2408	1-pyrroline-4-hydroxy-2-carboxylate deaminase (EC 3.5.4.22)	2.697271	0
Xag3078	Glycogen debranching enzyme (EC 3.2.1.- )	2.690393	0
Xag1879	Chemotaxis response regulator protein-glutamate methyltransferase CheB (EC 3.1.1.61)	2.688144	0
Xag1358	mRNA 3-end processing factor	2.686399	0
Xag3998	histone	2.68437	0
Xag1807	Biofilm PGA outer membrane secretin PgaA	2.683872	7.59E-202
Xag297	FIG01212070: hypothetical protein	2.683295	0
Xag4104	Bifunctional protein: zinc-containing alcohol dehydrogenase; quinone oxidoreductase ( NADPH:quinone reductase) (EC 1.1.1.-); Similar to arginate lyase	2.67622	0
Xag477	Serine/threonine protein kinase	2.669086	0
Xag724	TonB-dependent receptor	2.666684	0

Table 7 (Continued)

Locus ID	Function	Log2 fold change <sup>a</sup>	P_value <sup>a</sup>
	4-carboxymuconolactone decarboxylase		
Xag394	(EC 4.1.1.44)	2.658576	0
Xag1495	Putative oxidoreductase	2.656659	0
Xag3879	TonB-dependent receptor	2.653963	1.16E-152
Xag300	FIG01211436: hypothetical protein	2.649068	0
Xag355	hypothetical protein	2.644054	0
Xag3315	FIG01211877: hypothetical protein	2.643076	0
Xag3314	FIG01212107: hypothetical protein	2.642792	0
Xag3877	FIG01214789: hypothetical protein	2.638057	7.56E-74
Xag(1)_465	hypothetical protein	2.636577	0
Xag415	HpaF protein	2.629358	0
Xag2638	FIG01211039: hypothetical protein	2.620466	0
Xag3711	FIG01213187: hypothetical protein	2.611442	0
Xag(1)_254	hypothetical protein	2.608729	1.32E-22
Xag1182	YjeF protein, C-terminal domain	2.608104	0
Xag33	hypothetical protein	2.604395	0
Xag713	Osmotically inducible protein OsmY	2.601543	0
Xag1685	FIG01209797: hypothetical protein	2.600432	0
Xag3294	hypothetical protein	2.598892	0
	putative; ORF located using		
Xag(1)_886	Glimmer/Genemark	2.592473	0
Xag1635	hypothetical protein	2.587641	0
Xag454	FIG01210004: hypothetical protein	2.584484	0
	Vanillate O-demethylase oxygenase		
Xag385	subunit (EC 1.14.13.82)	2.58082	0
Xag696	probable outer membrane protein	2.575979	0
Xag3508	Mn-containing catalase	2.571067	0
Xag108	thioredoxin	2.57023	0
Xag3518	FIG01211279: hypothetical protein	2.569223	0
Xag3495	Glycosyl transferase, family 2	2.565908	0
	putative; ORF located using		
Xag630	Glimmer/Genemark	2.562544	0
Xag2018	hypothetical protein	2.560194	0
	Cytochrome c-type biogenesis protein		
Xag1675	CcmE, heme chaperone	2.559531	0
Xag787	hypothetical protein	2.553194	4.65E-78
Xag1667	response regulator	2.550504	0
Xag954	Hydrolase	2.550003	0
Xag384	phenoxybenzoate dioxygenase beta subunit	2.549643	0
Xag3444	FIG01212352: hypothetical protein	2.547267	0
	COG2110, Macro domain, possibly ADP-ribose binding module		
Xag3135	putative; ORF located using	2.54665	0
Xag(1)_67	Glimmer/Genemark	2.545956	0
	4'-phosphopantetheinyl transferase		
Xag3917	(EC 2.7.8.-)	2.541933	0
Xag(1)_194	FIG01210791: hypothetical protein	2.541366	0

Table 7 (Continued)

Locus ID	Function	Log2 fold change <sup>a</sup>	P_value <sup>a</sup>
Xag(1)_467	FIG01122584: hypothetical protein	2.537693	0
Xag371	HDIG domain protein	2.532825	0
Xag103	oxidoreductase ylbE	2.517639	0
	Cytochrome c-type biogenesis protein CcmG/DsbE, thiol:disulfide		
Xag1673	oxidoreductase	2.511094	0
Xag1677	FIG01211823: hypothetical protein	2.510339	0
Xag3472	FIG01210877: hypothetical protein	2.502104	0
	Ketoglutarate semialdehyde		
Xag2407	dehydrogenase (EC 1.2.1.26)	2.492239	0
	Betaine aldehyde dehydrogenase (EC		
Xag750	1.2.1.8)	2.488624	0
Xag(1)_59	avirulence protein	2.486833	0
Xag3969	FIG01212617: hypothetical protein	2.483513	0
Xag1880	Chemotaxis protein CheD	2.473038	0
	Chemotaxis protein methyltransferase		
Xag1881	CheR (EC 2.1.1.80)	2.472807	0
Xag1641	Urocanate hydratase (EC 4.2.1.49)	2.469097	0
Xag2412	4-hydroxyproline epimerase (EC 5.1.1.8)	2.464615	0
	2-dehydro-3-deoxyphosphogalactonate		
Xag1760	aldolase (EC 4.1.2.21)	2.460466	0
Xag187	FIG01211455: hypothetical protein	2.457645	0
Xag622	FIG01210193: hypothetical protein	2.451579	1.21E-178
	Aconitate hydratase (EC 4.2.1.3) @ 2-		
Xag1873	methylisocitrate dehydratase (EC 4.2.1.99)	2.450134	0
Xag2050	FIG01210791: hypothetical protein	2.450064	0
Xag2633	DUF378 domain-containing protein	2.449991	1.46E-303
Xag1688	glycosyl transferase	2.446087	1.68E-247
Xag749	Choline dehydrogenase (EC 1.1.99.1)	2.443377	0
Xag(1)_734	aklaviketone reductase	2.442412	2.56E-262
Xag(1)_826	FIG01211533: hypothetical protein	2.440523	4.84E-220
Xag4013	hypothetical protein	2.431504	0
Xag3713	hypothetical protein	2.428892	0
Xag(1)_545	hypothetical protein	2.428127	0
	D-amino acid dehydrogenase small subunit		
Xag3470	(EC 1.4.99.1)	2.427493	0
Xag4124	hypothetical protein	2.42623	0
Xag3506	FIG01214889: hypothetical protein	2.421505	0
	RND efflux system, inner membrane		
Xag1502	transporter CmeB	2.411775	0
Xag3918	transglycosylase associated protein	2.40448	0
	3-isopropylmalate dehydratase large		
Xag3249	subunit (EC 4.2.1.33)	2.394342	0
Xag4080	Urea carboxylase (EC 6.3.4.6)	2.38823	0
Xag2019	FIG01212799: hypothetical protein	2.387824	0
Xag1878	C-di-GMP phosphodiesterase A	2.387425	0
Xag2663	FIG01210449: hypothetical protein	2.383377	0

Table 7 (Continued)

Locus ID	Function	Log2 fold change <sup>a</sup>	P_value <sup>a</sup>
Xag1875	FIG01210619: hypothetical protein	2.382576	0
Xag3971	hypothetical protein	2.38038	0
Xag2017	FIG01211568: hypothetical protein	2.378819	0
Xag3970	FIG01212617: hypothetical protein	2.378157	0
Xag4106	FIG01210812: hypothetical protein	2.370456	2.96E-195
	NAD(P)H oxidoreductase YRKL (EC 1.6.99.-) @ Putative NADPH-quinone reductase (modulator of drug activity B) @		
Xag(1)_66	Flavodoxin 2	2.369863	0
	Branched-chain acyl-CoA dehydrogenase (EC 1.3.99.12)		
Xag1327		2.366308	0
Xag3305	Endoglucanase precursor (EC 3.2.1.4)	2.365424	6.45E-179
Xag2109	LmbE-like protein	2.36014	0
Xag1603	hypothetical protein	2.358054	0
Xag3944	Integral membrane protein	2.348523	0
Xag1505	FIG01214345: hypothetical protein	2.347879	0
Xag235	hypothetical protein	2.343218	0
Xag3902	Possible transferase	2.343022	3.03E-307
	Methylmalonate-semialdehyde dehydrogenase (EC 1.2.1.27)		
Xag1326		2.337059	0
Xag(1)_550	RpfN protein	2.333958	1.25E-302
Xag1383	FIG01209672: hypothetical protein	2.333469	0
Xag1704	general stress protein	2.331195	0
Xag1217	hypothetical protein	2.328361	0
Xag1439	FIG01213018: hypothetical protein	2.324353	0
Xag2273	ribonuclease	2.320333	0
	Membrane fusion component of tripartite multidrug resistance system		
Xag2336		2.303801	0
	Putative metal chaperone, involved in Zn homeostasis, GTPase of COG0523 family		
Xag290		2.30177	2.11E-211
Xag729	General secretion pathway protein G	2.297214	0
Xag4074	FIG01209846: hypothetical protein	2.292987	0
Xag157	Alpha-amylase (EC 3.2.1.1)	2.28836	0
Xag731	General secretion pathway protein I	2.28828	1.16E-141
Xag578	FIG01210185: hypothetical protein	2.282959	0
Xag2337	FIG01211017: hypothetical protein	2.282541	0
	Glycosyl transferase, group 2 family protein		
Xag2111		2.282144	0
Xag3726	FIG01210985: hypothetical protein	2.279887	0
Xag1701	MFS transporter	2.279282	0
Xag2747	Phenazine biosynthesis protein PhzF like	2.277034	0
Xag(1)_95	FIG01211636: hypothetical protein	2.275459	1.58E-244
	Membrane-bound lytic murein transglycosylase B precursor (EC 3.2.1.-)		
Xag4051		2.275363	0
Xag3556	hypothetical protein	2.27431	0
Xag844	FIG01210407: hypothetical protein	2.266725	0
Xag4089	hypothetical protein	2.262291	2.94E-43

**Table 7** (Continued)

<b>Locus ID</b>	<b>Function</b>	<b>Log2 fold change<sup>a</sup></b>	<b>P_value<sup>a</sup></b>
Xag1821	FIG01212631: hypothetical protein	2.257049	0
Xag4086	candidate type III effector HolPtoQ	2.255564	0
Xag577	Gluconolactonase (EC 3.1.1.17)	2.255188	0
Xag3053	avirulence protein	2.250459	0
Xag1080	hypothetical protein	2.248299	0
Xag3645	Ribonuclease BN (EC 3.1.-.-)	2.247595	0
Xag916	Long-chain-fatty-acid--CoA ligase (EC 6.2.1.3)	2.247501	0
Xag3038	Glucoamylase (EC 3.2.1.3)	2.240472	0
Xag489	FIG01210221: hypothetical protein	2.239162	0
Xag110	Permeases of the major facilitator superfamily	2.236794	0
Xag1260	SSU ribosomal protein S20p	2.22771	0
Xag1705	ExoD protein	2.220264	0
Xag3805	hypothetical protein	2.219592	0
Xag3248	3-isopropylmalate dehydratase small subunit (EC 4.2.1.33)	2.218397	0
Xag2368	RpfN protein	2.218256	0
Xag1181	Phosphoglycerate mutase family	2.217684	0
Xag824	FIG01210643: hypothetical protein	2.212787	0
Xag748	hypothetical protein	2.212154	0
Xag838	Methyltransferase	2.210411	0
Xag950	Thymidine phosphorylase (EC 2.4.2.4)	2.207894	0
Xag3724	FIG01210442: hypothetical protein	2.207846	0
Xag728	General secretion pathway protein F	2.205691	1.25E-148
Xag917	Aldehyde dehydrogenase (EC 1.2.1.3)	2.205093	0
Xag2424	Outer membrane lipoprotein Blc	2.202218	0
Xag380	Glycerol uptake facilitator protein	2.200758	0
Xag938	ThiJ/PfpI family protein	2.19756	0
Xag1874	FIG01211890: hypothetical protein	2.188359	0
Xag(1)_573	FIG01210741: hypothetical protein	2.186178	1.29E-68
Xag1369	FIG01211227: hypothetical protein	2.185484	0
Xag2782	Calcium-binding protein	2.180201	4.74E-276
Xag1380	MFS transporter	2.179349	0
Xag969	Extracellular protease precursor (EC 3.4.21.-)	2.177777	0
Xag2767	Iron-sulfur cluster regulator IscR	2.175904	0
Xag623	FIG01211375: hypothetical protein	2.174128	1.83E-42
Xag1884	chemotaxis protein	2.173856	0
Xag236	MFS transporter	2.172434	0
Xag3974	FIG01212617: hypothetical protein	2.169584	0
Xag446	Ubiquinone biosynthesis monooxygenase	2.168029	0
Xag3309	UbiB	2.163434	5.95E-180
Xag3458	hypothetical protein	2.16117	0
Xag1758	2-dehydro-3-deoxygalactonokinase (EC 2.7.1.58)	2.148713	0

Table 7 (Continued)

Locus ID	Function	Log2 fold change <sup>a</sup>	P_value <sup>a</sup>
Xag1220	Catalase (EC 1.11.1.6)	2.147362	0
Xag642	hypothetical protein	2.145618	0
Xag(1)_3	hypothetical protein	2.145592	0
Xag762	Phage tail fiber protein	2.144836	7.41E-202
Xag2419	hypothetical protein	2.144127	3.01E-35
Xag772	Permeases of the drug/metabolite transporter (DMT) superfamily	2.143766	0
Xag1461	Membrane fusion component of tripartite multidrug resistance system	2.141082	0
Xag1897	FIG01210234: hypothetical protein	2.138871	0
Xag4066	cardiolipin synthetase	2.133867	0
Xag1559	FIG01212491: hypothetical protein	2.129384	0
Xag1063	hypothetical protein	2.12937	3.02E-95
Xag2523	FIG01209698: hypothetical protein	2.125008	0
Xag1454	Bacterioferritin	2.11798	0
Xag1672	Cytochrome c heme lyase subunit CcmL	2.117686	0
Xag3827	FIG00476006: hypothetical protein	2.116523	0
Xag829	quinone reductase	2.115778	0
Xag657	outer membrane lipoprotein	2.11454	0
Xag1787	GAF domain/GGDEF domain/EAL domain protein	2.108951	0
Xag188	FIG01210717: hypothetical protein	2.10651	0
Xag3507	Protein yciF	2.106066	0
Xag1468	FIG01211598: hypothetical protein	2.104357	0
Xag(1)_905	Putative HTH-type transcriptional regulator YjgJ, TetR family	2.103392	1.06E-150
Xag217	FIG01209935: hypothetical protein	2.100145	0
Xag2335	Inner membrane component of tripartite multidrug resistance system	2.091178	0
Xag1895	chemotaxis protein	2.08918	0
Xag(1)_581	FIG01211154: hypothetical protein	2.087062	1.45E-52
Xag1674	Cytochrome c heme lyase subunit CcmF	2.084884	0
Xag1643	Histidine ammonia-lyase (EC 4.3.1.3)	2.07977	0
Xag269	Malate synthase (EC 2.3.3.9)	2.072296	0
Xag356	NADPH:quinone oxidoreductase 2 ## possible protective/detoxification role	2.062423	0
Xag(1)_255	hypothetical protein	2.061002	1.03E-28
Xag3039	Alpha, alpha-trehalose-phosphate synthase [UDP-forming] (EC 2.4.1.15)	2.060838	0
Xag2973	tolB protein precursor, periplasmic protein involved in the tonb-independent uptake of group A colicins	2.055801	0
Xag3306	Cyclic di-GMP binding protein precursor	2.053461	2.80E-106
Xag1219	hypothetical protein	2.05307	2.21E-301
Xag846	TonB-dependent receptor	2.052767	5.45E-213
Xag2702	FIG01211834: hypothetical protein	2.052257	0

**Table 7** (Continued)

<b>Locus ID</b>	<b>Function</b>	<b>Log2 fold change<sup>a</sup></b>	<b>P_value<sup>a</sup></b>
	3-oxoadipate CoA-transferase subunit B (EC 2.8.3.6); Glutaconate CoA-transferase subunit B (EC 2.8.3.12)		
Xag387		2.052176	0
Xag3537	hypothetical protein	2.035818	1.20E-35
	putative; ORF located using Glimmer/Genemark		
Xag94		2.034892	0
Xag3751	entericidin A	2.034226	0
Xag928	integral membrane protein	2.025003	0
Xag2256	FIG01210827: hypothetical protein	2.024013	0
	Enoyl-CoA hydratase [valine degradation] (EC 4.2.1.17)		
Xag1328		2.023318	0
Xag337	hypothetical protein	2.02023	0
	Putrescine transport ATP-binding protein		1.5296272395245e
Xag2333	PotG (TC 3.A.1.11.2)	2.018163	-320
	3-oxoacyl-[acyl-carrier protein] reductase (EC 1.1.1.100)		
Xag2114		2.018109	0
Xag2344	FIG01212240: hypothetical protein	2.017444	0
Xag(1)_469	transcriptional regulator lacI family	2.01733	0
Xag1469	FIG01211421: hypothetical protein	2.012822	0
Xag(1)_616	hypothetical protein	2.009655	1.34E-193
Xag370	4-hydroxybenzoate transporter	2.008372	0
Xag4015	Xylanase precursor (EC 3.2.1.8)	2.008247	0
Xag1604	FIG01212833: hypothetical protein	2.007441	0
Xag1039	Membrane protein	2.003671	0

<sup>a</sup>Fold change values (Log<sub>2</sub>) and adjusted P values are indicated for pairwise comparison of the differential gene expression between XagROX and wildtype using edgeR: a Bioconductor package.

**Table 8** The differentially plant downregulated genes in *Xanthomonas axonopodis* pv. *glycines* 12-2

Locus ID	Function	Log2 fold change <sup>a</sup>	P_value <sup>a</sup>
Xag(1)_302	putative; ORF located using Glimmer/Genemark	-6.39118	0
Xag1295	endo-1,3-beta-glucanase precursor	-6.01759	0
Xag2784	DNA transport competence protein	-5.98737	0
Xag2132	YapH protein	-5.90949	0
Xag2829	Lysyl endopeptidase (EC 3.4.21.50) ##		
Xag486	LysXxx (including Pro)	-5.56578	0
Xag(1)_442	putative neutral zinc metalloprotease	-5.52372	0
Xag(1)_330	hypothetical protein	-5.50733	0
Xag1073	hypothetical protein	-5.4026	0
Xag3303	peptidyl-Asp metalloendopeptidase	-5.32223	0
Xag(1)_574	Serine protease	-5.0693	0
Xag3337	putative; ORF located using Glimmer/Genemark	-5.0183	0
Xag2607	Protease	-4.79787	0
Xag2472	Extracellular protease precursor (EC 3.4.24.-)	-4.67098	0
Xag1868	Inner membrane protein forms channel for type IV secretion of T-DNA complex (VirB3)	-4.58168	0
Xag(1)_288	hypothetical protein	-4.35842	0
Xag(1)_800	hypothetical protein	-4.30571	0
Xag967	hypothetical protein	-4.28574	0
Xag966	hypothetical protein	-4.25885	0
Xag965	Extracellular protease precursor (EC 3.4.21.-)	-4.23896	0
Xag3338	hypothetical protein	-4.20433	0
Xag(1)_463	Outer membrane protein	-4.19449	0
Xag1483	hypothetical protein	-4.11422	0
Xag3290	major cold shock protein	-4.02213	0
Xag3302	Outer membrane receptor for ferric coprogen and ferric-rhodotorulic acid	-3.92004	0
Xag(1)_464	FIG01212861: hypothetical protein	-3.88985	0
Xag1443	1,4-beta-cellobiosidase	-3.82554	0
Xag3860	Sigma-fimbriae tip adhesin	-3.81725	0
Xag267	putative; ORF located using Glimmer/Genemark	-3.80904	0
Xag(1)_524	hypothetical protein	-3.78897	0
Xag2585	Type IV fimbrial biogenesis protein FimT	-3.76922	0
Xag27	TonB-dependent receptor	-3.72752	0
Xag(1)_69	Cellulase	-3.71866	0
Xag(1)_305	hypothetical protein	-3.71287	0
Xag1976	ankyrin repeat protein	-3.69006	0
Xag(1)_697	Flagellar basal-body rod protein FlgB	-3.66636	0
Xag2473	hypothetical protein	-3.6268	0
	Major pilus subunit of type IV secretion complex (VirB2)	-3.60814	0

Table 8 (Continued)

Locus ID	Function	Log2 fold change <sup>a</sup>	P_value <sup>a</sup>
Xag(1)_801	hypothetical protein putative; ORF located using Glimmer/Genemark	-3.59407	0
Xag1618	Glimmer/Genemark	-3.57724	0
Xag1245	Integral membrane protein	-3.57715	0
Xag(1)_448	hypothetical protein	-3.57365	4.01E-175
Xag3289	hypothetical protein	-3.56464	0
Xag(1)_70	hypothetical protein	-3.55157	0
Xag1243	hypothetical protein	-3.54932	0
Xag(1)_812	TonB-dependent receptor	-3.53542	0
Xag2674	TonB-dependent receptor	-3.5149	0
Xag1449	Asparagine synthetase [glutamine- hydrolyzing] (EC 6.3.5.4)	-3.50853	0
Xag(1)_462	hypothetical protein Probable Co/Zn/Cd efflux system membrane fusion protein	-3.50434	0
Xag2053	fusion protein	-3.49367	0
Xag1940	Flagellar motor switch protein FliM	-3.47872	0
Xag968	Extracellular protease precursor (EC 3.4.21.-)	-3.47095	0
Xag(1)_390	Oar protein	-3.45719	0
Xag(1)_523	Type IV fimbrial biogenesis protein PilV	-3.42588	0
Xag1941	Flagellar biosynthesis protein FliL	-3.42029	0
Xag3410	Copper resistance protein B	-3.35662	0
Xag3231	Pyrophosphate-energized proton pump (EC 3.6.1.1)	-3.35213	0
Xag3612	FIG01210023: hypothetical protein	-3.3179	0
Xag(1)_309	hypothetical protein	-3.3068	0
Xag2673	TonB-dependent receptor	-3.3019	0
Xag1442	Sigma-fimbriae chaperone protein	-3.29793	0
Xag(1)_537	hypothetical protein	-3.29382	0
Xag(1)_802	hypothetical protein putative; ORF located using Glimmer/Genemark	-3.28242	0
Xag1613	Glimmer/Genemark	-3.2658	0
Xag485	FIG01209882: hypothetical protein	-3.26078	0
Xag(1)_908	TonB-dependent receptor Flagellar hook-basal body complex protein	-3.23155	0
Xag1949	FliE	-3.21824	0
Xag3908	hypothetical protein	-3.1766	0
Xag2145	FIG002283: Isochorismatase family protein	-3.17453	0
Xag2030	Manganese transport protein MntH	-3.15143	0
Xag2779	putative exported protein putative; ORF located using Glimmer/Genemark	-3.12785	0
Xag(1)_339	Glimmer/Genemark	-3.10896	0
Xag858	Haemin uptake system outer membrane receptor Forms the bulk of type IV secretion complex that spans outer membrane and periplasm	-3.08857	0
Xag2477	(VirB9)	-3.07708	0
Xag3104	TonB-dependent receptor	-3.07584	0

Table 8 (Continued)

Locus ID	Function	Log2 fold change <sup>a</sup>	P_value <sup>a</sup>
Xag(1)_542	hypothetical protein	-3.07343	0
Xag(1)_443	Phage T7 exclusion protein	-3.06895	0
Xag(1)_268	Flagellar biosynthesis protein FliQ	-3.06017	0
Xag4031	OmpA-related protein	-3.05768	0
Xag3353	TonB-dependent receptor	-3.05109	0
Xag2587	Oar protein	-3.0331	0
Xag1936	Flagellar biosynthesis protein FliQ	-3.01929	0
Xag1773	sensor kinase	-3.00067	0
Xag3409	Multicopper oxidase	-3.00005	0
Xag(1)_449	hypothetical protein	-2.9974	0
Xag(1)_521	Type IV fimbrial biogenesis protein PilX	-2.99683	0
Xag3656	Cytochrome c oxidase polypeptide I (EC 1.9.3.1)	-2.99485	0
Xag2133	GAF domain/GGDEF domain/EAL domain protein	-2.97095	0
Xag1939	Flagellar motor switch protein FliN	-2.96686	0
Xag135	Aldehyde dehydrogenase (EC 1.2.1.3)	-2.96455	0
Xag1513	Serine peptidase	-2.96336	0
Xag(1)_682	hypothetical protein	-2.95579	0
Xag960	NAD(P) transhydrogenase alpha subunit (EC 1.6.1.2)	-2.95557	0
Xag2470	FIG01213965: hypothetical protein	-2.95484	0
Xag2478	Inner membrane protein forms channel for type IV secretion of T-DNA complex (VirB8)	-2.95117	0
Xag2775	Iron-uptake factor PiuC	-2.93698	0
Xag2475	ATPase provides energy for both assembly of type IV secretion complex and secretion of T-DNA complex (VirB11)	-2.93191	0
Xag2774	TonB-dependent receptor	-2.92801	0
Xag2464	TonB-dependent receptor	-2.90923	0
Xag2953	N-acetylglucosamine-regulated TonB-dependent outer membrane receptor	-2.90179	0
Xag1948	Flagellar M-ring protein FliF	-2.87556	0
Xag(1)_644	Cyclic beta-1,2-glucan synthase (EC 2.4.1.-)	-2.8595	0
Xag(1)_340	VirB6 protein	-2.85542	0
Xag2777	putative membrane protein	-2.84761	0
Xag(1)_291	hypothetical protein	-2.84265	0
Xag3933	cytochrome C biogenesis protein	-2.84073	0
Xag4085	FIG01214495: hypothetical protein	-2.83615	0
Xag833	Alpha-amylase	-2.83484	0
Xag(1)_515	hypothetical protein	-2.82906	0
Xag(1)_374	FIG01210862: hypothetical protein	-2.81245	0
Xag2465	Maltodextrin glucosidase (EC 3.2.1.20)	-2.81005	0
Xag1297	Alpha-N-arabinofuranosidase 2 (EC 3.2.1.55)	-2.81	0
Xag(1)_445	FIG014574: hypothetical protein	-2.80975	0
Xag(1)_44	probable ATP /GTP binding protein	-2.80211	0

Table 8 (Continued)

Locus ID	Function	Log2 fold change <sup>a</sup>	P_value <sup>a</sup>
Xag(1)_810	hypothetical protein	-2.79182	0
Xag855	putative; ORF located using Glimmer/Genemark	-2.77203	0
Xag1611	putative; ORF located using Glimmer/Genemark	-2.77053	0
Xag(1)_441	hypothetical protein	-2.76014	0
Xag(1)_436	hypothetical protein	-2.7543	0
Xag(1)_61	hypothetical protein	-2.74659	0
Xag(1)_10	hypothetical protein	-2.7405	0
Xag2176	Type IV secretory pathway, VirB4 components	-2.74046	6.97E-148
Xag(1)_446	Putative deoxyribonuclease similar to YcfH, type 4	-2.73936	0
Xag2780	Thiamin biosynthesis lipoprotein ApbE	-2.72598	0
Xag1614	FIG01212788: hypothetical protein	-2.72257	0
Xag(1)_710	hypothetical protein	-2.72203	0
Xag1336	Serine protease precursor MucD/AlgY associated with sigma factor RpoE	-2.72189	0
Xag1183	Glycosyl hydrolase	-2.71933	0
Xag2778	putative exported protein	-2.70684	0
Xag(1)_437	hypothetical protein	-2.70333	0
Xag3653	Cytochrome c oxidase polypeptide III (EC 1.9.3.1)	-2.70331	0
Xag1612	FIG01212272: hypothetical protein	-2.70047	0
Xag3655	FIG01210764: hypothetical protein	-2.68771	0
Xag(1)_514	hypothetical protein	-2.67579	0
Xag1610	SECRETION ACTIVATOR PROTEIN	-2.67081	0
Xag(1)_307	hypothetical protein	-2.66361	0
Xag3657	Cytochrome c oxidase polypeptide II (EC 1.9.3.1)	-2.65406	0
Xag3934	FIG01212148: hypothetical protein	-2.65011	0
Xag285	FIG01212647: hypothetical protein	-2.64714	0
Xag3394	TonB-dependent receptor	-2.63704	0
Xag3070	hypothetical protein	-2.62848	0
Xag182	Fatty acid desaturase (EC 1.14.19.1); Delta-9 fatty acid desaturase (EC 1.14.19.1)	-2.62079	0
Xag(1)_554	hypothetical protein	-2.61028	0
Xag2820	pectate lyase II	-2.60932	0
Xag859	Hemin transport protein	-2.60837	0
Xag(1)_633	hypothetical protein	-2.60257	0
Xag(1)_306	hypothetical protein	-2.5793	0
Xag1971	Flagellar basal-body rod protein FlgG	-2.57876	0
Xag67	hypothetical protein	-2.57773	0
Xag(1)_872	Programmed cell death antitoxin MazE like	-2.57614	0
Xag(1)_522	Type IV fimbrial biogenesis protein PilW	-2.57413	0
Xag2776	FOG: TPR repeat, SEL1 subfamily	-2.56464	0
Xag(1)_879	Nucleotidyltransferase (EC 2.7.7.-)	-2.56335	0

Table 8 (Continued)

Locus ID	Function	Log2 fold change <sup>a</sup>	P_value <sup>a</sup>
Xag3498	FIG01210787: hypothetical protein	-2.55956	0
Xag1244	FIG01212000: hypothetical protein	-2.54505	0
Xag(1)_42	hypothetical protein Probable Co/Zn/Cd efflux system membrane	-2.54313	0
Xag(1)_328	fusion protein	-2.54278	0
Xag(1)_520	Type IV fimbrial biogenesis protein PilY1	-2.53395	0
Xag2166	FIG036757: Plasmid-related protein	-2.52682	2.55E-249
Xag2513	Oar protein	-2.51829	0
Xag2054	Transport protein Methanol dehydrogenase large subunit	-2.51598	0
Xag679	protein (EC 1.1.99.8)	-2.5155	0
Xag1405	ABC transporter ATP-binding protein	-2.51107	0
Xag(1)_231	hypothetical protein	-2.509	0
Xag1970	Flagellar L-ring protein FlgH	-2.50533	0
Xag(1)_461	TonB-dependent receptor	-2.50134	0
Xag(1)_678	hypothetical protein	-2.50102	0
Xag(1)_894	cell wall hydrolase/autolysin	-2.49123	0
Xag(1)_341	hypothetical protein	-2.48639	0
Xag(1)_555	hypothetical protein	-2.4754	0
Xag(1)_769	response regulator	-2.47037	0
Xag(1)_385	FIG076676: Hypothetical protein TldD family protein, Actinobacterial	-2.46931	0
Xag124	subgroup	-2.46445	0
Xag860	FIG01212468: hypothetical protein	-2.45725	0
Xag(1)_651	hypothetical protein	-2.4393	0
Xag(1)_321	hypothetical protein	-2.43057	0
Xag1321	hypothetical protein	-2.42627	0
Xag(1)_239	hypothetical protein	-2.41882	0
Xag(1)_530	phage-related integrase	-2.40705	6.38E-224
Xag(1)_649	phospholipase D/Transphosphatidylase	-2.40653	0
Xag1964	Flagellar hook-associated protein FliD	-2.40534	0
Xag(1)_708	hypothetical protein	-2.40009	1.35E-191
Xag2461	Six-hairpin glycosidase-like protein	-2.39765	0
Xag1619	FIG01212609: hypothetical protein ABC-type bacteriocin/lantibiotic exporters, contain an N-terminal double-glycine	-2.3937	0
Xag(1)_646	peptidase domain	-2.39314	0
Xag2883	hypothetical protein	-2.3886	0
Xag(1)_665	deoxycytidylate deaminase( EC:3.5.4.12 )	-2.38405	0
Xag(1)_45	ATP-dependent helicase	-2.38009	0
Xag(1)_312	hypothetical protein ubiquinol cytochrome C oxidoreductase,	-2.37808	0
Xag2316	cytochrome C1 subunit	-2.36761	0
Xag1448	hypothetical protein	-2.36117	0
Xag26	hypothetical protein	-2.36059	0
Xag(1)_481	hypothetical protein	-2.36058	0

Table 8 (Continued)

Locus ID	Function	Log2 fold change <sup>a</sup>	P_value <sup>a</sup>
	Flagellar basal-body rod modification protein		
Xag1974	FlgD	-2.36039	0
Xag(1)_680	GlyA	-2.35789	0
Xag(1)_736	MchC protein	-2.35076	0
Xag3658	FIG01209735: hypothetical protein	-2.34698	0
	Inner membrane protein of type IV secretion		
Xag(1)_836	of T-DNA complex, VirB6	-2.34579	0
Xag(1)_400	hypothetical protein	-2.34145	0
Xag(1)_880	hypothetical protein	-2.32738	0
Xag3393	peptidase	-2.32421	0
	Inner membrane protein forms channel for		
	type IV secretion of T-DNA complex		
Xag2476	(VirB10)	-2.32374	0
Xag2107	O-methyltransferase	-2.31812	0
Xag(1)_494	hypothetical protein	-2.31796	0
Xag(1)_401	hypothetical protein	-2.31387	0
	Probable Co/Zn/Cd efflux system membrane		
Xag3909	fusion protein	-2.2982	0
	TonB-dependent receptor; Outer membrane		
Xag3400	receptor for ferrienterochelin and colicins	-2.29726	0
Xag1269	PDZ domain family protein	-2.29018	0
Xag1518	Ferric uptake regulation protein FUR	-2.29006	0
Xag1343	Response regulator	-2.27182	0
Xag(1)_543	wall-associated protein	-2.26854	0
Xag(1)_338	Sensor kinase	-2.26119	0
Xag(1)_270	Flagellar biosynthesis protein FliP	-2.26015	0
	Cytosine-specific DNA methyltransferase		
Xag2161	(EC 2.1.1.37)	-2.25908	9.71E-77
	Outer membrane receptor for ferric coprogen		
Xag3161	and ferric-rhodotorulic acid	-2.2544	0
Xag(1)_532	hypothetical protein	-2.25035	0
	POSSIBLE LINOLEOYL-CoA		
	DESATURASE (DELTA(6)-		
Xag3703	DESATURASE)	-2.24351	0
Xag2055	Transport protein	-2.23698	0
Xag3788	TonB-dependent receptor	-2.23225	0
Xag(1)_245	hypothetical protein	-2.23211	0
	ATPase provides energy for both assembly of		
	type IV secretion complex and secretion of		
Xag2471	T-DNA complex (VirB4)	-2.23203	0
	2-keto-3-deoxy-D-arabino-heptulosonate-7-		
Xag573	phosphate synthase I alpha (EC 2.5.1.54)	-2.22421	0
Xag(1)_751	hypothetical protein	-2.22354	0
	2-keto-3-deoxy-D-arabino-heptulosonate-7-		
Xag(1)_435	phosphate synthase I alpha (EC 2.5.1.54)	-2.21806	0
Xag(1)_632	hypothetical protein	-2.21294	0
Xag2930	FIG01211050: hypothetical protein	-2.2069	0

Table 8 (Continued)

Locus ID	Function	Log2 fold change <sup>a</sup>	P_value <sup>a</sup>
Xag(1)_289	conserved hypothetical protein	-2.20201	0
	Cobalt-zinc-cadmium resistance protein		
Xag3907	CzcA; Cation efflux system protein CusA	-2.20113	0
Xag3203	FIG019278: hypothetical protein	-2.1952	0
	FIG024214: Transcriptional regulator, AraC family		
Xag2146		-2.17718	1.75E-150
Xag(1)_650	Serine/threonine protein kinase	-2.17176	0
Xag(1)_813	TonB-dependent receptor	-2.16613	0
Xag1947	Flagellar motor switch protein FliG	-2.16355	0
Xag(1)_39	hypothetical protein	-2.16093	0
Xag1935	Flagellar biosynthesis protein FliR	-2.15326	0
Xag(1)_132	hypothetical protein	-2.1524	0
Xag2460	Predicted maltose transporter MalT	-2.15144	0
Xag3505	FIG01211680: hypothetical protein	-2.14582	5.61E-259
Xag3413	FIG01209832: hypothetical protein	-2.14167	0
Xag618	hypothetical protein	-2.14046	0
	putative; ORF located using Glimmer/Genemark		
Xag1918		-2.13984	0
Xag2704	FIG01209686: hypothetical protein	-2.13872	0
Xag(1)_643	hypothetical protein	-2.13736	0
Xag(1)_658	hypothetical protein	-2.13632	4.288e-314
Xag1938	Flagellar biosynthesis protein FliO	-2.13616	0
Xag3330	General secretion pathway protein K	-2.13258	0
Xag3112	Aminopeptidase N	-2.13225	0
Xag3652	hypothetical protein	-2.12998	0
Xag3340	outer membrane protein	-2.12891	0
	Ubiquinol--cytochrome c reductase, cytochrome B subunit (EC 1.10.2.2)		
Xag2317		-2.12244	0
Xag(1)_447	hypothetical protein	-2.12038	1.12E-38
	Phage T7 exclusion protein associated		
Xag(1)_444	hypothetical protein	-2.11451	0
Xag2309	chemotaxis protein	-2.11324	0
Xag(1)_737	putative hemolysin activation protein	-2.11234	0
Xag3059	hypothetical protein	-2.10898	0
Xag3420	ABC transporter permease	-2.10343	0
Xag(1)_777	RelA/SpoT domain protein	-2.10039	0
Xag(1)_287	Rhs family protein	-2.09943	0
	TldE/PmbA family protein, Actinobacterial subgroup		
Xag123		-2.09854	0
Xag(1)_275	FIG01214483: hypothetical protein	-2.09638	0
Xag(1)_46	hypothetical protein	-2.09281	0
Xag3105	TonB-dependent receptor	-2.0918	0
	Ubiquinol-cytochrome C reductase iron-sulfur subunit (EC 1.10.2.2)		
Xag2318		-2.09083	0
Xag(1)_308	Superfamily I DNA helicase	-2.09074	0
Xag1959	RNA polymerase sigma-54 factor RpoN	-2.09058	0

**Table 8** (Continued)

Locus ID	Function	Log2 fold change <sup>a</sup>	P_value <sup>a</sup>
Xag(1)_172	FIG045374: Type II restriction enzyme, methylase subunit YeeA	-2.08608	0
Xag1908	FIG01214483: hypothetical protein	-2.08118	9.47E-303
Xag(1)_556	hypothetical protein	-2.0796	0
Xag(1)_322	hypothetical protein	-2.0771	0
Xag(1)_645	MchC protein	-2.07488	0
Xag(1)_499	DNA-binding protein H-NS	-2.06946	0
Xag(1)_377	FIG036757: Plasmid-related protein	-2.06945	0
Xag1927	Flagellar biosynthesis protein FlhF	-2.06013	0
Xag(1)_700	IS1595 transposase	-2.05826	6.43E-125
Xag(1)_387	FIG01214131: hypothetical protein	-2.05064	4.16E-216
Xag2819	FIG01210039: hypothetical protein	-2.04467	3.94E-238
Xag1441	Sigma-fimbriae usher protein	-2.03833	0
Xag(1)_325	hypothetical protein	-2.03566	0
Xag(1)_372	Superfamily II DNA/RNA helicases, SNF2 family	-2.03522	0
Xag2858	Histidine kinase/response regulator hybrid protein	-2.03396	8.32E-306
Xag(1)_867	response regulator	-2.03299	0
Xag(1)_656	hypothetical protein	-2.02918	0
Xag(1)_929	3-oxoacyl-[acyl-carrier-protein] synthase, KASIII (EC 2.3.1.41)	-2.02791	0
Xag(1)_519	Type IV pilus biogenesis protein PilE	-2.02502	0
Xag1978	Flagellar basal-body P-ring formation protein FlgA	-2.01943	0
Xag2544	NADH ubiquinone oxidoreductase chain A (EC 1.6.5.3)	-2.01933	0
Xag2468	carboxypeptidase	-2.01712	0
Xag1958	response regulator	-2.01558	0
Xag(1)_683	hypothetical protein	-2.0142	0
Xag284	FIG024006: iron uptake protein	-2.00621	0

<sup>a</sup>Fold change values (Log<sub>2</sub>) and adjusted P values are indicated for pairwise comparison of the differential gene expression between XagROX and wildtype using edgeR: a Bioconductor package.

## Discussion

Bacterial pustule (BP) disease remains a key production constraint in worldwide including Thailand, where its endemic occurrence continues to have effects on subsistence from communities. Bacterial pustule caused by *X. axonopodis* pv. *glycines* is a foliar pathogen of soybean that Thailand local cultivars such as SJ group are particularly susceptible to the disease. Generally, when bacterial plant pathogens penetrate host cells through stomata or wounds, a series of defense responses is induced in host plants resulting to hypersensitive response (HR) or disease symptoms occur depend on it interaction between soybean. Bacterial pustule symptoms of natural infection under farming system are small pale green spots, yellow to brown lesions with raised pustules in the center (Weber *et al.*, 1966). Spots of BP vary from minute specks to large, irregular, mottled brown areas that arise when smaller lesion coalesce in later stages. The dried lesions, broken remnants of pustules seen on small brown necrotic are surrounded by narrow yellowing haloes. When the disease is severe, the leaves cause premature defoliation resulting in reducing photosynthesis and decreased yield both in quantity and quality (Weber *et al.*, 1966). Understanding how pathogen infects plants and how plants respond to pathogen attack is essential for developing efficient management strategies of plant disease.

Recent studies about the interaction between soybean and *X. axonopodis* pv. *glycines* that cover a biology of pathogen, disease development, and development of biological control. The quorum sensing system of *X. axonopodis* pv. *glycines* 12-2 is essential for virulence on soybean. The *rpfF* mutant of *X. axonopodis* pv. *glycines* strain 12-2 was attenuated in DSF production, extracellular polysaccharide, the extracellular enzymes cellulase, protease, endo- $\beta$ -1,4-mannanase, and pectate lyase, which would normally be expressed when cell densities are high. Significant reductions in biofilm formation, population density, and virulence on soybean as well as DSF abolishment were also observed. In contrast, the siderophore production was increased in *X. axonopodis* pv. *glycines* *rpfF* mutant (Thowthampitak *et al.*, 2008). The gene involved in motility also have been report in *X. axonopodis* pv. *glycines*

strain 12-2 and strain SW005. Flagellar and pili proteins are also a virulence factor in this bacterium. The *flgC*, *flgK*, *fliC*, and *fliD* mutants were decreased virulence on soybean and lost swimming movement, except *fliD* mutant decreased swim on the Luria Bertani (LB) agar with 0.4% agar. Likewise, *pilD* mutant was lost twitching motility (Athiniwat 2009). Another gene, *xagP*, that encodes a pectate lyase in *X. axonopodis* pv. *glycines*, was shown to be essential for induction of HR on tobacco but not on pepper, cucumber, sesame, and tomato. The *xagP* mutant failed to induce HR on tobacco and epiphytic fitness analysis of the *xagP* mutant on nutrient glucose broth and tobacco leaves indicated that its population density was similar with the wildtype (Kaewnum *et al.*, 2006). The another Xag phosphoenol pyruvate synthase (*ppsA*) genes of *X. axonopodis* pv. *glycines* mutant strain KUMNTP2 reduced cell multiplication and affected extracellular cellulase secretion protein related to HR induction on tobacco (*Nicotiana tabacum* cv. Xanthi), but still induced cell death on tomato (*Lycopersicon esculentum* cv. Sridatip-II). This result indicated that *ppsA* might be affected to HR induction on tobacco base on protein secretions involved in the number of cell multiplication (Kasem *et al.*, 2007).

To gain more knowledge of *X. axonopodis* pv. *glycines* 12-2 and soybean interaction the draft genome of *X. axonopodis* pv. *glycines* 12-2 was performed in this study. Recent developments in DNA-sequencing technology provide opportunities for rapid and cost-effective comparative genomics studies (MacLean *et al.*, 2009). We used the 'Next Generation' 454 sequencing and Illumina Solexa GA technology (Bentley *et al.*, 2008) to generate draft genome sequences for bacterial pustule pathogen *X. axonopodis* pv. *glycines* 12-2. This *Xag* 12-2 shared significantly greater nucleotide identity with *Xanthomonas* foliar pathogen genome other than with the genome of vascular pathogen *Xanthomonas* genome. Genetic differences may also reflect adaptations for epiphytic fitness and for invasion and colonization in the host cells. Plant-pathogenic *Xanthomonas* pathovars require a type III secretion to secrete and translocate effector proteins in order to cause disease. The unique gene of *X. axonopodis* pv. *glycines* 12-2 also found the gene encoded avirulence protein that might play an important role for soybean and *X. axonopodis* pv. *glycines* specific interaction. These effectors have evolved to manipulate host cellular processes to the

benefit of the pathogen; however, many plants have evolved resistance whereby they can recognize specific effectors, triggering the HR. Therefore, in the context of a resistant plant, these effectors show an 'avirulence' activity, thus limiting the pathogen's host range (Alfano and Collmer, 2004; Buttner and Bonas, 2009). In addition, mobile genetic elements, such as phage-related and IS elements, were well represented in *X. axonopodis* pv. *glycines* 12-2 unique genes list. These pathovar-specific differences in gene content might give us some clues about targeted approaches for disease control and will last but not least allow the precise PCR-based diagnosis of bacterial diseases.

Several genes are related to bacterial adhesin and flagellar protein were found as unique genes in *X. axonopodis* pv. *glycines* 12-2. Bacterial attachment to host tissues by various adhesins is a first step in the pathogenesis of many animal pathogens, but a role for attachment in plant pathogenesis is less clear. The necrogenic pathogens have been reported to produce a variety of potential adhesins, including fimbriae by *Erwinia rhapontici*, *E. carotovora*, *P. syringae*, *X. campestris* and *Ralstonia solanacearum*, type IV pili by *P. syringae* and adhesive factors such as lipopolysaccharide by *R. solanacearum* (Romantschuk, 1992). Attachment to leaf surfaces by type IV pili slightly promotes the epiphytic fitness of *P. syringae*, and the related process of self aggregation is also promoted in *P. syringae* by type IV pili and in *X. campestris* by FimA fimbriae (Buttner and Bonas, 2009). Much more is known about the adhesins produced by animal pathogens. These are usually proteins that are assembled in a structure, such as a pilus or fimbriae, or are surface exposed (afimbrial adhesins). The afimbrial adhesins are anchored directly in the outer membrane with the adhesin domain exposed to the extracellular surface. The adhesin HecA family was found in *X. axonopodis* pv. *glycines* 12-2 unique genes. HecA and related proteins found in other plant pathogenic bacteria are highly diverse.

In addition, the *flgC* (flagellar basal body rod protein), *flgK* (flagellar hook-associated protein), and *fliC* (flagellin proteins) mutants of *X. axonopodis* pv. *glycines* SW005 lacked a monopolar flagellum and lost swimming motility where *fliD* mutant lost flagellar filament capping protein and reduced swimming motility that may

produce an altered monopolar flagellum or may be not. These results demonstrate that *flgC*, *flgK*, and *fliC* are required for flagella biosynthesis and swimming motility. The *flgC*, *flgK*, *fliC*, and *fliD* mutants were also altered in biofilm production (Athinuwat, 2009).

The genus *Xanthomonas* comprises a large number of bacterial plant pathogens that infect at least 124 monocotyledonous and 268 dicotyledonous plants (Chan and Goodwin, 1999). So far, the bacterial factors that determine host range and mode of infection in different pathovars are largely unknown. Comparative genomic sequence analyses of *X. axonopodis* pv. *citri*, *X. campestris* pv. *campestris* and *X. campestris* pv. *vesicatoria* have already revealed differences among putative virulence factors that might bear host-specific functions. The obvious differences in the genetic virulence equipment validate genome sequencing of more than one subspecies. Currently, the genomes of *X. axonopodis* pv. *glycines* 12-2 are being sequenced. The successful termination of these sequencing projects will provide the unique opportunity to identify and compare putative virulence factors from four different members of one bacterial genus.

In this study we have analyzed the dynamics of *X. axonopodis* pv. *glycines* interactions with soybean during the infection process with particular attention to the role of the transcriptional regulator XagR. The primary structure of XagR is similar to that of OryR and XccR, having a typical modular structure of other LuxR-family response regulators involved in quorum sensing with an inducer-binding domain in the N terminus contains and a helix-turn-helix DNA-binding domain in the C terminus. While *xagR* is constitutively expressed both in culture and *in planta*, XagR only accumulates in cells in infected plants. While XagR was not stabilized by any of the structurally different AHLs tested, unidentified compounds in the plant may enable its accumulation, apparently in a way similar to that seen for OryR (Ferluga and Venturi, 2009).

The plant factor(s) that activate XagR are apparently not host plant specific since some induction of *pip* was observed when *X. axonopodis* pv. *glycines* was

infiltrated into rice and cabbage as well as soybean. In contrast to studies of OryR, however, no XagR function, as measured by the activation of *pip*, could be observed *in vitro* with extracts of any plants including rice, suggesting that the inducing compounds for OryR and XagR differ. Since homologs of *xagR* are present in the genomes of several other beneficial and pathogenic plant-associated bacteria such as *Pseudomonas fluorescens* and *Pseudomonas syringae* (Zhang *et al.*, 2007), it seems likely that they may have evolved to interact with specific host-derived compounds. PsoR, a LuxR homolog in *P. fluorescens* CHA0 was recently shown to be stabilized by rice and wheat extracts, but not by cucumber extracts (Subramoni and Venturi, 2009) lending support to this idea. To date, the identity of these plant compounds remain unknown. Those from rice and cabbage that interact with OryR and XccR are suggested to be small molecules (<1 kDa) (Ferluga and Venturi, 2009; Wang *et al.*, 2011). While the signal molecules in rice and cabbage are apparently relatively abundant even in uninfected plants, the compound(s) in soybean seem to accumulate only after infection, since little induction of *pip* is seen for at least 24 to 48 hr after inoculation and does not reach a maximum until 72 hr or more. Identification of the plant compound needed for stabilization of XagR should help unravel the complex interactions that occur during infection events.

Both XagR and Pip are required for full virulence of *X. axonopodis* pv. *glycines* to soybean and XagR is required for *pip* expression similar to that seen for OryR and XccR in *X. oryzae* pv. *oryzae* and *X. campestris* pv. *campestris*. The role of Pip in virulence remains unclear. Pip catalyzes the removal of N-terminal prolines from peptides with fairly high specificity. D-Alanine is also removed, with much lower efficiency than the L-isomer (Alonso and Garcia, 1996). In *X. campestris* pv. *campestris*, Pip is a periplasmic protein and might hydrolyze some small molecules from the host plant (Zhang *et al.*, 2007). In *X. oryzae* pv. *oryzae*, the activity of the *pip* promoter in media containing extracts of infected rice (10-days after inoculation) was somewhat higher than that containing uninfected rice macerates (Ferluga and Venturi, 2009) suggesting that its induction might be associated with adaptation to the presence of inhibitory compounds made by the plant during infection. The delayed induction of *pip* in *X. axonopodis* pv. *glycines* in soybean until many hours after

inoculation strongly suggests that its role might be to respond to increases in defensive compounds that occur during the infection event. Although XagR controls at least 79 genes, given that *xagR* and *pip* mutants exhibit similarly reduced virulence to soybean, it appears that Pip contributes substantially to the virulence phenotypes regulated by XagR.

Compounds found in infected soybean likely stabilize XagR, although its pattern of transcriptional regulation appears to differ from that of related proteins. Many LuxR regulators are insoluble and/or unstable and susceptible to proteolytic degradation unless they bind to their cognate AHL. TraR of *A.tumefaciens*, a member of the LuxR family, required 3-oxo-octanoyl homoserine lactone-mediated folding for resistance to cytoplasmic proteases (Zhu and Winans, 1999) and dimerization also enhances its resistance to cellular proteases (Pinto and Winans, 2009). The expression of *xccR* in *X. campestris* pv. *campestris* was repressed in culture media by XerR, a NtrC-type response regulator which was relieved when the bacteria were grown *in planta* (Wang *et al.*, 2011). In *X. oryzae* pv. *oryzae*, OryR negatively regulated its own transcription but its expression was independent of the presence of rice extract (Ferluga and Venturi, 2009). However, accumulation of OryR occurred in the presence of a rice signal molecule (Ferluga *et al.*, 2007). In this study we found that *xagR* transcription was constitutive, but that XagR accumulated only in soybean plants. Interestingly, although *xagR* was expressed both in culture and *in planta*, XagR was detected only in cells recovered from soybean plants 72 hours or more after infiltration, or in minimal media when *xagR* was over-expressed *in trans*. While the number of *X. axonopodis* pv. *glycines* cells present in plants soon after inoculation are relatively low, we found no evidence of XagR in cells at early stages of infection, suggesting that it accumulates relatively late in the infection process. This suggests that a signal molecule(s) that accumulates in soybean only during the infection process is 1) indirectly controlling XagR abundance, perhaps by altering its proteolytic degradation and 2) post transcriptionally modulating XagR levels. Interestingly, the virulence of XagROX, in which XagR does accumulate, was very low in soybean suggesting that early accumulation of XagR during the infection process is inhibitory. Given the relatively large number of genes regulated by XagR, it

remains unclear which ones might inhibit the infection process if prematurely expressed.

Deep RNA sequencing proved a very effective means to compare the transcriptomes of strain XagROX in which XagR was overexpressed, allowing XagR to accumulate even in culture, with that of the wildtype strain in which XagR does not accumulate in culture. XagR apparently regulates a large number of genes directly or indirectly since 44 percent of the annotated genes of *X. axonopodis* pv. *glycines* were differentially expressed (P=0.01). The high sequencing depth, due to the substantial removal of ribosomal RNAs that we achieved, and the high reproducibility of the RNA sequencing process enabled measures of expression of nearly all *X. axonopodis* pv. *glycines* genes with high resolution. Estimates of transcript abundance obtained by RNA sequencing with the Illumina HiSeq 2000 System correlated well with those made by quantitative RT-PCR. Noteworthy genes positively regulated by XagR include the gene encoding proline iminopeptidase (*pip*) that is located immediately downstream of *xagR* and which contains a putative *lux* box in the intergenic region with *xagR*. Similar to that shown for XccR and OryR, XagR likely binds to a low molecular weight plant compound and subsequently regulates *pip* expression via its well conserved *lux*-box. In contrast, the *pip* gene of the biocontrol strain *P. fluorescens* CHA0, which is adjacent to the *xagR* homolog *psoR*, does not have a *lux* box and is not regulated by *psoR* (Subramoni and Venturi, 2009); the *pip* gene in *P. fluorescens* likewise also lacks a *lux* box (Subramoni and Venturi, 2009). While the mechanism by which Pip contributes to the virulence of *Xanthomonas* pathogens remains unknown, LuxR-type regulators appear to play a direct role in their regulation. The predicted gene coding for a membrane protease related to stomatin/prohibitin (XAC3964 homolog from *Xac* strain 306) and *rtcB* (homolog to XAC3965) also exhibited substantial increases in transcript levels in XagROX. The membrane protease may contribute to posttranslational modification of other proteins, perhaps in a manner similar to that proposed for Pip (Kihara *et al.*, 1996). RtcB enzymes are novel RNA ligases that join 2', 3'-cyclic phosphate and 5'-OH ends of RNA that might afford bacteria a means to recover from stress-induced damage (Tanaka *et al.*, 2011). While no function of these genes have been reported in

bacterial plant pathogens, the disruption of either of them significantly reduced the virulence of *X. axonopodis* pv. *glycines*. Four genes in an operon defined by XagID 2143-2146 encoding, respectively, exoenzyme regulatory protein AepA, membrane protein 2 having some similarity to the thiosulphate: quinone oxidoreductase DoxD, a isochorismatase family protein, and a putative transcriptional regulator in the AraC family were also up-regulated by XagR. The proteins belonging to the AraC family of transcriptional regulators have three main regulatory functions in common: carbon metabolism, stress response, and pathogenesis (Gallegos *et al.*, 1993). Again, as they presumably are expressed primarily late in the infection process, they may be required mainly to deal with events that occur after initial plant interactions.

We observed up-regulation of several genes that mediate responses to low water availability including the choline dehydrogenase and betaine aldehyde dehydrogenase loci as well as the potassium-transporting ATPase operon in strain XagROX compared to the wildtype strain. Increases in the osmolarity of bacterial environments usually results in changes in intracellular solute concentration and cell volume (Poolman and Glaasker, 1998). To cope with such stresses, bacteria accumulate osmotically-active solutes, including, proline, glutamic acid, glutamine,  $\alpha$ -aminobutyric acid, ectoine, betaine and potassium (Galinski and Truper, 1994). Choline dehydrogenase catalyzes the oxidation of choline to glycine betaine, with betaine aldehyde as an intermediate (Landfald and Strom, 1986). Numerous *in vitro* studies have shown that betaine acts as an osmoprotectant by stabilizing both the quaternary structure of proteins and membrane integrity against the adverse effects of high salinity and extreme temperatures (Le Rudulier *et al.*, 1984). Plant restriction of water availability has been demonstrated in both compatible and incompatible interactions of plant pathogenic bacteria with plants (Beattie, 2011). Therefore it is possible that *X. axonopodis* pv. *glycines* anticipates the lower water availability that might accompany later stages of infection of soybean, with the accumulation of XagR triggering the accumulation of osmoprotectants.

Interestingly, the expression of *yapH* and a GAF/GGDEF/EAL domain protein were both down-regulated in XagROX compared to the wildtype strain. GGDEF-

domain proteins are involved in the synthesis of cyclic di-GMP, which is a second messenger in bacteria that regulates a range of external cellular functions such as motility and adhesion that often contribute to the virulence of pathogens (Simm *et al.*, 2004; Tamayo *et al.*, 2007; Hengge, 2009). The modulation of *yapH* expression might therefore have been via alteration of cyclic di-GMP signaling. YapH was required for adhesion of the vascular pathogen *Xanthomonas fuscans* subsp. *fuscans* to seeds, leaves, and abiotic surfaces, but not for *in planta* transmission to seeds or for infection of bean leaves (Darsonval *et al.*, 2009); *yapH* was thus considered a potential anti-virulence gene (Foreman-Wykert and Miller, 2003). *yapH* mutants of *X. oryzae* pv. *oryzae* also exhibit deficiencies in leaf attachment or entry into rice xylem vessels (Das *et al.*, 2009).

Importantly, we also found that a *yapH* mutant and XagROX were deficient in adhesion to both abiotic surfaces and to soybean leaf surfaces. Since XagR does not accumulate in cells in culture we were not surprised that cultured cells of the *xagR* mutant did not differ from the wildtype strain in adhesiveness. In contrast, while egress of the *yapH* mutant and XagROX from infected leaves was only slightly greater than that of the wildtype strain, the *xagR* mutant was much more strongly retained in the infected tissue compared to the wildtype strain. In infected leaves XagR would have accumulated and suppressed the expression of YapH, while no such repression of YapH would have occurred in the *xagR* mutant, leading to a greater adhesiveness.

The virulence contribution of *yapH* and other genes in *X. axonopodis* pv. *glycines* under the control of XagR are strongly context-dependent. Indeed, we observed that disruption of *yapH* increased the ability of *X. axonopodis* pv. *glycines* to cause leaf lesions on soybean under relatively dry conditions, but under wet conditions in which simulated rain was applied to plants after inoculation the *yapH* mutant incited significantly fewer lesions compared to the wildtype strain. It is easy to imagine that the lower adhesiveness of the *yapH* mutant allows it to more easily move on moist leaves (not experiencing rain) after inoculation; since they are not immobilized by attachment to the leaf surface they would have more opportunities to

enter stomata and begin intercellular growth leading, eventually to lesions. In contrast, such a strain would be more easily washed from leaves during rainfall events, thereby removing them from the infection court.

Considerations of the temporal pattern of accumulation of XagR during the infection process, and the traits that are under the control of XagR, enable us to develop a plausible model for the role of this LuxR-regulator in the cycle of bacterial pustule disease of soybean (Figure 28). Upon arrival at a healthy plant, *X. axonopodis* pv. *glycines* apparently does not perceive any plant signals that would enable the accumulation of XagR. Under such conditions *pip* is not induced and adhesins such as YapH are not suppressed, leading to an adhesive state, allowing the strong attachment of cells to the leaf surface, thereby becoming resistant to removal by rain. Those cells that enter the leaf begin to grow in the apoplast and after 2 or more days the plant has accumulated enough of a signal molecule that is produced during the infection process that XagR is stabilized and accumulates in cells, triggering numerous changes in gene expression such as *pip* induction and *yapH* repression. Genes associated with biosurfactant production is also induced at this time. Such intercellular cells would be of low adhesiveness and the surfactants would enable the cells to spread within the apoplast, thereby expanding the lesion and increasing population size. Such cells would also be more capable of egression from the plant via the pustules that form on leaves.

Upon escape from the plant and perhaps rain splash to other leaves, the cells would initially be of low adhesiveness, enabling them to invade new leaves. However, the plant factor to which the cells had responded within infection sites would be diluted and XagR might quickly be degraded, enabling the restoration of an adhesive state and the suppression of virulence genes such as *pip* and others that are useful or required only in later stages of plant infection. Thus perhaps distinct from other LuxR regulators, XagR seems to play a particularly large role in coordinating the temporally distinct phases of the life cycle of this pathogen. That is, phenotypes that are beneficial in one setting can be temporally regulated to avoid conflicts via such a regulator which appears to sense different stages in the infection process.

Until now, various plant-regulated virulence genes of *Xanthomonas* sp. have been identified, but little information is available on general host upregulated genes of the bacterium at a genomic level. To broaden our understanding in this area, whole transcriptome analysis using RNA sequencing technique was introduced in this study to identify genes in *X. axonopodis* pv. *glycines* 12-2 that are upregulated in a soybean host plant. The major plant-upregulated genes identified in this assays include *Hrp* cluster included *Hpa*, *HrpB*, *HrpD*, *HrpF*, *HrpX*, type III secretion system and type III effector. The analysis of non-polar mutants in the *hrp* gene cluster of *X. campestris* pv. *vasicatoria* also identified *hpa* (*hrp* associated) genes that contribute to, but are not essential for the pathogenic interaction with the plant (Buttner *et al.*, 2004). For example, *hpaA* encodes a protein that is needed for the HR and full pathogenicity. HpaA is secreted by the type III secretion system and localizes to the plant nucleus when expressed in planta (Huguet *et al.*, 1998). In contrast, HpaB remains in the bacterium where it plays an important role in the control of type III protein export (Buttner *et al.*, 2004). Interestingly, the type III-secreted protein XopA (*Xanthomonas* outer protein) also shows features of an Hpa protein: The *xopA* gene is located adjacent to the left border of the *hrp* region, its expression is HrpG and HrpX-dependent. XopA shows homology to Hpa1 from *X. oryzae* pv. *oryzae* (Zhu *et al.*, 2000). However, XopA shows no harpin HR eliciting activity as it was shown for Hpa1 from *X. oryzae* pv. *oryzae* and the homolog HpaG from *X. axonopodis* pv. *glycines* (Kim *et al.*, 2003). *xopA* mutants are affected in bacterial virulence, but not in type III-mediated secretion. As XopA is not translocated into the host cell, it might be part of the translocon (Buttner *et al.*, 2004).

Expression of the type III secretion system in phytopathogenic bacteria is induced *in planta* or in specific minimal media mimicking the plant apoplast (Schulte and Bonas, 1992; Lindgren, 1997). The regulatory cascade controlling expression of *hrp* genes varies in different plant pathogens. Based on similarities in gene organization and regulation, the *hrp* regions of different pathogens were classified into two groups. Group I comprises species of *Erwinia*, *Pantoea* and *P. syringae*, whereas *R. solanacearum* and *Xanthomonas* spp. belong to group II (Alfano and Collmer, 1996). The key regulatory proteins in *Xanthomonas* are HrpG and HrpX,

which are encoded outside of the *hrp* gene cluster. HrpG belongs to the OmpR-family of two-component system response regulators (Wengelnik *et al.*, 1996) and controls the expression of the regulator HrpX (Wengelnik and Bonas, 1996; Noel *et al.*, 2001, 2002, 2003).

Also, *hrpX* gene of *X. axonopodis* pv. *glycines* was differentially expressed in soybean. HrpX, an AraCtype transcriptional activator, regulates the expression of most genes of the HrpG regulon including the *hrp* operons *hrpB* to *hrpF* (Wengelnik and Bonas, 1996; Noel *et al.*, 2001, 2002, 2003). Many *hrpX*-regulated genes contain a PIP box (plant-inducible promoter box; consensus TTCGCN15-TTCGC) in their promoter region, which was proposed to serve as a regulatory element (Wengelnik and Bonas, 1996). However, this motif is not sufficient to confer HrpX inducibility, because there are HrpX-independent PIP-box containing promoters, e.g., *avrRxxv* (Ciesiolka *et al.*, 1999). It appears that additionally, as described above for HrpB a  $\_10$  box is needed for HrpX inducibility (Tsuge *et al.*, 2005). Remarkably, this 10 box is absent in the promoter of the constitutively expressed *avrRxxv* mentioned above. Whether HrpX or a still unknown protein binds to the PIP box remains to be elucidated.

The HrpF protein is probably inserted into the plantcell membrane and may be required for the bacterium's type III effector proteins to enter host cells (Butter and Bonas, 2002). As a bacterial translocon, HrpF would therefore be in direct contact with the plant-cell membrane and even possibly subjected to the plant's surveillance mechanisms while it mediates effector protein delivery across the host-cell membrane. In *X. oryzae* pv. *oryzae*, found that HrpF is required for pathogenicity, which had a reduced ability to either grow within rice plants or cause lesions (Sugio *et al.*, 2005).

*Xanthomonas* pathogenicity is highly dependent on the type III secretion system injecting effector proteins into the eukaryotic host cell (Buttner and Bonas, 2009; White and Yang, 2009). Knowledge on the type III secretion system in *X. axonopodis* pv. *glycines* is based on studies of the AvrXg1 belonging to AvrBs3/pthA

family of *Xanthomonas* effector proteins. This family includes proteins with avirulence activities, virulence functions, or both (Athinuwat *et al.*, 2009). Avirulent gene homolog to *avrXg1* and candidate type III effector HolPtoQ are up-regulated. *AvrXg1* of *X. axonopodis* pv. *glycines* SW005 enhanced virulence and bacterial population on resistant and susceptible soybean cultivars. Expression of *avrXg1* in Race 1, that was predicted to confer a non-specific HR, led to virulence on susceptible cultivars. This *avrXg1* was also expressed in Race 2 resulting in increased virulence and additive pathogen fitness on resistant and susceptible cultivars. Race 2 was shown to carry *avrBs3*-like genes but apparently not *avrXg1* (Athinuwat *et al.*, 2009).

Among the virulence factors secreted by the type II secretion system of phytopathogens, cell-wall degrading enzymes (CWDE), such as polygalacturonases (PG), cellulases, xylanases, and proteases, have been studied due to their clear or potential functions in bacterial pathogenesis, and comprehensive studies on the structures and functions of CWDE have been undertaken. The type II secretion system allows most Gram-negative bacteria to deliver extracellular hydrolytic enzymes and toxins to their surroundings and hosts, many of which are responsible for pathogenesis in plants and animals (Sandkvist, 2001). CWDE function to break down the components of host cell walls and may play a crucial role in virulence and bacterial nutrition. In this study the gene coding for polygalacturonases were also up-regulated *in planta*. PG are hydrolytic enzymes of CWDE that selectively degrade the pectic polymers, the major components of higherplant middle lamellae and primary cell walls. PG are classified by activity as endo-PG (EC 3. 2. 1. 15) and exo-PG (EC 3. 2. 1. 67). Endo-PG randomly hydrolyze polygalacturonic acid, releasing oligosaccharidic chains of variable length, whereas exo-PG release either galacturonate monomer, in the case of exoPG (EC 3.2.1.67), or dimer (digalacturonate), in the case of exo-poly-a-D-galacturonosidase (EC 3.2.1.82), starting from the nonreducing end (Huang and Allen, 1997). In other *Xanthomonas*, two novel PG genes (*pghAxc* and *pghBxc*) encoding functional PG from *X. campestris* pv. *campestris* 8004. The expressions of these two PG genes are regulated by the type III secretion regulators HrpX and HrpG and the global regulator Clp. These PG genes could be efficiently induced in planta and were required for the full virulence of *X. campestris* pv. *campestris* to *Arabidopsis*. In addition, these PG were confirmed to be

secreted via the type II secretion system in an Xps-dependent manner (Wang *et al.*, 2008). As we found the *hrpX* and gene coding for polygalacturonase were also upregulated in soybean resulting that *hrpX* of Xag might regulated the PG expression as shown in *X. campestris* pv. *campestris*. The fact that HrpX is also involved in the regulation of some extracellular enzymes of the type II secretion system suggests that HrpX controls the expression of the majority of genes containing a PIP box in *Xanthomonas* spp. and, therefore, may be involved in regulation of many *Xanthomonas* genes. This regulation of HrpX suggested that the signal transduction networks of pathogens are cross-linked and that the type III secretion system and type II secretion system may cooperate via various regulators to promote the virulence of the pathogen in the host.

In addition, the gene coding for xylanase was also up-regulated in soybean. Cell-wall-degrading enzymes, including cellulases, pectinases, xylanases and proteases, are secreted by phytopathogenic bacteria for breaking down the components of host cell walls. Xylan is a polymer consisting of a linear backbone of 1,4-linked D-xylanopyranosyl residues and side chains of arabinose, glucuronic acid, or methylglucuronic acid. Additional modifications in the form of acetyl and phenolic esters contribute to the complexity of xylan. Several sets of enzymes are required to degrade xylan to xylose monomers. The endo- or exo- $\beta$ -xylanases hydrolyze the backbone to yield xylo-oligosaccharides. Another enzyme,  $\beta$ -xylosidase, cleaves the 1-4- $\beta$  linkages to yield xylose monomers. Additional sets of enzymes are required for cleaving the side-chain residues, which vary depending on the nature of the side chains among different plant types. Of particular relevance to this study are the esterases that are involved in hydrolyzing acetyl ester and phenolic ester bonds in xylan. Xylanases and esterases as well as the other enzymes that cleave the side chains have been shown to act cooperatively in degrading xylan (Bachmann and McCarthy, 1991; Biely *et al.*, 1986). Due to the xylanase of *X. axonopodis* pv. *glycines* 12-2 was expressed *in planta* it might be involved in virulence on soybean. Since these enzymes are constitutively secreted into the extracellular medium *in vitro*, and Western analysis indicates that the XynB protein also is released into the xylem sap during *in planta* growth of *X. oryzae* pv. *oryzae*. Mutations that affect either the

secreted xylanase or lipase/esterase have slight effects on virulence, which may be due to redundancy caused by the production of multiple cell-wall-degrading enzymes in *X. oryzae* pv. *oryzae* (Rajeshwari *et al.*, 2005).

Interestingly, the gene related to attachment and movement mechanism were downregulated when *X. axonopodis* pv. *glycines* colonization in soybean plant. Athinuwat 2009 has been report that the flagellar and type IV pili genes including *flgC*, *flgK*, and *pilD* are important virulence factors for pathogenesis of *X. axonopodis* pv. *glycines* SW005. These *flgC*, *flgK*, and *pilD* controlled swimming, twitching motility and biofilm formation functioned by bacterial flagellum and pillus was required for full expression of disease and severity initiation when spray inoculation. However, *in planta* observations by Zoller and Kosuge, 1971 showed that *X. campestris* pv. *campestris* is nonmotile and nonflagellated in the xylem fluid of infected cabbage leaves and suggested that the movement of the bacteria in the xylem was due to diffusion rather than to motility. In contrast, vascular pathogen, four genes fimbrial assembly protein (FI978267), pilin (FI978178), type IV pilin (FI978319), and the *pilY1* gene (FI978318) that are associated with bacterial adhesion and biofilm formation were found as up-regulated in *X. oryzae* pv. *oryzae* MA11 *in planta* at 6 day after inoculation. Type IV pili are bacterial major virulence factors supporting adhesion, surface motility, and gene transfer in vascular pathogens. Adhesion of bacteria to biotic surfaces is key for the invasion of the host tissue. Also, type IV pili were proposed to play a role in the attachment of *X. campestris* pv. *hyacinthi* to the stomata of its host plant (van Doorn *et al.*, 1994). However, a contribution of type IV pili to the attachment of leaf spot *X. campestris* pv. *vesicatoria* to tomato leaves was not observed (Ojanen-Reuhs *et al.*, 1997). In this study, the YapH protein was suppressed by XagR, also downregulated in plant upregulatory gene experiment. This suggest the role of flagella genes in *X. axonopodis* pv. *glycines* that swimming and swarming motility and biofilm formation important to adhere to the soybean leave surface and motile into the intercellular space of plant tissue. After *X. axonopodis* pv. *glycines* colonization in the plant the flagellar and adhesion gene were suppressed to promoted the *X. axonopodis* pv. *glycines* is a nonflafellted and movement to anoter plant cell via diffusion. This result confirm the role of

XagR in contributed virulent in infection process by interact with plant signaling and control other gene that effect to virulent on soybean (Figure 28).



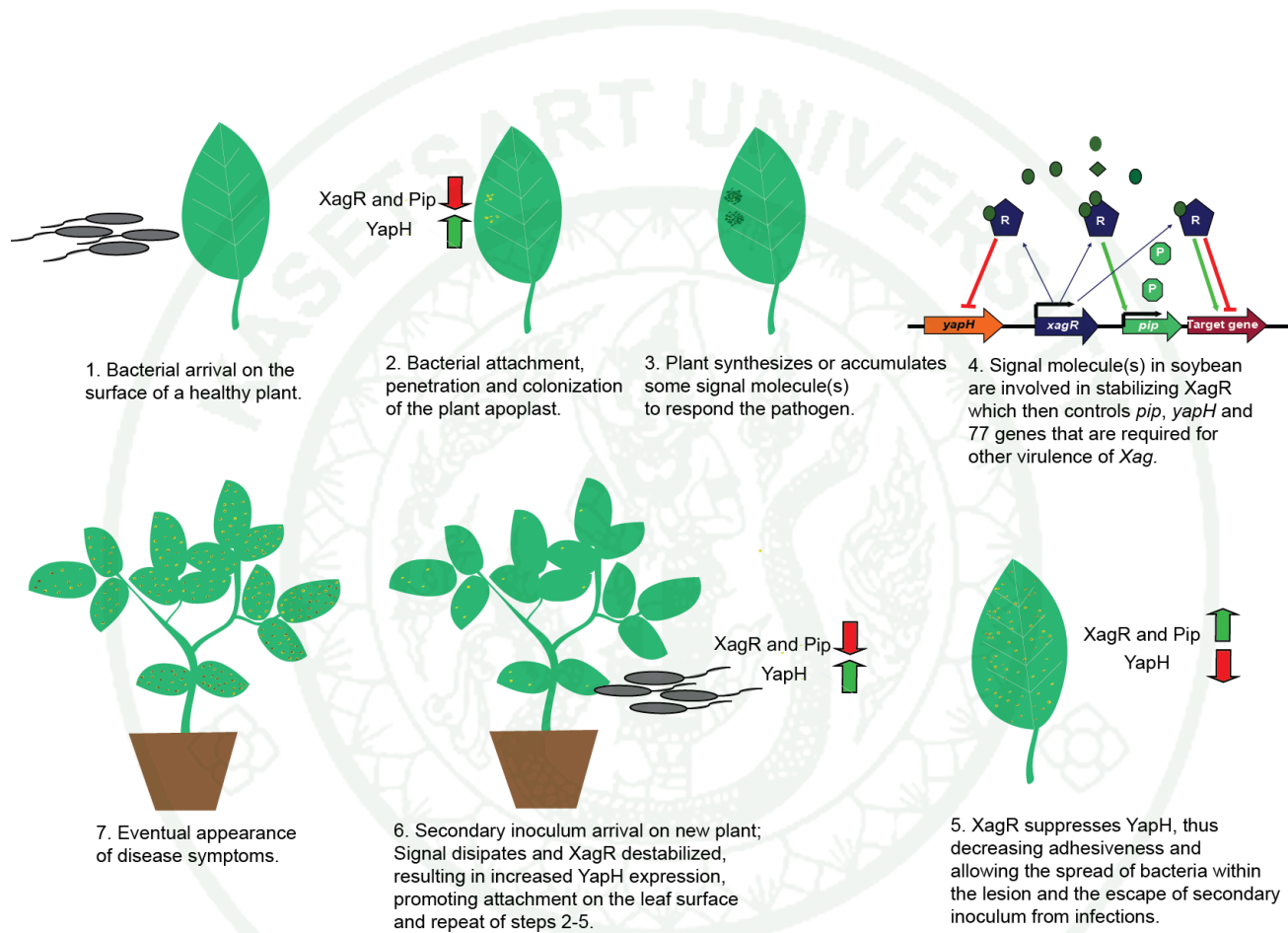


**Figure 28** A model of the temporal regulation of different traits of *Xanthomonas axonopodis* pv. *glycines* that are regulated by XagR in relation to the process of disease development in a population of plants. ● Represents the putative signal molecules from the host.

## CONCLUSIONS

1. This is the first report to generated draft genome of the *X. axonopodis* pv. *glycines* 12-2.
2. A total of 5062 putative coding genes (ORFs) were identified in the *X. axonopodis* pv. *glycines* 12-2 draft genome.
3. A novel *luxR* homolog, termed *xagR*, presence in *X. axonopodis* pv. *glycines* 12-2, the cause of soybean pustule, and controls expression of *pip*, *yapH* and at least 77 other genes.
4. *XagR*, *pip* and *yapH* contributes to virulence of *X. axonopodis* pv. *glycines* to soybean.
5. A biosurfactant that is induced by XagR may contribute to the movement of cells of *X. axonopodis* pv. *glycines* through the apoplast of soybean and hence in lesion formation; the role of other XagR-regulated genes in the disease process is still being investigated.
6. While transcription of *xagR* is constitutive, XagR protein only accumulates in infected soybean plants and thus appears to be stabilized by a plant signal molecule.
7. XagR-dependent induction of *pip* occurs only 2 days or more after inoculation suggesting that plant signal molecules are produced after the initial infection event.
8. Constitutive over-production of XagR suppresses the virulence of *X. axonopodis* pv. *glycines* to soybean.

9. XagR modulates the adhesiveness of the *X. axonopodis* pv. *glycines* 12-2 during the infection process by suppressing the adhesin YapH.

10. *yapH* mutants and cells in which XagR was over-expressed exhibited much more egress from infected leaves than the wildtype strain.

11. Results suggest a role of XagR in modulating the pattern of expression of *Xag* genes during the infection event in response to feedback from plant molecules elaborated during infection.

12. This is the first report to compare bacterial gene expression *in planta* during infection. Of 5062 predicted genes in Xag draft genome, 534 and 289 were identified as plant upregulated and downregulated respectively.

13. Plant upregulated genes included *hrp* cluster, avirulent and typeIII effector protein, extracellular enzyme, chemotaxis components and several already known or new putative virulence factors.

14. Plant downregulated genes included the gene involved in attachment and movement process. The *yapH* were also highly suppressed *in planta*.

15. Molecular genetics include genomic sequencing and RNA sequencing technology can now be employed to determine the role of these genes in plant-microbe interactions.

16. The gained knowledge will be instrumental for improving soybean bacterial pustule control.

**LITTERATURE CITED**

- Aldon, D., B. Brito, C. Boucher and S. Genin. 2000. A bacterial sensor of plant cell contact controls the transcriptional induction of *Ralstonia solanacearum* pathogenicity genes. **Eur. Mol. Biol. Organ. J.** 19: 2304-2314.
- Alfano, J.R. and A. Collmer. 1996. Bacterial pathogens in plants: life up against the wall. **Plant Cell** 8: 1683-1698.
- Alfano, J. R. and A. Collmer. 2004. Type III secretion system effector proteins: Double agents in bacterial disease and plant defense. **Annu. Rev. Phytopathol.** 42: 385-414.
- Alonso, J. and J.L. Garcí'a. 1996. Proline iminopeptidase gene from *Xanthomonas campestris* pv. *citri*. **Microbiology** 142: 2951-2957.
- Ankenbauer, R.G. and E.W. Nester. 1990. Sugar-mediated induction of *Agrobacterium tumefaciens* virulence genes: structural specificity and activities of monosaccharides. **J. Bacteriol.** 172: 6442-6446.
- Arlat, M., C.L. Gough, C. Zischek, P.A. Barberis, A. Trigalet and C.A. Boucher. 1992. Transcriptional organization and expression of the large *hrp* gene cluster of *Pseudomonas solanacearum*. **Mol. Plant-Microbe Interact.** 5: 187-193.
- Aslam, S.N., M.A. Newman and G. Erbs. 2008. Bacterial polysaccharides suppress induced innate immunity by calcium chelation. **Curr. Biol.** 18: 1078-1083.
- Athinuwat, D. 2009. **Specificity of avirulence genes of *Xanthomonas axonopodis* pv. *glycines* on different soybean cultivars.** Ph.D. Thesis, Kasetsart University.

- Athinuwat, D., S. Prathuangwong and T.J. Burr. 2009. *Xanthomonas axonopodis* pv. *glycines* –soybean cultivar virulence specificity determinate by *avrBs3* homolog, *avrXag1*. **Phytopathology** 99: 996-1004.
- Aziz, R.K., D. Bartels, A.A. Best, M. DeJongh, T. Disz, R.A. Edwards, K. Formsma, S. Gerdes, E.M. Glass, M. Kubal, F. Meyer, G.L. Olsen, R. Olson, A.L. Osterman, R.A. Overbeek, L.K. McNeil, D. Paarmann, T. Paczian, B. Parrello, G.D. Pusch, C. Reich, R. Stevens, O. Vassieva, V. Vonstein, A. Wilke and O. Zagnitko. 2008. The RAST server: rapid annotations using subsystems technology. **BMC. Genom.** 9: 75.
- Bachmann, S.L. and A.J. McCarthy. 1991. Purification and cooperative activity of enzymes constituting the xylan-degrading system of *Thermomonospora fusca*. **Appl. Environ. Microbiol.** 57: 2121-2130.
- Barber, C.E., J.L.Tang, J.X. Feng, M.Q. Pan, T.J.G. Wilson, H. Slater, J.M. Dow, P. Williams and M.J. Daniels. 1997. A novel regulatory system required for pathogenicity of *Xanthomonas campestris* is mediated by a small diffusible signal molecule. **Mol. Microbiol.** 24(3): 555-566.
- Bassler, B.L. and R. Losick. 2006. Bacterially speaking. **Cell.** 125: 237-246.
- Bauer, W. D. and U. Mathesius. 2004. Plant responses to bacterial quorum sensing signals. **Curr. Opin. Plant Biol.** 7:429-433.
- Beattie, G.A. 2011. Water relations in the interaction of foliar bacterial pathogens with plants. **Annu. Rev. Phytopathol.** 49: 533-555.
- Bentley, D.R., S. Balasubramanian and H.P. Swerdlow. 2008. Accurate whole human genome sequencing using reversible terminator chemistry. **Nature.** 456: 53-59.

- Bergman, K., M. Gulashhoffee, R.E. Hovestadt, R.C. Larosiliere, P.G. Ronco and L. Su. 1988. Physiology of behavioral mutants of *Rhizobium meliloti*-evidence for a dual chemotaxis pathway. **J. Bacteriol.** 170: 3249-3254.
- Becker, A., F. Katzen, A. Puhler and L. Ielpi. 1998. Xanthan gum biosynthesis and application: a biochemical/genetic perspective. **Appl. Microbiol. Biot.** 50: 145-152.
- Biely, P., C.R. MacKenzie, J. Puls and H. Schneider. 1986. Cooperativity of esterases and xylanases in the enzymatic degradation of acetyl xylan. **Biotechnology** 4: 731-733.
- Block, A., G. Li G, Z.Q. Fu and J.R. Alfano. 2008. Phytopathogen type III effector weaponry and their plant targets. **Curr. Opin. Plant Biol.** 11: 396-403.
- Burch, A. Y., B.K. Shimada, P.J. Browne and S.E. Lindow. 2010. Novel high throughput detection method to assess bacterial surfactant production. **Appl. Environ. Microbiol.** 76: 5363-5372.
- Buttner, D. and U. Bonas. 2002. Getting across-bacterial type III effector proteins on their way to the plant cell. **Eur. Mol. Biol. Organ. J.** 21: 5313-5322.
- Buttner, D., D. Gurlebeck, L.D. Noel and U. Bonas. 2004. HpaB from *Xanthomonas campestris* pv. *vesicatoria* acts as an exit control protein in type III-dependent protein secretion. **Mol. Microbiol.** 54: 755-768.
- Buttner, D. and U. Bonas. 2009. Regulation and secretion of *Xanthomonas* virulence factors. **FEMS. Microbiol. Rev.** 34: 107-133.
- Caetano-Anolles, G., D.K. Cristestes and W.D. Bauer. 1988. Chemotaxis of *Rhizobium meliloti* to the plant flavone luteolin requires functional nodulation genes. **J. Bacteriol.** 170: 3164-3169.

- Cao, J.G. and E.A. Meighen. 1989. Purification and structural identification of an autoinducer for the luminescence system of *Vibrio harveyi*. **J. Biol. Chem.** 264(36): 21670-21676.
- Castañeda, A., J.D. Reddy, B.E. Yacoubi and D.W. Gabriel. 2005. Mutagenesis of all eight *avr* genes in *Xanthomonas campestris* pv. *campestris* had no detected effect on pathogenicity, but one *avr* gene affected race specificity. **Mol. Plant-Microbe Interact.** 18: 1306-1317.
- Ciesiolka, L.D., T. Hwin, J.D. Gearlds, G.V. Minsavage, R. Saenz and M. Bravo. 1999. Regulation of expression of avirulence gene *avrRxv* and identification of a family of host interaction factors by sequence analysis of *avrBsT*. **Mol. Plant-Microbe Interact.** 12: 35-44.
- Champoiseau, P., J.H. Daugrois, I. Pieretti, S. Cociancich, M. Royer and P. Rott. 2006. High variation in pathogenicity of genetically closely related strains of *Xanthomonas albilineans*, the sugarcane leaf scald pathogen, in Guadeloupe. **Phytopathology** 96: 1081-1091.
- Chan, J.W.Y.F. and P.H. Goodwin. 1999. The molecular genetics of virulence of *Xanthomonas campestris*. **Biotechnol. Adv.** 17: 489-508.
- Chen, X., S. Schauder, N. Potier, A.V. Drosselaer and I. Pelczer. 2002. Structural identification of a bacterial quorum sensing signal containing boron. **Nature.** 415: 545-549.
- Chatterjee, S. and R.V. Sonti. 2002. *rpfF* mutants of *Xanthomonas oryzae* pv. *oryzae* are deficient for virulence and growth under low iron conditions. **Mol. Plant-Microbe Interact.** 15: 463-471.

- Choi, S.H. and E.P. Greenberg. 1991. The C-terminal region of the *Vibrio fischeri* LuxR protein contains an inducer-independent *lux* gene activating domain. **Proc. Natl. Acad. Sci. USA.** 88: 11115-11119.
- Cui, Y., A. Chatterjee, H. Hasegawa, V. Dixit, N. Leigh and K. Chatterjee. 2005. ExpR, a LuxR homolog of *Erwinia carotovora* subspecies *carotovora*, activates transcription of *rsmA* which specifies a global regulatory RNA-binding protein. **J. Bacteriol.** 187: 4792-4803.
- Darsonval, A., A. Darrasse, K. Durand, C. Bureau, S. Cesbron and M.A. Jacques. 2009. Adhesion and fitness in the bean phyllosphere and transmission to seed of *Xanthomonas fuscans* subsp. *fuscans*. **Mol. Plant-Microbe Interact.** 22: 747-757.
- Das, A., N. Rangaraj and R.V. Sonti. 2009. Multiple adhesin-like functions of *Xanthomonas oryzae* pv. *oryzae* are involved in promoting leaf attachment, entry, and virulence on rice. **Mol. Plant-Microbe Interact.** 22: 73-85.
- da Silva, A.C., J.A. Ferro and F.C. Reinach. 2002. Comparison of the genomes of two *Xanthomonas* pathogens with differing host specificities. **Nature.** 417: 459-463.
- da Silva, F.G., Y. Shen, C. Dardick, S. Burdman, R.C. Yadav, A.L. de Leon and P.C. Ronald. 2004. Bacterial genes involved in type I secretion and sulfation are required to elicit the rice Xa21-mediated innate immune response. **Mol. Plant-Microbe Interact.** 17: 593-601.
- Datsenko, A.K. and B.L. Wanner. 2000. One-step inactivation of chromosomal genes in *Escherichia coli* K-12 using PCR products. **Proc. Natl. Acad. Sci. USA.** 97: 6640-6645.

- Davey, M. E. and G.A. O'Toole. 2000. Microbial biofilms: from ecology to molecular genetics. **Microbiol. Mol. Biol. Rev.** 64: 847-867.
- Denny, T.P. 1995. Involvement of bacterial polysaccharide in plant pathogenesis. **Annu. Rev. Phytopathol.** 32: 173-197.
- Denton, M. and K.G. Kerr. 1998. Microbiological and clinical aspects of infection associated with *Stenotrophomonas maltophilia*. **Clin. Microbiol. Rev.** 11: 57-80.
- Dow, J.M., D.E. Milligan, L. Jaison, C.E. Barber and M.J. Daniels. 1987. A gene cluster in *Xanthomonas campestris* required for pathogenicity controls the excretion of polygalacturonate lyase and other enzymes. **Physiol. Mol. Plant P.** 31: 261-271.
- Dow, J.M. and M.J. Daniels. 2000. *Xylella* genomics and bacterial pathogenicity to plants. **Yeast** 17: 263-271.
- Dunlap, P.V. and E.P. Greenberg. 1985. Control of *Vibrio fischeri* luminescence gene expression in *Escherichia coli* by cyclic AMP and cyclic AMP receptor protein. **J. Bacteriol.** 164: 45-60.
- Dunny, G.M and S.C. Winans. 1999. Bacterial life: neither lonely nor boring. pp. 1-5. **In Cell-Cell Signaling in Bacteria**, ed. GM Dunny, SC Winans, Washington, DC: ASM Press.
- Dye, E.W. and R.A. Lelliott. 1974. **Genus II Xanthomonas. Bergey's Manual of Determinative Bacteriology** (Buchanan RE & Gibbons NE, eds), pp. 243-249. Williams and Wilkins, Baltimore.
- Eberhard, A., A.L. Burlingame, C. Eberhard, G.L. Kenyon, K.H. Nealson and N.J. Oppenheimer. 1981. Structural identification of autoinducer of *Photobacterium fischeri* luciferase. **Biochemistry** 20(9): 2444-2449.

- Espinosa, A. and J.R. Alfano. 2004. Disabling surveillance: bacterial type III secretion system effectors that suppress innate immunity. **Cell Microbiol.** 6: 1027-1040.
- Ferluga, S., J. Bigirimana, M. Höfte and V. Venturi. 2007. A LuxR homolog of *Xanthomonas oryzae* pv. *oryzae* is required for optimal rice virulence. **Mol. Plant Pathol.** 8: 529-538.
- Ferluga, S. and V. Venturi. 2009. OryR is a LuxR-family protein involved in interkingdom signaling between pathogenic *Xanthomonas oryzae* pv. *oryzae* and rice. **J. Bacteriol.** 191: 890-897.
- Fett, W.F., and M.F. Dunn. 1987. Auxin production by plant-pathogenic pseudomonads and xanthomonads. **Appl. Environ. Microbiol.** 53: 1839-1845.
- Fett, W.F., M.F. Dunn, G.T. Maher and B. Maleeff. 1987. Bacteriocins and temperature phase of *Xanthomonas campestris* pv. *glycines*. **Curr. Microbiol.** 16: 137-144.
- Flavier, A.B., S.J. Clough, M.A. Schell and T.P. Denny. 1997. Identification of 3-hydroxypalmitic acid methyl ester as a novel autoregulator controlling virulence in *Ralstonia solanacearum*. **Mol. Microbiol.** 26: 251-259.
- Foreman-Wykert, A.K. and J.F. Miller. 2003. Hypervirulence and pathogen fitness. **Trends. Microbiol.** 11: 105-108.
- Fuqua, C. and S.C. Winans. 1996. Localization of the OccR-activated and TraR-activated promoters that express two ABC-type permeases and the *traR* gene of the Ti plasmid pTiR10. **Mol. Microbiol.** 120: 1199-1210.

- Fuqua, C. and E.P. Greenberg. 2002. Listening in on bacteria: acylhomoserine lactone signaling. **Nat. Rev. Mol. Cell Biol.** 3: 685-695.
- Furutani, A., S. Tsuge, K. Ohnishi, Y. Hikichi, T. Oku, K. Tsuno, Y. Inoue, H. Ochiai, H. Galinski, E. A. and H.G. Truper. 1994. Microbial behavior in salt stress ecosystems. **FEMS. Microbiol. Rev.** 15: 95-108.
- Furutani, A., S. Tsuge, K. Ohnishi, Y. Hikichi, T. Oku, K. Tsuno, Y. Inoue, H. Ochiai, H. Kaku and Y. Kubo. 2004. Evidence for HrpXodependent expression of type II secretory proteins in *Xanthomonas oryzae* pv. *oryzae*. **J. Bacteriol.** 186: 1374-1380.
- Galinski, E.A., and Trüper, H.G. 1994. Microbial behaviour in salt-stressed ecosystems. **FEMS Microbiol. Rev.** 15: 95-108.
- Gallegos, M.T., C. Michalín and J.L. Ramos. 1993. The XylS/AraC family of regulators. **Nucleic Acids Res.** 21: 807-810.
- Gao, M., M. Teplitski, J.B. Robinson and W.D. Bauer. 2003. Production of substances by *Medicago truncatula* that affect bacterial quorum sensing. **Mol. Plant-Microbe Interact.** 16: 827-834.
- Gentleman, R.C., V.J. Carey, D.M. Bates, B. Bolstad, M. Dettling, S. Dudoit, B. Ellis, L. Gautier, Y. Ge, J. Gentry, K. Hornik, T. Hothorn, W. Huber, S. Iacus, R. Irizarry, F. Leisch, C. Li, M. Maechler, A.J. Rossini, G. Sawitzki, C. Smith, G. Smyth, L. Tierney, J.Y. Yang and J. Zhang. 2004. Bioconductor: Open software development for computational biology and bioinformatics. **Genome Biol.** 5: 80.
- Gerlach, R.G. and M. Hensel. 2007. Protein secretion systems and adhesins: the molecular armory of Gram-negative pathogens. **Int. J. Med. Microbiol.** 297: 401-415.

- Geurts, R. and H. Franssen. 1996. Signal transduction in *Rhizobium*-induced nodule formation. **Plant Physiol.** 112: 447-453.
- Ghosh, P. 2004. Process of protein transport by the type III secretion system. **Microbiol. Mol. Biol. R.** 68: 771-795.
- Gottig, N., B.S. Garavaglia, C.G. Garofalo, E.G. Orellano and J. Ottado. 2009. A filamentous hemagglutinin-like protein of *Xanthomonas axonopodis* pv. citri, the phytopathogen responsible for citrus canker, is involved in bacterial virulence. **PLoS. One** 4: e4358.
- Gough, C.L., J.M. Dow, C.E. Barber and M.J. Daniels. 1988. Cloning of two endoglucanase genes of *Xanthomonas campestris* pv. campestris: analysis of the role of the endoglucanase in pathogenesis. **Mol. Plant-Microbe Interact.** 1: 275-281.
- Grant, S.R., E.J. Fisher, J.H. Chang, B.M. Mole and J. Dangel. 2006. Subterfuge and manipulation: type III effector proteins of phytopathogenic bacteria. **Annu. Rev. Microbiol.** 60: 425-449.
- Hao, G., H. Zhang, D. Zheng and T.J. Burr. 2005. *luxR* homolog *avhR* in *Agrobacterium vitis* affects the development of a grape-specific necrosis and a tobacco hypersensitive response. **J. Bacteriol.** 187: 185-192.
- Hawes, M.C. and L.Y. Smith. 1989. Requirement for chemotaxis in pathogenicity of *Agrobacterium tumefaciens* on roots of soil-grown pea plants. **J. Bacteriol.** 171: 5668-5671.
- Hengge, R. 2009. Principles of c-di-GMP signaling in bacteria. **Nat. Rev. Microbiol.** 7: 263-273.

- Hokawat, S. 1978. **Soybean pustule bacteria in Thailand**. M.S. Thesis, Kasetsart University, Bangkok, Thailand.
- Hokawat, S. and K. Rudolph. 1993. **The hosts of *Xanthomonas***. Pages 44-48 In: *Xanthomonas*. J. G. Swings and E. L. Civerolo, eds. Chapman and Hall, London.
- Holden, M.T., C.S. Ram, R.D. Nys, P. Stead, N.J. Bainton, P.J. Hill, M. Manefield, N. Kumar, M. Labatte and D. England. 1999. Quorum-sensing cross talk: isolation and chemical characterization of cyclic dipeptides from *Pseudomonas aeruginosa* and other Gram-negative bacteria. **Mol. Microbiol.** 33: 1254-1266.
- Hu, J., W. Qian and C. He. 2007. The *Xanthomonas oryzae* pv. *oryzae* eglXoB endoglucanase gene is required for virulence to rice. **FEMS. Microbiol. Lett.** 269: 273-279.
- Huynh, T.V., D. Dahlbeck and B.J. Staskawicz. 1989. Bacterial blight of soybean: regulation of a pathogen gene determining host cultivar specificity. **Science** 245: 1374-1377.
- Hugouvieux-Cotte-Pattat, N., H. Dominguez and J. Robert-Baudouy. 1992. Environmental conditions affect transcription of the pectinase genes of *Erwinia chrysanthemi* 3937. **J. Bacteriol.** 174: 7807-7818.
- Hugouvieux-Cotte-Pattat, N., G. Condemine, W. Nasser and S. Reverchon. 1996. Regulation of pectinolysis in *Erwinia chrysanthemi*. **Annu. Rev. Microbiol.** 50: 213-257.
- Huang, Q. and C. Allen. 1997. An exo-poly-alpha-D-galacturonosidase, PehB, is required for wildtype virulence of *Ralstonia solanacearum*. **J. Bacteriol.** 179:7369-7378.

- Huguet, E., K. Hahn, K. Wengelnik and U. Bonas. 1998. *hpaA* mutants of *Xanthomonas campestris* pv. *vesicatoria* are affected in pathogenicity but retain the ability to induce host-specific hypersensitive reaction. **Mol. Microbiol.** 29:1379-1390.
- Jansson, P.E., L. Kenne and B. Lindberg. 1975. Structure of extracellular polysaccharide from *Xanthomonas campestris*. **Carbohydr. Res.** 45: 274-282.
- Jha, G., R. Rajeshwari and R.V. Sonti. 2007. Functional interplay between two *Xanthomonas oryzae* pv. *oryzae* secretion systems in modulating virulence on rice. **Mol. Plant-Microbe Interact.** 20: 31-40.
- Ji, G., R.C. Beavis and R.P. Novick. 1995. Cell density control of staphylococcal virulence mediated by an octapeptide pheromone. **Proc. Natl. Acad. Sci. USA.** 92: 12055-12059.
- Johnson, T.L., J. Abendroth, W.G.J. Hol and M. Sandkvist. 2006. Type II secretion: from structure to function. **FEMS. Microbiol. Lett.** 255: 175-186.
- Jones, S.B. and W.F. Fett. 1985. Fate of *Xanthomonas campestris* infiltrated into soybean leaves: an ultrastructural study. **Phytopathology** 25:733-741.
- Jones, J.D. and J.L Dangl. 2006 The plant immune system. **Nature.** 444: 323-329.
- Kaewnum, S., S. Prathuangwong and T.J. Burr. 2005. Aggressiveness of *Xanthomonas axonopodis* pv. *glycines* isolates to soybean and hypersensitivity responses by other plants. **Plant Pathol.** 54: 409-415.
- Kaewnum, S., S. Prathuangwong and T.J. Burr. 2006. A pectate lyase homolog, *xagP*, in *Xanthomonas axonopodis* pv. *glycines* is associated with hypersensitive response induction on tobacco. **Phytopathology** 96: 1230-1236.

- Kaplan, H.B. and E.P. Greenberg. 1985. Diffusion of autoinducer is involved in regulation of the *Vibrio fischeri* luminescence system. **J. Bacteriol.** 163(3): 1210-1214.
- Kasem, S., S. Prathuangwong and S. Tsuyumu. 2007. Evidence that *ppsA* in *Xanthomonas axonopodis* pv. *glycines* affects carbon utilization and secretion of virulence factors. **Thai J. Agri. Sci.** 40(1-2): 73-89.
- Katzen, F., D.U. Ferreira, C.G. Oddo, M.V. Ielmini, A. Becker, A. Puhler and L. Ielpi. 1998. *Xanthomonas campestris* pv. *campestris* gummutants: effects on xanthan biosynthesis and plant virulence. **J. Bacteriol.** 180: 1607-1617.
- Keshavarzi, M., S. Soylu, I. Brown, U. Bonas, M. Nicole, J. Rossiter and J. Mansfield. 2004. Basal defenses induced in pepper by lipopolysaccharides are suppressed by *Xanthomonas campestris* pv. *vesicatoria*. **Mol. Plant-Microbe Interact.** 17: 805-815.
- Kihara, A., Y. Akiyama and K. Ito. 1996. A protease complex in the *Escherichia coli* plasma membrane: HfIKC (HfIA) forms a complex with FtsH (HfIB), regulating its proteolytic activity against SecY. **Eur. Mol. Biol. Organ. J.** 15: 6122-6131.
- Kim, J.G., B.K. Park, C.H. Yoo, E. Jeon, J. Oh and I. Hwang. 2003. Characterization of the *Xanthomonas axonopodis* pv. *glycines* Hrp pathogenicity island. **J. Bacteriol.** 185: 3155-3166.
- Kim, J.G., S.-H. Choi, J. Oh, J.S. Moon and I. Hwang. 2006. Comparative analysis of three indigenous plasmids from *Xanthomonas axonopodis* pv. *glycines*. **Plasmid** 56: 79-87.

- Kitten, T. and D.K. Willis. 1996. Suppression of a sensor kinase-dependent phenotype in *Pseudomonas syringae* by ribosomal proteins L35 and L20. **J. Bacteriol.** 178: 1548-1555.
- Kleerebezem, M. and L.E. Quadri. 2001. Peptide pheromone-dependent regulation of antimicrobial peptide production in Gram-positive bacteria: a case of multicellular behaviour. **Peptides.** 22: 1579-1596.
- Kovach, E.M., P.H. Elzer, D.S. Hill, G.T. Robertson, M.A. Farris, R.M. Roop II and K.M. Peterson. 1995. Four new derivatives of the broad-host-range cloning vector pBBR1MSC, carrying different antibiotic-resistance cassettes. **Gene** 166: 175-176.
- Landfald, B. and A.R. Strom. 1986. Choline-glycine betaine pathway confers a high level of osmotic tolerance in *Escherichia coli*. **J. Bacteriol.** 165: 849-855.
- Langmead, B. C. Trapnell, M. Pop and S.L. Salzberg. 2009. Ultrafast and memory-efficient alignment of short DNA sequences to the human genome. **Genome Biol.** 10: R25.
- Laviolette, F.A., K.L. Athow, A.H. Probst and J.R. Wilcox. 1976. Effect of bacterial pustule on yield of soybeans. **Crop Science** 10: 150-151.
- Lee, B.M, Y.J. Park and D.S. Park. 2005. The genome sequence of *Xanthomonas oryzae* pathovar *oryzae* KACC10331, the bacterial blight pathogen of rice. **Nucleic Acids. Res.** 33: 577-586.
- Le Rudulier, D., A.R. Strom, A.M. Dandekar, L.T. Smith and R. Valentine. 1984. Molecular biology of osmoregulation. **Science** 224: 1064-1068.
- Lelliott, R.A. and D.E. Stead. 1987. **Methods for the Diagnosis of Bacterial Diseases of Plants**, Blackwell Scientific Publications, Oxford.

- Lequette, Y., J.H. Lee, F. Ledgham, A. Lazdunski and E.P. Greenberg. 2006. A distinct QscR regulon in the *Pseudomonas aeruginosa* quorum sensing circuit. **J. Bacteriol.** 188: 3365-3370.
- Lindgren, P.B. 1997. The role of *hrp* genes during plant-bacterial interactions. **Annu. Rev. Phytopathol.** 35:129-152.
- \_\_\_\_\_, R.C. Peet and N.J. Panopoulos. 1986. Gene-cluster of *Pseudomonas syringae* pv. phaseolicola controls pathogenicity of bean plants and hypersensitivity on nonhost plants. **J. Bacteriol.** 168: 512-522.
- Loh, J., R.W. Carlson, W.S. York, and G. Stacey. 2002. Bradyoxetin, a unique chemical signal involved in symbiotic gene regulation. **Proc. Natl. Acad. Sci. USA.** 99: 146-151.
- Loper, J.E. and S.E. Lindow. 1996. **Reporter gene systems useful in evaluating in situ gene expression by soil and plant associated bacteria.** Pages 482-491 *In* : Manual of environmental microbiology. C. J. Hurst, ed. American Society for Microbiology, Washington, D.C.
- Lu, H., P. Patil and M.A. Van Sluys. 2008. Acquisition and evolution of plant pathogenesis-associated gene clusters and candidate determinants of tissue-specificity in *Xanthomonas*. **PLoS. One** 3: e3828.
- MacLean, D., J.D. Jones and D. Studholme. 2009. Application of ‘next-generation’ sequencing technologies to microbial genetics. **Nat. Rev. Microbiol.** 7: 287-296.
- Malott, R.J., E.P. O’Grady, J. Toller, S. Inhülsen, L. Eberl and P.A. Sokol. 2009. A *Burkholderia cenocepacia* orphan LuxR homolog is involved in quorum-sensing regulation. **J. Bacteriol.** 191: 2447-2460.

- Marketon, M.M., M.R. Gronquist, A. Eberhard and J.E. González. 2002. Characterization of the *Sinorhizobium meliloti* sinR/sinI locus and the production of novel N-acyl homoserine lactones. **J. Bacteriol.** 184: 5686-5695.
- Millar, R.K. 1955. **Studies on the nature of pathogenicity of *Xanthomonas phasioli* (E.F. Smith) Downson and *Xanthomonas phaseoli* var. *sojensis* (Hedges) Starr and Burk.** Ph.D. thesis, Cornell University. Cited J. G. Swings and E.L. Civerolo, eds. 1993. *Xanthomonas*. Chapman and Hall, London.
- Miller, W. G. and S.E. Lindow. 1997. An improved GFP cloning cassette designed for prokaryotic transcriptional fusions. **Gene** 191: 149–153.
- Miller, W.G., J.H.J. Leveau and S.E. Lindow. 2000. Improved *gfp* and *inaZ* broad-host-range promoter-probe vectors. **Mol. Plant-Microbe Interact.** 13: 1243-1250.
- Miller, M.B. and B.L. Bassler. 2001. Quorum Sensing in Bacteria. **Annu. Rev. Microbiol.** 55: 165-199.
- Mo, Y.Y. and D.C. Gross. 1991. Plant signal molecules activate the *syrB* gene, which is required for syringomycin production by *Pseudomonas syringae* pv. *syringae*. **J. Bacteriol.** 173: 5784-5792.
- \_\_\_\_\_, M. Geibel, R.F. Bonsall and D.C. Gross. 1995. Analysis of sweet cherry (*Prunus avium* L.) leaves for plant signal molecules that activate the *syrB* gene required for synthesis of the phytotoxin, syringomycin, by *Pseudomonas syringae* pv *syringae*. **Plant Physiol.** 107: 603-612.

- Moreira, L.M., N.F. Jr Almeida and N. Potnis. 2010. Novel insights into the genomic basis of citrus canker based on the genome sequences of two strains of *Xanthomonas fuscans* subsp. *aurantifolii*. **BMC. Genomics** 11: 238.
- Morgan, F.L. 1963. Bacterial pustule of soybean. **Soybean Dig.** 23: 8-9.
- Newman, K.L., R.P.P. Almeida, A.H. Purcell and S.E. Lindow. 2004. Cell-cell signaling controls *Xylella fastidiosa* interactions with both insects and plants. **Proc. Natl. Acad. Sci. U.S.A.** 101: 1737-1742.
- Newton, J.A. and R.G. Fray. 2004. Integration of environmental and host-derived signals with quorum sensing during plant-microbe interactions. **Cell. Microbiol.** 6: 213-224.
- Noel, L., F. Thieme, D. Nennstiel and U. Bonas. 2001. cDNA-AFLP analysis unravels a genome-wide hrpG-regulon in the plant pathogen *Xanthomonas campestris* pv. *vesicatoria*. **Mol. Microbiol.** 41:1271-1281.
- \_\_\_\_\_, \_\_\_\_\_, \_\_\_\_\_, \_\_\_\_\_.2002. Two novel type III-secreted proteins of *Xanthomonas campestris* pv. *vesicatoria* are encoded within the *hrp* pathogenicity island. **J. Bacteriol.** 184:1340-1348.
- \_\_\_\_\_, \_\_\_\_\_, J. Gabler, D. Buttner and U. Bonas. 2003. XopC and XopJ, two novel type III effector proteins from *Xanthomonas campestris* pv. *vesicatoria*. **J. Bacteriol.** 185:7092-7102.
- Ochiai, H., Y. Inoue, M. Takeya, A. Sasaki and H. Kaku. 2005. Genome sequence of *Xanthomonas oryzae* pv. *oryzae* suggests contribution of large numbers of effector genes and insertion sequences to its race diversity. **Jpn. Agr. Res. Q.** 39: 275-287.

- Ojanen-Reuhs, T., I.M. Helander, K. Haahtela, T.K. Korhonen and T. Laakso. 1993. Outer- membrane proteins and lipopolysaccharides in pathovars of *Xanthomonas campestris*. **Appl. Environ. Microb.** 59: 4143-4151.
- \_\_\_\_\_, N. Kalkkinen, B. Westerlund-Wikstrom, J. van Doorn, K. Haahtela, E.L. Nurmiäho-Lassila, K. Wengelnik, U. Bonas and T.K. Korhonen. 1997. Characterization of the *fimA* gene encoding bundle-forming fimbriae of the plant pathogen *Xanthomonas campestris* pv. *vesicatoria*. **J. Bacteriol.** 179:1280-1290.
- Parke, D. L.N. Ornston and E.W. Nester. 1987. Chemotaxis to plant phenolic inducers of virulence genes is constitutively expressed in the absence of the Ti-plasmid in *Agrobacterium tumefaciens*. **J. Bacteriol.** 169: 5336-5338.
- Pearson, J.P., K.M. Gray, L. Passador, K.D. Tucker, A. Eberhard, B.H. Iglewski and E.P. Greenberg. 1994. Structure of the autoinducer required for expression of *Pseudomonas aeruginosa* virulence genes. **Proc. Natl. Acad. Sci. USA.** 91: 197-201.
- Pieretti, I., M. Royer and V. Barbe. 2009. The complete genome sequence of *Xanthomonas albilineans* provides new insights into the reductive genome evolution of the xylem-limited Xanthomonadaceae. **BMC. Genomics** 10: 616.
- Pinto, U.M. and S.C. Winans. 2009. Dimerization of the quorum-sensing transcription factor TraR enhances resistance to cytoplasmic proteolysis. **Mol. Microbiol.** 73: 32-42.
- Piper, K.R., S. Beck Von Bodman, I. Hwang and S.K. Farrand. 1999. Hierarchical gene regulatory systems arising from fortuitous gene associations: controlling quorum sensing by the opine regulon in *Agrobacterium*. **Mol. Microbiol.** 32: 1077-1089.

- Poellinger, K.A., J.P. Lee, J.V. Parales and E.P. Greenberg. 1995. Intragenic suppression of a *luxR* mutation: Characterization of an autoinducer-independent LuxR. **FEMS. Microbiol. Lett.** 129(1): 97-101.
- Poolman, B. and E. Glaasker. 1998. Regulation of compatible solute accumulation in bacteria. **Mol. Microbiol.** 29: 397-407.
- Prathuangwong, S. 1983. Effects of different soybean plant ages on susceptibility of *Xanthomonas campestris* pv. *glycines*. **J. Thai Phytopathol. Soc.** 3: 148-153.
- \_\_\_\_\_ and K. Amnuaykit. 1987. Studies on tolerance and rate reducing bacterial pustule of soybean cultivars/lines. **Kasetsart J.** 21: 408-420.
- \_\_\_\_\_, S. Kasem, N. Thaveechai and S. Tsuyumu. 2000. Evaluation of thermotolerant bacteria from soybean phyllospheres and rhizospheres for secondary metabolite production and biological control of soybean bacterial pustule. **Proc. of the 2<sup>nd</sup> JSPS-NRCT Joint Seminar on Development of Thermoterant Microbial Resources**, Japan. 69: 04-05.
- \_\_\_\_\_, S. Saisangthong, A. Fareaendee and P. Chutuwantana. 1996. The incidence and new occurrence of soybean diseases at central area of Thailand during 1994-1996. **Proc. of the 6th Nat. Soybean Res. Con.**, Sept. 3-6, 1996. Chiang Mai, Thailand: 242-258.
- \_\_\_\_\_, J. Thowthampitak, S. Kasem and S. Tsuyumu. 2004. New application strategies of thermotolerant bacteria for managing soybean diseases under farming production. **Proc. of the 4th JSPS-NRCT Joint Seminar on Development Microbial Resources and Their Application**. Nov. 7-10, 2004. Fukuoka.

- Qian, W, Y.T. Jia, S.X. Ren, Y.Q. He, J.X. Feng, L.F. Lu, Q.H. Sun, G. Ying, D.J. Tang, H. Tang, W. Wu, P. Hao, L.F. Wang, B.L. Jiang, S.Y. Zeng, W.Y. Gu, G. Lu, L. Rong, Y.C. Tian, Z.J. Yao, G. Fu, B.S. Chen, R.X. Fang, B.Q. Qiang, Z. Chen, G.P. Zhao, J.L. Tang and C.Z. He. 2005. Comparative and functional genomic analyses of the pathogenicity of phytopathogen *Xanthomonas campestris* pv. *campestris*. **Genome Res.** 15: 757-767.
- Rademaker, J.L., F.J. Louws, M.H. Schultz, U. Rossbach, L. Vauterin, J. Swings and F.J. de Bruijn. 2005. A comprehensive species to strain taxonomic framework for *Xanthomonas*. **Phytopathology** 95: 1098-1111.
- Raetz, C.R.H. and C. Whitfield. 2002. Lipopolysaccharide endotoxins. **Ann. Rev. Biochem.** 71: 635-700.
- Rahme, L.G., M.N. Mindrinos and N.J. Panopoulos. 1992. Plant and environmental sensory signals control the expression of *hrp* genes in *Pseudomonas syringae* pv. *Phaseolicola*. **J. Bacteriol.** 174: 3499-3507.
- Rajeshwari, R., G. Jha and R.V. Sonti. 2005. Role of an *in plant* a expressed xylanase of *Xanthomonas oryzae* pv. *oryzae* in promoting virulence on rice. **Mol. Plant-Microbe Interact.** 18: 830-837.
- Ray, S.K., R. Rajeshwari and R.V. Sonti. 2000. Mutants of *Xanthomonas oryzae* pv. *oryzae* deficient in general secretory pathway are virulence deficient and unable to secrete xylanase. **Mol. Plant-Microbe Interact.** 13: 394-401.
- Robinson, M.D., D.J. McCarthy and G.K. Smyth. 2010. edgeR: a Bioconductor package for differential expression analysis of digital gene expression data. **Bioinformatics** 26: 139-140.

- Romantschuk, M. 1992. Attachment of plant pathogenic bacteria to plant surfaces. **Annu. Rev. Phytopathol.** 30: 225-243.
- Salzberg, S.L., D.D. Sommer and M.C. Schatz. 2008. Genome sequence and rapid evolution of the rice pathogen *Xanthomonas oryzae* pv. *oryzae* PXO99A. **BMC. Genomics** 9: 204.
- Sambrook, J., E.F. Fritsch and T. Maniatis. 1989. **Molecular cloning: a laboratory manual, 2<sup>nd</sup> ed.** Cold Spring Harbor Laboratory, Cold Spring Harbor, N.Y.
- Sandkvist, M. 2001. Biology of type II secretion. **Mol. Microbiol.** 40: 271-283.
- Santiago-Vazquez, L.Z., L.K. Ranzer and R.G. Kerr. 2006. Comparison of two total RNA extraction protocols using the marine gorgonian coral *Pseudopterogorgia elisabethae* and its symbiont *Symbiodinium* sp. **Electron. J. Biotechnol.** 9: 598-603.
- Schaad, N.W., A.K. Vidaver, G.H. Lacy, K. Rudolph and J.B. Jones. 2000. Evaluation of proposed amended names of several pseudomonads and xanthomonads and recommendations. **Phytopathology** 90: 208-213.
- Schroter, K., E. Flaschel, A. Puhler and A. Becker. 2001. *Xanthomonas campestris* pv. *campestris* secretes the endoglucanases ENGXCA and ENGXCB: construction of an endoglucanase deficient mutant for industrial xanthan production. **Appl. Microbiol. Biotol.** 55: 727-233.
- Schulte, R. and U. Bonas. 1992. Expression of the *Xanthomonas campestris* pv. *vesicatoria* *hrp* gene cluster, which determines pathogenicity and hypersensitivity on pepper and tomato, is plant inducible. **J. Bacteriol.** 174: 815-823.

- Shen, Y., P. Sharma, F.G. da Silva and P. Ronald. 2002. The *Xanthomonas oryzae* pv. *oryzae* raxP and raxQ gene encode an ATP sulphurylase and adenosine-5'-phosphosulphate kinase that are required for AvrXa21 avirulence activity. **Mol. Microbiol.** 44: 37-48.
- Simm, R., M. Morr, A. Kader, M. Nimtz and U. Romling. 2004. GGDEF and EAL domains inversely regulate cyclic di-GMP levels and transition from sessility to motility. **Mol. Microbiol.** 53: 1123-1134.
- Sinclair, J.B. and O.D. Dhingra. 1975. **An annotated bibliography of soybean diseases**, 1882-1974. Urbana, International Soybean Program, University of Illinois.
- Slater, H., A. Alvarez-Morales, C.E. Barber, M.J. Daniels and J.M. Dow. 2000. A two-component system involving an HD-GYP domain protein links cell-cell signalling to pathogenicity gene expression in *Xanthomonas campestris*. **Mol. Microbiol.** 38: 986-1003.
- Slock, J., D. VanRiet, D. Kolibachuk and E.P. Greenberg. 1990. Critical regions of the *Vibrio fischeri* LuxR protein defined by mutational analysis. **J. Bacteriol.** 172(7): 3974-3979.
- Smith, J.N. and B.M. Ahmer. 2003. Detection of other microbial species by *Salmonella*: expression of the SdiA regulon. **J. Bacteriol.** 185: 1357-1366.
- Stevens, K.M. and E.P. Greenberg. 1994. Synergistic binding of the *Vibrio fischeri* LuxR transcriptional activator domain and RNA polymerase to the *lux* promoter region. **Proc. Natl. Acad. Sci. USA.** 91(26): 12619-12623.

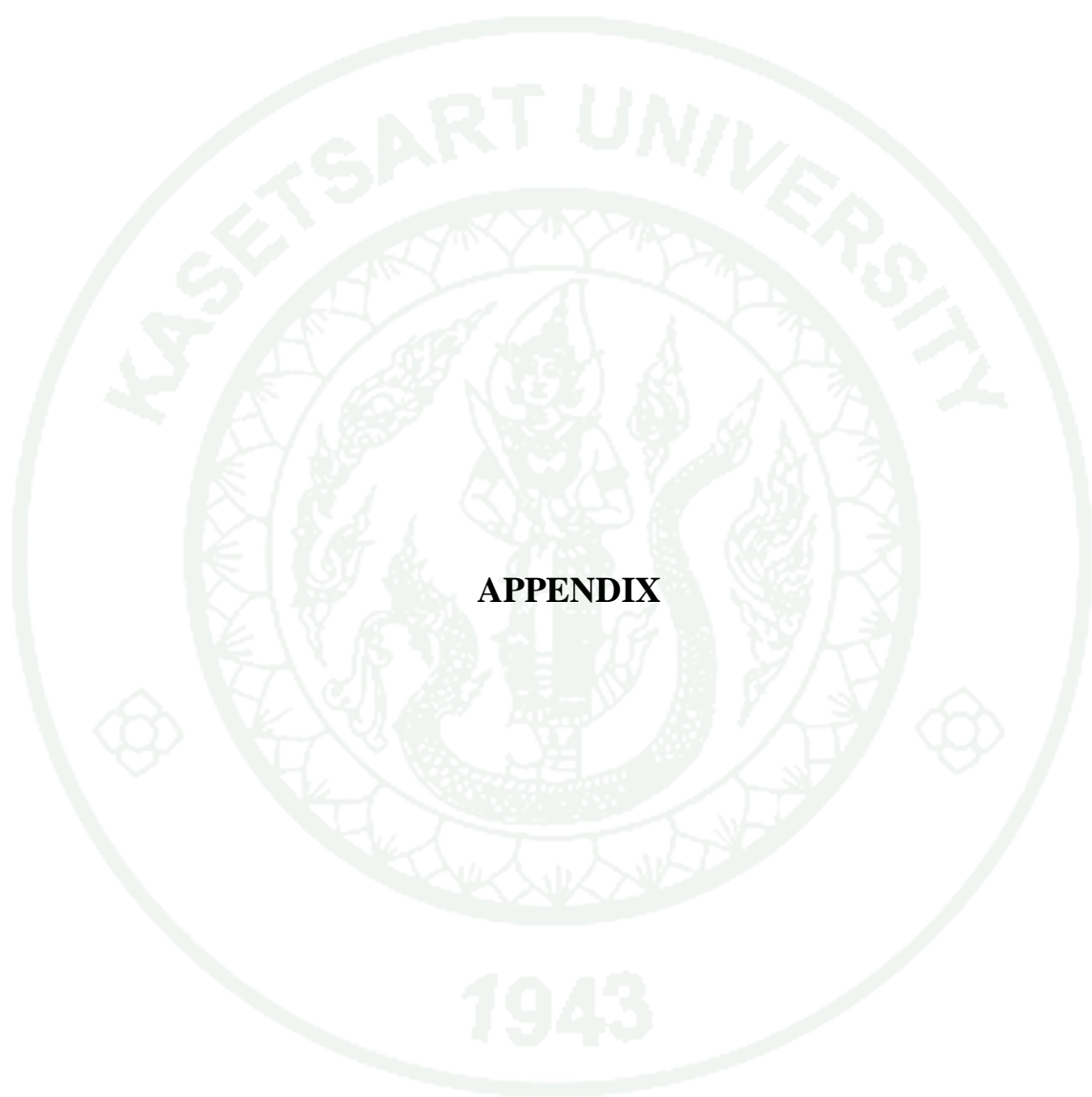
- Stevens, A.M. and E.P. Greenberg. 1997. Quorum sensing in *Vibrio fischeri*: Essential elements for activation of the luminescence genes. **J. Bacteriol.** 179(2): 557-562.
- Stevens, N.F., A. Ishihama and E.P. Greenberg. 1999. Involvement of the RNA polymerase alpha-subunit C-terminal domain in LuxR-dependent activation of the *Vibrio fischeri* luminescence genes. **J. Bacteriol.** 181(15): 4704-4707.
- Subramoni, S. and V. Venturi. 2009. LuxR-family 'solos': bachelor sensors/regulators of signaling molecules. **Microbiology** 155: 1377-1385.
- \_\_\_\_\_, J.F. Gonzalez, A. Johnson, M. Péchy-Tarr, L. Rochat, I. Paulsen, J.E. Loper, C. Keel and V. Venturi. 2011. Bacterial subfamily of LuxR regulators that respond to plant compounds. **Appl. Environ. Microbiol.** 77: 4579-4588.
- Sugio, A., B. Yang, F.F. White. 2005. Characterization of the hrpF Pathogenicity Peninsula of *Xanthomonas oryzae* pv. *oryzae*. **Mol. Plant-Microbe Interact.** 18: 546-554.
- Sun, Q.H., J. Hu, G.X. Huang, C. Ge, R.X. Fang and C.Z. He. 2005. Type-II secretion pathway structural gene xpsE, xylanase and cellulase secretion and virulence in *Xanthomonas oryzae* pv. *oryzae*. **Plant Pathol.** 54: 15-21.
- Tamayo, R., J.T. Pratt and A. Camilli. 2007. Roles of cyclic diguanylate in the regulation of bacterial pathogenesis. **Annu. Rev. Microbiol.** 61: 131-148.
- Tanaka, N., K. Nagasaka and Y. Komatsu. 2011. RtcB, a novel RNA ligase, can catalyze tRNA splicing and HAC1 mRNA splicing *in vivo*. **J. Biol. Chem.** 286: 30253-30257.

- Tang, J. L., Y.N. Liu, C.E. Barber, J.M. Dow, J.C. Wootton and M.J. Daniels. 1991. Genetic and molecular analysis of a cluster of *rpf* genes involved in positive regulation of synthesis of extracellular enzymes and polysaccharide in *Xanthomonas campestris* pathovar *campestris*. **Mol. Gen. Genet.** 226: 409-417.
- Teplitski, M., J.B. Robinson and W.D. Bauer. 2000. Plants secrete substances that mimic bacterial *N*-acyl homoserine lactone signal activities and affect population density dependent behaviors in associated bacteria. **Mol. Plant-Microbe Interact.** 13: 637-648.
- Thieme, F, R. Koebnik and T. Bekel. 2005. Insights into genome plasticity and pathogenicity of the plant pathogenic bacterium *Xanthomonas campestris* pv. *vesicatoria* revealed by the complete genome sequence. **J. Bacteriol.** 187: 7254-7266.
- Thowthampitak, J., B. Shaffer, S. Prathuangwong and J. Loper. 2008. Role of *rpfF* in virulence and exoenzyme production of *Xanthomonas axonopodis* pathovar *glycines*, the causal agent of bacterial pustule of soybean. **Phytopathol.** 98(12): 1252-1260.
- Tsuge, S., S. Terashima, A. Furutani, H. Ochiai, T. Oku and K. Tsuno. 2005. Effects on promoter activity of base substitutions in the cis-acting regulatory element of *HrpXo* regulons in *Xanthomonas oryzae* pv. *oryzae*. **J. Bacteriol.** 187:2308-2314.
- van Doorn, J., P.M. Boonekamp and B. Oudega. 1994. Partial characterization of fimbriae of *Xanthomonas campestris* pathovar *hyacinthi*. **Mol. Plant-Microbe Interact.** 7: 334-344.
- Vauterin. L., J. Rademaker, and J. Swings. 2000. Synopsis on the taxonomy of the genus *Xanthomonas*. **Phytopathol.** 90: 677-682.

- Vojnov, A.A., A. Zorreguieta, J.M. Dow, M.J. Daniels and M.A. Dankert. 1998. Evidence for a role for the gumB and gumC gene products in the formation of xanthan from its pentasaccharide repeating unit by *Xanthomonas campestris*. **Microbiol.** 144: 1487-1493.
- Vorholter, F.J., S. Schneiker and A. Goesmann. 2008. The genome of *Xanthomonas campestris* pv. *campestris* B100 and its use for the reconstruction of metabolic pathways involved in xanthan biosynthesis. **J. Biotechnol.** 134: 33-45.
- Wang, L.H., Y. He, Y. Gao, J.E. Wu, Y.H. Dong, C. He, S.X. Wang, L.X. Weng, J.L. Xu, L. Tay, R.X. Fang and L.H. Zhang. 2004. A bacterial cell-cell communication signal with cross-kingdom structural analogues. **Mol. Microbiol.** 51: 903-912.
- Wang, L., W. Rong and C. He. 2008. Two *Xanthomonas* extracellular polygalacturonases, PghAxc and PghBxc, are regulated by type III secretion regulators HrpX and HrpG and are required for virulence. **Mol. Plant-Microbe Interact.** 21: 555-563.
- \_\_\_\_\_, L. Zhang, Y. Geng, W. Xi, R. Fang and Y. Jia. 2011. XerR, a negative regulator of XccR in *Xanthomonas campestris* pv. *campestris*, relieves its repressor function *in planta*. **Cell Res.** 10: 64.
- Weber, C.R., J.M. Dunleavy and W.R. Fehr. 1966. Effect of bacterial pustule on closely related soybean lines. **Agron. J.** 58: 544-545.
- Weber, E., T. Ojanen-Reuhs., E. Huguet, G. Hause and M. Romantschuk. 2005. The type III-dependent Hrp pilus is required for productive interaction of *Xanthomonas campestris* pv. *vesicatoria* with pepper host plants. **J. Bacteriol.** 187: 2458-68.

- Wei, Z.M., B.J. Sneath and S.V. Beer. 1992. Expression of *Erwinia amylovora* *hrp* genes in response to environmental stimuli. **J. Bacteriol.** 174: 1875-1882.
- Wengelnik, K and U. Bonas. 1996. HrpXv, an AraC-type regulator, activates expression of five out of six loci in the *hrp* cluster of *Xanthomonas campestris* pv. *vesicatoria*. **J. Bacteriol.** 178: 3462-3469.
- \_\_\_\_\_, G. Van den Ackerveken and U. Bonas. 1996. HrpG, a key *hrp* regulatory protein of *Xanthomonas campestris* pv. *vesicatoria* is homologous to two-component response regulators. **Mol. Plant-Microbe Interact.** 9: 704-712.
- White, F.F. and B. Yang. 2009. Host and Pathogen Factors Controlling the Rice-*Xanthomonas oryzae* Interaction. **Plant Physiol.** 150: 1677-1686.
- Xiao, Y., Y. Lu, S. Heu and S.W. Hutcheson. 1992. Organization and environmental regulation of the *Pseudomonas syringae* pv. *syringae* 61 *hrp* cluster. **J. Bacteriol.** 174: 1734-1741.
- Xavier, K.B. and B.L. Bassler. 2003. LuxS quorum sensing: more than just a numbers game. **Curr. Opin. Microbiol.** 6: 191-197.
- Yamada, Y. and T. Nihira. 1998. Microbial hormones and microbial chemical ecology. pp. 377-413. *In* **Comprehensive Natural Products Chemistry**. Vol. 8, ed. DHR Barton, K Nakanishi, Oxford, UK: Elsevier.
- Yamazaki, A., H. Hirata and S. Tsuyumu. 2008. HrpG regulates type II secretory proteins in *Xanthomonas axonopodis* pv. *citri*. **J. Gen. Plant Pathol.** 74: 138-150.

- Yun, M.H., P.S. Torres, M. El Oirdi, L.A. Rigano, R. Gonzalez-Lamothe, M.R. Marano, A.P. Castagnaro, M.A. Dankert, K. Bouarab and A.A. Vojnov. 2006. Xanthan induces plant susceptibility by suppressing callose deposition. **Plant Physiol.** 141: 178-187.
- Zhang, L., Y. Jia, L. Wang and R. Fang. 2007. A proline iminopeptidase gene upregulated in planta by a LuxR homolog is essential for pathogenicity of *Xanthomonas campestris* pv. *campestris*. **Mol. Microbiol.** 65: 121-136.
- Zhu, J. and S.C. Winans. 1999. Autoinducer binding by the quorum-sensing regulator TraR increase affinity for target promoters *in vitro* and decreases TraR turnover rates in whole cells. **Proc. Natl. Acad. Sci. USA.** 96: 4832-4837.
- Zhu, W.G., M.M. Magbanua and F.F. White. 2000. Identification of two novel hrp-associated genes in the hrp gene cluster of *Xanthomonas oryzae* pv. *oryzae*. **J. Bacteriol.** 182: 1844-1853.
- Zoller, B.G. and T. Kosuge. 1971. Growth and movement of *Xanthomonas campestris* in natural fluids in relation to infection of cabbage. **Phytopathology** 61: 919.



**APPENDIX**

### Recipes of media in this study

#### 1. Nutrient glucose agar (NGA) and nutrient broth (NGB)\*

	per L
Beef extract	3.0 g
Bacto peptone	5.0 g
Glucose	2.5 g
Agar	15.0 g

Nutrient agar or nutrient broth may be purchased in dehydrated form Difco.

\* Do not add agar if nutrient broth is desired.

#### 2. Nutrient-broth yeast extract agar (NBY) and nutrient-broth yeast extract broth\*

	per L
Nutrient broth	8.0 g
Yeast extract	2.0 g
K <sub>2</sub> HPO <sub>4</sub>	2.0 g
KH <sub>2</sub> PO <sub>4</sub>	0.5 g
Glucose	2.5 g
Agar	15.0 g

After autoclaving, add 1.0 ml of a sterile solution of 1M MgSO<sub>4</sub>. 7H<sub>2</sub>O<sub>2</sub>

\*Do not add agar if nutrient broth is desired.

#### 3. Luria bertani (LB) agar and Luria bertani broth \*

	per L
Bacto typtone	10.0 g
Yeast extract	5.0 g
NaCl	10.0 g
Agar	15.0 g

\*Do not add agar if nutrient broth is desired.

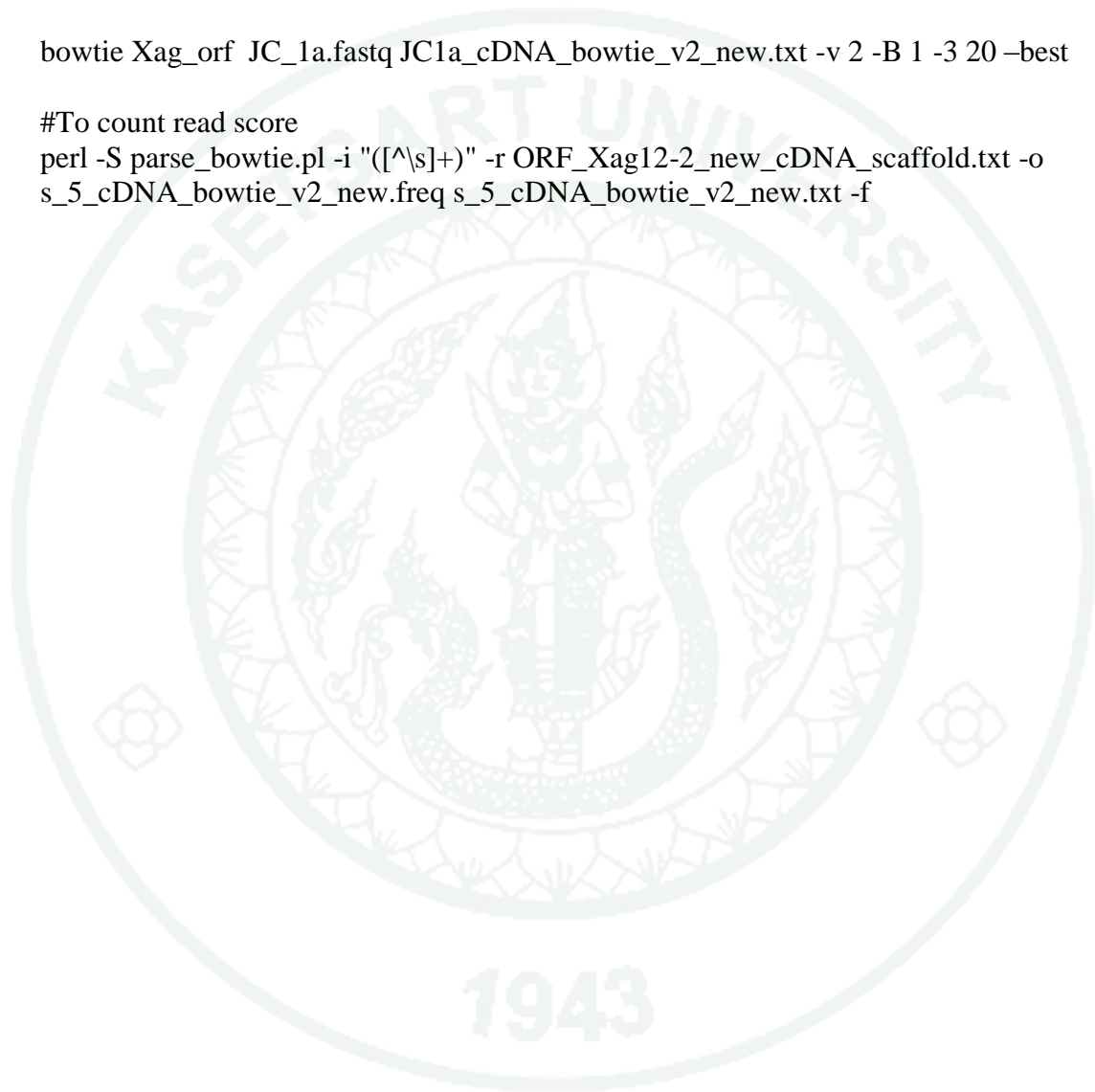
**Command line use for RNA sequencing analysis**

```
# To combine multi fastq.file to single file  
cat *.fastq > new_filename.fastq
```

```
#To run bowtie for short read alignment  
trim 20 bp at 3 prime
```

```
bowtie Xag_orf JC_1a.fastq JC1a_cDNA_bowtie_v2_new.txt -v 2 -B 1 -3 20 -best
```

```
#To count read score  
perl -S parse_bowtie.pl -i "([^\s]+)" -r ORF_Xag12-2_new_cDNA_scaffold.txt -o  
s_5_cDNA_bowtie_v2_new.freq s_5_cDNA_bowtie_v2_new.txt -f
```



**Additional Table 1** The unique genes of *Xanthomonas axonopodis* pv. *glycines* 12-2

<b>Feature ID</b>	<b>Length (bp)</b>	<b>Function</b>
Unique 1	984	Aldo-keto reductase
Unique ma.1	72	tRNA-Val-CAC
Unique 2	1137	hypothetical protein
Unique 3	210	hypothetical protein
Unique 4	402	hypothetical protein
Unique 5	321	hypothetical protein
Unique 6	174	hypothetical protein
Unique 7	240	FIG01214491: hypothetical protein
Unique 8	147	hypothetical protein
Unique 9	138	hypothetical protein
Unique 10	879	COGs COG2378
Unique 11	489	hypothetical protein
Unique 12	579	conserved hypothetical protein
Unique 13	2253	hypothetical protein
Unique 14	765	hypothetical protein
Unique 15	132	FIG01205497: hypothetical protein
Unique 16	1371	phage-related integrase
Unique 17	897	hypothetical protein
Unique 18	291	hypothetical protein
Unique 19	438	hypothetical protein
Unique 20	1245	hypothetical protein
Unique 21	1122	hypothetical protein
Unique 22	483	hypothetical protein
Unique 23	138	hypothetical protein
Unique 24	837	DNA primase (EC 2.7.7.-), phage-associated
Unique 25	651	hypothetical protein
Unique 26	216	hypothetical protein
Unique 27	210	FIG01213968: hypothetical protein
Unique 28	177	hypothetical protein
Unique 29	198	hypothetical protein

**Additional Table 1** (Continued)

<b>Feature ID</b>	<b>Length (bp)</b>	<b>Function</b>
Unique 30	129	hypothetical protein
Unique 31	1143	Integrase
Unique 32	336	hypothetical protein
Unique 33	690	filamentous phage Cf1c related protein
Unique 34	804	thioesterase
Unique 35	213	MbtH-like protein
Unique 36	1374	Acriflavin resistance protein
Unique 37	1371	hypothetical protein
Unique 38	1515	SAM-dependent methyltransferases
Unique 39	408	Type IV pilin PilA
Unique 40	126	hypothetical protein
Unique 41	237	Transposase
Unique 42	447	hypothetical protein
Unique 43	2364	Cyclic beta-1,2-glucan synthase (EC 2.4.1.-)
Unique 44	1293	MchC protein
Unique 45	2166	ABC-type bacteriocin/lantibiotic exporters, contain an N-terminal double-glycine peptidase domain
Unique 46	351	hypothetical protein
Unique 47	117	hypothetical protein
Unique 48	207	Unknown, probable hemolysin/adhesin
Unique 49	153	hypothetical protein
Unique 50	501	Unknown, probable hemolysin/adhesin
Unique 51	132	Acyl carrier protein
Unique 52	987	3-oxoacyl-[acyl-carrier-protein] synthase, KASIII (EC 2.3.1.41)
Unique 53	765	short-chain dehydrogenase/reductase SDR
Unique 54	735	dehydrogenase with different specificities
Unique 55	654	Acetyltransferase
Unique 56	159	hypothetical protein
Unique 57	465	hypothetical protein

**Additional Table 1** (Continued)

<b>Feature ID</b>	<b>Length (bp)</b>	<b>Function</b>
Unique 58	192	hypothetical protein
Unique 59	1659	CELL SURFACE PROTEIN
Unique 60	216	Transposase
Unique 61	420	FIG01213324: hypothetical protein
Unique 62	240	FIG01212390: hypothetical protein
Unique 63	924	Tn5045 resolvase
Unique 64	990	IncW-like replication protein
Unique 65	807	serine protease, putative
Unique 66	159	hypothetical protein
Unique 67	141	hypothetical protein
Unique 68	195	hypothetical protein
Unique 69	651	Chromosome (plasmid) partitioning protein ParA
Unique 70	645	ParA, short form
Unique 71	123	hypothetical protein
Unique 72	114	hypothetical protein
Unique 73	258	Programmed cell death antitoxin PemI
Unique 74	333	Programmed cell death toxin PemK
Unique 75	819	MJ0042 family finger-like protein
Unique 76	2178	involved in conjugative DNA transfer
Unique 77	303	hypothetical protein
Unique 78	420	hypothetical protein
Unique 79	681	Protein mobD
Unique 80	591	hypothetical protein
Unique 81	1533	Putative conjugative transfer protein TraD_F
Unique 82	327	hypothetical protein
Unique 83	711	Minor pilin of type IV secretion complex (VirB5)
Unique 84	237	IncQ plasmid conjugative transfer protein TraG
Unique 85	1041	Inner membrane protein of type IV secretion of T-DNA complex, VirB6
Unique 86	342	Protein export cytoplasm protein SecA ATPase RNA helicase (TC 3.A.5.1.1)

**Additional Table 1** (Continued)

<b>Feature ID</b>	<b>Length (bp)</b>	<b>Function</b>
Unique 87	177	hypothetical protein
Unique 88	237	hypothetical protein
Unique 89	234	hypothetical protein
Unique 91	546	hypothetical protein
Unique 92	639	hypothetical protein
Unique 93	468	hypothetical protein
Unique 95	225	hypothetical protein
Unique 96	114	hypothetical protein
Unique 97	159	hypothetical protein
Unique 98	516	hypothetical protein
Unique 99	123	hypothetical protein
Unique ma.2	73	tRNA-Thr-TGT
Unique 100	162	hypothetical protein
Unique 101	333	hypothetical protein
Unique 102	717	hypothetical protein
Unique 103	987	hypothetical protein
Unique 104	960	hypothetical protein
Unique 105	834	TVG0570508 protein
Unique 106	747	hypothetical protein
Unique 107	1659	Serine/threonine protein kinase
Unique 108	1365	phospholipase D/Transphosphatidylase
Unique 109	240	FIG01213867: hypothetical protein
Unique 110	282	hypothetical protein
Unique 111	312	FIG01211154: hypothetical protein
Unique 112	255	hypothetical protein
Unique 113	606	Phage-related protein
Unique 114	144	hypothetical protein
Unique 115	312	hypothetical protein
Unique 116	1149	hypothetical protein
Unique 117	525	phage-related tail protein
Unique 118	120	hypothetical protein

**Additional Table 1** (Continued)

<b>Feature ID</b>	<b>Length (bp)</b>	<b>Function</b>
Unique 119	246	filamentous hemagglutinin-related protein
Unique 120	1827	adhesin HecA family
Unique 121	297	hemagglutinin/hemolysin-related protein
Unique 122	669	hypothetical protein
Unique 123	1362	hemagglutinin/hemolysin-related protein
Unique 124	267	Error-prone repair protein UmuD
Unique 125	174	hypothetical protein
Unique 126	1200	phage-related integrase
Unique 127	222	FIG01210286: hypothetical protein
Unique 128	207	FIG01210871: hypothetical protein
Unique 129	381	Very-short-patch mismatch repair endonuclease (G-T specific)
Unique 130	117	hypothetical protein
Unique 131	129	hypothetical protein
Unique 132	1224	DNA-cytosine methyltransferase (EC 2.1.1.37)
Unique 133	141	putative transposase
Unique 134	117	hypothetical protein
Unique 135	1386	hypothetical protein
Unique 136	651	conserved hypothetical protein
Unique 137	2835	FIG01112839: hypothetical protein
Unique 138	456	hypothetical protein
Unique 139	738	hypothetical protein
Unique 140	834	DNA primase traC (EC 2.7.7.-)
Unique 141	675	phage-related tail protein
Unique 142	252	hypothetical protein
Unique 143	210	phage-related tail protein
Unique 144	114	hypothetical protein
Unique 145	261	Phage-related protein
Unique 146	381	VirB6 protein
Unique 147	117	hypothetical protein
Unique 148	1500	FIG01214843: hypothetical protein

**Additional Table 1** (Continued)

<b>Feature ID</b>	<b>Length (bp)</b>	<b>Function</b>
Unique 149	576	outer membrane protein
Unique 150	306	Putative surface protein
Unique 151	780	CDP-diacylglycerol pyrophosphatase (EC 3.6.1.26)
Unique 152	126	transcriptional regulator lacI family
Unique 153	642	FIG01214410: hypothetical protein
Unique 154	219	FIG01213968: hypothetical protein
Unique 155	279	FIG01212736: hypothetical protein
Unique 156	264	FIG01210340: hypothetical protein
Unique 157	411	putative; ORF located using Glimmer/Genemark
Unique 158	177	FIG01210741: hypothetical protein
Unique 159	276	FIG01210866: hypothetical protein
Unique 160	123	hypothetical protein
Unique 161	177	Type IV pilus biogenesis protein PilQ
Unique 162	1329	FIG00964775: hypothetical protein
Unique 163	162	hypothetical protein
Unique 164	168	hypothetical protein
Unique 165	1224	GlyA
Unique 166	135	GlyB
Unique 167	159	hypothetical protein
Unique 168	1056	dTDP-glucose 4,6-dehydratase (EC 4.2.1.46)
Unique 169	888	Glucose-1-phosphate thymidyltransferase (EC 2.7.7.24)
Unique 170	558	dTDP-4-dehydrorhamnose 3,5-epimerase (EC 5.1.3.13)
Unique 171	129	hypothetical protein
Unique 172	435	COG0065: 3-isopropylmalate dehydratase large subunit
Unique 173	1332	FIG01197885: hypothetical protein
Unique 174	1125	metallophosphoesterase
Unique 175	2685	Chromosome partition protein smc

**Additional Table 1** (Continued)

<b>Feature ID</b>	<b>Length (bp)</b>	<b>Function</b>
Unique 176	1293	hypothetical protein
Unique 177	1770	Nucleotidyltransferase (EC 2.7.7.-)
Unique 178	474	hypothetical protein
Unique 179	903	hypothetical protein
Unique 180	690	hypothetical protein
Unique 181	3762	hypothetical protein
Unique 182	1251	hypothetical protein
Unique 183	183	Programmed cell death antitoxin MazE like
Unique 184	351	hypothetical protein
Unique 185	129	hypothetical protein
Unique 186	219	hypothetical protein
Unique 187	177	hypothetical protein
Unique 188	135	hypothetical protein
Unique 189	129	hypothetical protein
Unique 190	126	hypothetical protein
Unique 191	114	hypothetical protein
Unique 192	189	hypothetical protein
Unique 193	177	GII2891 protein
Unique 194	1518	Avirulence protein
Unique 195	258	hypothetical protein
Unique 196	201	FIG01211154: hypothetical protein
Unique 197	279	FIG01210817: hypothetical protein
Unique 198	213	FIG01213867: hypothetical protein
Unique 199	324	hypothetical protein
Unique 200	273	hypothetical protein
Unique 201	180	Baseplate assembly protein J
Unique 202	1539	cell wall hydrolase/autolysin
Unique 203	237	Phage tail completion protein
Unique 204	477	hypothetical protein
Unique 205	1632	Sulfur carrier protein adenylyltransferase ThiF

**Additional Table 1** (Continued)

<b>Feature ID</b>	<b>Length (bp)</b>	<b>Function</b>
Unique 206	1137	FIG01197816: hypothetical protein
Unique 207	987	Patatin
Unique 208	393	transcriptional regulator, XRE family
Unique 209	870	hypothetical protein
Unique 210	120	hypothetical protein
Unique 211	363	hypothetical protein
Unique 212	231	hypothetical protein
Unique 213	276	Shufflon-specific DNA recombinase
Unique 214	1188	phage-related integrase
Unique 215	225	FIG01210286: hypothetical protein
Unique 216	123	hypothetical protein
Unique 217	216	FIG01213394: hypothetical protein
Unique 218	1014	FIG01211087: hypothetical protein
Unique 219	144	hypothetical protein
Unique 220	3234	hypothetical protein
Unique 221	1299	probable ATP /GTP binding protein
Unique 222	2199	ATP-dependent helicase
Unique 223	162	hypothetical protein
Unique 224	483	ankyrin repeat protein
Unique 225	579	ankyrin repeat protein
Unique 226	234	hypothetical protein
Unique 227	651	hypothetical protein
Unique 228	219	hypothetical protein
Unique 229	4665	RhsD protein
Unique 230	120	hypothetical protein
Unique 231	138	hypothetical protein
Unique 232	1839	1,4-beta-cellobiosidase
Unique 233	129	hypothetical protein
Unique 234	720	FIG01122584: hypothetical protein
Unique 235	138	hypothetical protein
Unique 236	234	transcriptional regulator lacI family
Unique 237	1212	hypothetical protein

**Additional Table 1** (Continued)

<b>Feature ID</b>	<b>Length (bp)</b>	<b>Function</b>
Unique 238	3282	structural elements; cell exterior; surface polysaccharides/antigens
Unique 239	645	structural elements; cell exterior; surface polysaccharides/antigens
Unique 240	798	Transposase
Unique 241	210	ISXo8 transposase
Unique 242	837	Putative lipoprotein
Unique 243	138	hypothetical protein
Unique 244	675	hypothetical protein
Unique 245	354	putative; ORF located using Glimmer/Genemark
Unique 246	165	FIG01212243: hypothetical protein
Unique 247	861	Beta-lactamase (EC 3.5.2.6)
Unique 248	861	Beta-lactamase (EC 3.5.2.6)
Unique 249	480	ankyrin repeat protein
Unique 250	234	hypothetical protein
Unique 251	651	hypothetical protein
Unique 252	114	hypothetical protein
Unique 253	138	hypothetical protein
Unique 254	189	hypothetical protein
Unique 255	936	FIG01113227: hypothetical protein
Unique 256	225	FIG01212625: hypothetical protein
Unique 257	291	hypothetical protein
Unique 258	447	hypothetical protein
Unique 259	651	hypothetical protein
Unique 260	678	hypothetical protein
Unique 261	312	hypothetical protein
Unique 262	4398	Phage tail fiber protein
Unique 263	393	hypothetical protein
Unique 264	462	hypothetical protein
Unique 265	357	hypothetical protein
Unique 266	3354	Phage tail length tape-measure protein 1

**Additional Table 1** (Continued)

<b>Feature ID</b>	<b>Length (bp)</b>	<b>Function</b>
Unique 267	315	hypothetical protein
Unique 268	393	hypothetical protein
Unique 269	468	hypothetical protein
Unique 270	399	hypothetical protein
Unique 271	426	conserved hypothetical protein
Unique 272	1098	hypothetical protein
Unique 273	357	hypothetical protein
Unique 274	513	hypothetical protein
Unique 275	531	hypothetical protein
Unique 276	948	Mlr8009 protein
Unique 277	441	hypothetical protein
Unique 278	1095	Phage-related protein
Unique 279	2004	hypothetical protein
Unique 280	1815	probable bacteriophage protein STY1048
Unique 281	1533	Phage terminase, large subunit
Unique 282	495	Terminase small subunit
Unique 283	318	hypothetical protein
Unique 284	435	hypothetical protein
Unique 285	321	hypothetical protein
Unique 286	312	hypothetical protein
Unique 287	492	Phage lysin
Unique 288	135	hypothetical protein
Unique 289	162	hypothetical protein
Unique 290	678	hypothetical protein
Unique 291	255	hypothetical protein
Unique 292	537	hypothetical protein
Unique 293	249	hypothetical protein
Unique 294	522	hypothetical protein
Unique 295	222	hypothetical protein
Unique 296	174	hypothetical protein
Unique 297	141	hypothetical protein

**Additional Table 1** (Continued)

<b>Feature ID</b>	<b>Length (bp)</b>	<b>Function</b>
Unique 298	312	hypothetical protein
Unique 299	447	hypothetical protein
Unique 300	642	hypothetical protein
Unique 301	1494	Replicative DNA helicase (EC 3.6.1.-)
Unique 302	936	hypothetical protein
Unique 303	198	hypothetical protein
Unique 304	477	hypothetical protein
Unique 305	207	hypothetical protein
Unique 306	423	hypothetical protein
Unique 307	246	hypothetical protein
Unique 308	675	phage-related repressor protein
Unique 309	426	hypothetical protein
Unique 310	282	hypothetical protein
Unique 311	372	hypothetical protein
Unique 312	264	hypothetical protein
Unique 313	216	hypothetical protein
Unique 314	114	hypothetical protein
Unique 315	255	hypothetical protein
Unique 316	609	hypothetical protein
Unique 317	279	hypothetical protein
Unique 318	843	hypothetical protein
Unique 319	972	hypothetical protein
Unique 320	225	phage transcriptional regulator, AlpA
Unique 321	879	RecA-family ATPase
Unique 322	699	FIG01205749: hypothetical protein
Unique 323	216	hypothetical protein
Unique 324	834	Conjugative transfer protein TrbJ
Unique 325	231	Conjugative transfer entry exclusion protein TrbK
Unique 326	1470	Conjugative transfer protein TrbL
Unique 327	246	hypothetical protein
Unique 328	258	hypothetical protein

**Additional Table 1** (Continued)

<b>Feature ID</b>	<b>Length (bp)</b>	<b>Function</b>
Unique 329	300	transcriptional regulator, Fis family
Unique 330	174	hypothetical protein
Unique 331	264	hypothetical protein
Unique 332	318	plasmid stabilization protein
Unique 333	252	plasmid stabilization protein
Unique 334	876	ParA, short form
Unique 335	162	hypothetical protein
Unique 336	1701	hypothetical protein
Unique 337	591	hypothetical protein
Unique 338	2451	bll1593; unknown protein
Unique 339	126	Pyruvate oxidase [ubiquinone, cytochrome] (EC 1.2.2.2)
Unique 340	660	RNA polymerase sigma factor for flagellar operon
Unique 341	753	Flagellar biosynthesis protein FljP
Unique 342	324	hypothetical protein
Unique 343	255	hypothetical protein
Unique 344	690	hypothetical protein
Unique 345	1164	Flagellar hook protein FlgE
Unique 346	417	Flagellar basal-body rod modification protein FlgD
Unique 347	744	hypothetical protein
Unique 348	462	hypothetical protein
Unique 349	1326	Flagellum-specific ATP synthase FliI
Unique 350	645	hypothetical protein
Unique 351	465	hypothetical protein
Unique 352	1377	Flagellar M-ring protein FliF
Unique 353	297	hypothetical protein
Unique 354	384	Flagellar basal-body rod protein FlgC
Unique 355	378	hypothetical protein
Unique 356	1116	Flagellar P-ring protein FlgI
Unique 357	564	Flagellar L-ring protein FlgH

**Additional Table 1** (Continued)

<b>Feature ID</b>	<b>Length (bp)</b>	<b>Function</b>
Unique 358	699	hypothetical protein
Unique 359	768	Flagellar basal-body rod protein FlgG
Unique 360	672	putative flagellar basal-body rod protein flgF
Unique 361	2064	Flagellar biosynthesis protein FlhA
Unique 362	1074	Flagellar biosynthetic protein FlhB
Unique 363	771	Flagellar biosynthesis pathway, component FliR
Unique 364	264	Flagellar biosynthesis protein FliQ
Unique 365	1170	FOG: TPR repeat
Unique 366	282	hypothetical protein
Unique 367	11136	Rhs family protein
Unique 368	816	saccharide biosynthesis regulatory protein
Unique 369	390	hypothetical protein
Unique 370	558	hypothetical protein
Unique 371	372	Phage-related protein
Unique 372	219	hypothetical protein
Unique 373	708	phage-related tail protein
Unique 374	1287	FIG01212243: hypothetical protein
Unique 375	222	hypothetical protein
Unique 376	141	hypothetical protein
Unique 377	288	hypothetical protein
Unique 378	546	FIG01213968: hypothetical protein
Unique 379	294	FIG01214410: hypothetical protein
Unique 380	213	FIG01213867: hypothetical protein
Unique 381	279	FIG01210817: hypothetical protein
Unique 382	201	FIG01211154: hypothetical protein
Unique 383	228	ATPase provides energy for both assembly of type IV secretion complex and secretion of T-DNA complex (VirB4)
Unique 384	1188	FIG01214986: hypothetical protein
Unique 385	342	transcriptional regulator, XRE family
Unique 387	195	hypothetical protein

**Additional Table 1** (Continued)

<b>Feature ID</b>	<b>Length (bp)</b>	<b>Function</b>
Unique 388	891	plasmid mobilization protein
Unique 389	174	hypothetical protein
Unique 390	960	hypothetical protein
Unique 391	1275	hypothetical protein
Unique 392	1392	phage-related integrase
Unique 393	114	hypothetical protein
Unique 394	1197	hypothetical protein
Unique 395	1053	Protein kinase
Unique 396	1083	Protein kinase
Unique 397	153	hypothetical protein
Unique 398	318	hypothetical protein
Unique 399	507	hypothetical protein
Unique 400	114	hypothetical protein
Unique 401	609	ISPpu14, transposase Orf2
Unique 402	783	hypothetical protein
Unique 403	1581	hypothetical protein
Unique 404	927	hypothetical protein
Unique 405	588	ankyrin repeat protein
Unique 406	201	hypothetical protein
Unique 407	1686	deoxycytidylate deaminase( EC:3.5.4.12 )
Unique 408	150	hypothetical protein
Unique 409	264	hypothetical protein
Unique 410	243	Adenine-specific methyltransferase (EC 2.1.1.72)
Unique 411	138	hypothetical protein
Unique 412	165	site-specific DNA-methyltransferase
Unique 413	1041	Transposase
Unique 414	120	hypothetical protein
Unique 415	234	hypothetical protein
Unique 416	186	Adenine-specific methyltransferase (EC 2.1.1.72)
Unique 417	1335	RelA/SpoT domain protein
Unique 418	141	AmpG permease

**Additional Table 1** (Continued)

<b>Feature ID</b>	<b>Length (bp)</b>	<b>Function</b>
Unique 419	525	hypothetical protein
Unique 420	603	hypothetical protein
Unique 421	123	Integrase
Unique 422	306	hypothetical protein
Unique 423	141	hypothetical protein
Unique 424	1014	hypothetical protein
Unique 425	123	hypothetical protein
Unique 426	144	hypothetical protein
Unique 427	936	hypothetical protein
Unique 428	333	hypothetical protein
Unique 429	177	hypothetical protein
Unique 430	2013	RhsD protein
Unique 431	147	hypothetical protein
Unique 432	156	hypothetical protein
Unique 433	342	hypothetical protein
Unique 434	168	hypothetical protein
Unique 435	276	FIG01210268: hypothetical protein
Unique 436	672	hypothetical protein
Unique 437	219	hypothetical protein
Unique 438	282	hypothetical protein
Unique 439	1167	General secretion pathway protein D
Unique 440	906	hypothetical protein
Unique 441	276	hypothetical protein
Unique 442	501	hypothetical protein
Unique 443	2673	TonB-dependent receptor
Unique 444	147	FIG01213922: hypothetical protein
Unique 445	378	hypothetical protein
Unique 446	618	hypothetical protein
Unique 447	708	wall-associated protein
Unique 448	189	hypothetical protein
Unique 449	294	hypothetical protein

**Additional Table 1** (Continued)

<b>Feature ID</b>	<b>Length (bp)</b>	<b>Function</b>
Unique 450	990	Rossmann fold nucleotide-binding protein Smf possibly involved in DNA uptake
Unique 451	1269	DNA topoisomerase I
Unique 452	501	hypothetical protein
Unique 453	1389	phage-related integrase
Unique 454	447	hypothetical protein
Unique 455	1125	hypothetical protein
Unique 456	501	hypothetical protein
Unique 457	639	plasmid mobilization protein
Unique 458	750	Error-prone, lesion bypass DNA polymerase V (UmuC)
Unique 459	132	hypothetical protein
Unique 460	1179	Zn peptidase with DNA binding
Unique 461	468	hypothetical protein
Unique 462	150	Adenine-specific methyltransferase (EC 2.1.1.72)
Unique 463	549	hypothetical protein
Unique 464	1026	FIG01210548: hypothetical protein
Unique 465	126	hypothetical protein
Unique 466	129	hypothetical protein
Unique 467	519	hypothetical protein
Unique 468	252	hypothetical protein
Unique 469	1182	phage-related integrase
Unique 470	222	FIG01210286: hypothetical protein
Unique 471	1518	hypothetical protein
Unique 472	426	GDP-mannose 4,6 dehydratase (EC 4.2.1.47)
Unique 473	957	UDP-glucose 4-epimerase (EC 5.1.3.2)
Unique 474	1440	hypothetical protein
Unique 475	1068	methyltransferase FkbM family
Unique 476	2040	putative carbohydrate translocase
Unique 477	657	COG1232: Protoporphyrinogen oxidase
Unique 478	696	COG1232: Protoporphyrinogen oxidase

**Additional Table 1** (Continued)

<b>Feature ID</b>	<b>Length (bp)</b>	<b>Function</b>
Unique 479	327	hypothetical protein
Unique 480	957	glycosyl transferase
Unique 481	225	hypothetical protein
Unique 482	270	phage-related protein
Unique 483	228	hypothetical protein
Unique 484	303	hypothetical protein
Unique 485	258	hypothetical protein
Unique 486	156	hypothetical protein
Unique 487	1254	DNA-cytosine methyltransferase (EC 2.1.1.37)
Unique 488	2517	Superfamily II DNA/RNA helicases, SNF2 family
Unique 489	219	hypothetical protein
Unique 490	216	hypothetical protein
Unique 491	639	Putative DnaJ-class molecular chaperone with C-terminal Zn finger domain, heat shock protein
Unique 492	225	hypothetical protein
Unique 493	1041	Phage integrase: Phage integrase, N-terminal SAM-like
Unique 494	1083	Type IV fimbrial biogenesis protein PilW
Unique 495	513	Type IV fimbrial biogenesis protein PilX
Unique 496	261	Phage tail fibers
Unique 497	1206	phage-related tail fiber protein
Unique 498	228	putative; ORF located using Glimmer/Genemark
Unique 499	873	hypothetical protein
Unique 500	180	hypothetical protein
Unique 501	141	hypothetical protein
Unique 502	279	hypothetical protein

**CIRRICULUM VITAE**

**NAME:** : Miss Tiyakhon Chatnaparat

**DATE OF BIRTH** : 30 June 1984

**PLACE OF BIRTH** : Burirum, THAILAND

**ADDRESS OFFICE:**

Department of Plant Pathology, Faculty of Agriculture, Kasetsart University  
50 Paholyothin Rd. Ladyao, Chatuchak, Bangkok, THAILAND 10900  
Phone : (66) 8-91478390

**INSTITUTION ATTENDED:**

1. Kasetsart University, Thailand, 2003-2006, Bachelor Degree of Science (Integrated Pest Management) (first class honor)
2. Kasetsart University, Bangkok, Thailand, 2006- present, Doctor of Philosophy (Plant Pathology)

**AWARDS AND SCHOLARSHIPS:**

1. The Royal Golden Jubilee Ph.D. Scholarship, from the Thailand Research Fund, 2006-2011.
2. The Louisiana State Agricultural Center Summer Internship for Graduate Students of Kasetsart University, Thailand, 2008.
3. The first honorable mention award of article and oral presentation of The 46<sup>th</sup> Kasetsart University Annual Conference 2008.
4. The first honorable award of article and oral presentation for Graduate Students Conference of Faculty Agriculture Kasetsart University 2010.
5. The first honorable mention award of article and oral presentation of The 49<sup>th</sup> Kasetsart University Annual Conference 2011.
6. The outstanding award of oral presentation of the Royal Golden Jubilee Conference 2011.